Efficient Identification and Utilization of Spectrum Opportunities in Cognitive Radio Networks

by

Hyoil Kim

A dissertation submitted in partial fulfillment
of the requirements for the degree of
Doctor of Philosophy
(Electrical Engineering: Systems)
in The University of Michigan
2010

Doctoral Committee:

Professor Kang G. Shin, Chair
Associate Professor Achilleas Anastasopoulos
Associate Professor Jason N. Flinn
Associate Professor Mingyan Liu

To my wife Hee Sun, and my parents

ACKNOWLEDGEMENTS

I would like to express my sincere gratitude to Professor Kang G. Shin for his extraordinary support and guidance during my doctoral studies. He has inspired me with many critical aspects of becoming a good researcher such as completeness, imagination, practicality, and agility. He has advised me not only on my research, but also on my career and life. I thus feel fortunate to work with him and proud of being a member of his research group, Real-Time Computing Laboratory. I am also thankful to my research committee, Professor Mingyan Liu, Professor Achilleas Anastasopoulos, and Professor Jason N. Flinn for their support and valuable suggestions on my dissertation.

My special thanks go to my beloved wife, Hee Sun Min, and my parents. Hee Sun has been my biggest supporter during my doctoral studies enduring hard times together. I am indebted to my parents for their unconditional love and support throughout my life. It would not have been possible to stand where I am now without them.

I feel grateful to Professor Mingyan Liu, Dr. Carlos Cordeiro, Dr. Chun-Ting Chou, and Professor Demosthenis Teneketzis for serving as my reference. I also thank my mentors and collaborators, Dr. Bong-Jun Ko at IBM T.J. Watson Research Center and Dr. Kiran Challapali and Dr. Dave Cavalcanti at Philips Research North America. My appreciation also goes to Alexander W. Min, Dr. Jaehyuk Choi, and Ashwini Kumar for their kind support and collaboration in co-authoring

conference and journal papers, and also goes to other former/current members of RTCL especially Dr. Daji Qiao, Dr. Taejoon Park, Dr. Jai-Jin Lim, Dr. Abhijit Bose, Dr. Kyu-Han Kim, Dr. Min-gyu Cho, Dr. Pradeep Padala, Dr. Jisoo Yang, Dr. Bechir Hamdaoui, Dr. Young-June Choi, Dr. Sangsoo Park, Dr. Ji-Hoon Yun, Eugene Chai, and Xinyu Zhang.

I also want to thank for the financial support from the Korea Science and Engineering (KOSEF) scholarship foundation, Samsung scholarship foundation, NSF, Intel Corporation, Philips Research North America, and NEC Labs North America.

TABLE OF CONTENTS

LIST OF FIGURES

Figure

LIST OF TABLES

Table

ABSTRACT

There has been an exponential increase in spectrum demands due to new emerging wireless services and applications, making it harder to find unallocated spectrum bands for future usage. This potential resource scarcity is rooted at inefficient utilization of spectrum under static spectrum allocation. Therefore, a new concept of *dynamic spectrum access* (DSA) has been proposed to opportunistically utilize the legacy spectrum bands by *cognitive radio* (CR) users. Cognitive radio is a key technology for alleviating this inefficient spectrum utilization, since it can help discover *spectrum opportunities* (or *whitespaces*) in which legacy spectrum users do not temporarily use their assigned spectrum bands.

In a DSA network, it is crucial to efficiently identify and utilize the whitespaces. We address this issue by considering *spectrum sensing* and *resource allocation*. Spectrum sensing is to discover spectrum opportunities and to protect the legacy users (or incumbents) against harmful interference from the CR users. In particular, sensing is an interaction between PHY and MAC layers where in the PHY-layer signal detection is performed, and in the MAC-layer spectrum sensing is scheduled and spectrum sensors are coordinated for collaborative sensing. Specifically, we propose an efficient MAC-layer sensing scheduling algorithm that discovers spectrum opportunities as much as possible for better quality-of-service (QoS), and as fast as possible for seamless service provisioning. In addition, we propose an optimal in-band spectrum sensing algorithm to protect incumbents by achieving the detectability requirements set by regulators (e.g., FCC) while incurring minimal sensing overhead.

For better utilization of discovered spectrum opportunities, we pay our attention to resource allocation in the secondary spectrum market where legacy license holders temporarily lease their own spectrum to secondary wireless service providers (WSPs) for opportunistic spectrum access by CR users. In this setting, we investigate how a secondary WSP can maximize its profit by optimally controlling the admission and eviction of its customers (i.e., CR users). In addition, we also focus on the price and quality competition between co-located WSPs where they contend for enticing customers by providing more competitive service fee while leasing the channels with best matching quality.

CHAPTER I

INTRODUCTION

Over the last two decades, there has been an exponential increase in spectrum demands due to the new emerging wireless services, which causes a shortage of allocatable wireless spectrum resources. According to the current *static* spectrum allocation policy, each new wireless service/protocol should be assigned a spectrum band which has never been allocated, and therefore most parts of the spectrum under 3GHz are now allocated to specific use. Although wireless spectrum is considered in theory an unlimited resource, its poor transmission characteristics at higher frequency bands (e.g., 60GHz) restrict their usage to specific applications (e.g., personal area networks). As a result, in the near future we expect a shortage of allocatable spectrum bands with fair transmission characteristics.

This potential resource scarcity is actually solvable, since the shortage derives from inefficient utilization of spectrum by the static spectrum allocation. A recent measurement study [55] revealed that the average spectrum utilization is only about 5.2% over time for spectrum bands under 3GHz, measured at many geographical locations. Nevertheless, the remaining unused portion of time in those bands cannot be used for other purposes, since the current static policy strictly prohibits such usage. Therefore, since 2000, FCC has been searching for a new spectrum policy to

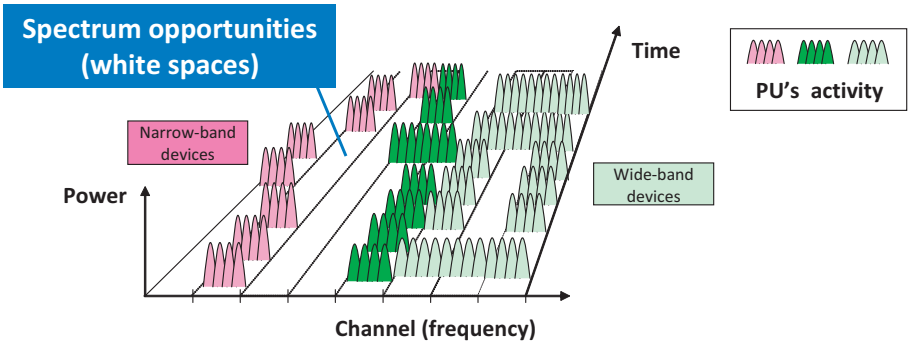

Figure 1.1: An illustration of spectrum opportunities.

dynamically utilize the legacy spectrum bands [24–28].

Dynamic Spectrum Access (DSA) is a new paradigm for alleviating the inefficient spectrum-utilization problem by exploiting the spectrum agility (SA) feature of the *Cognitive Radio* (CR) technology. In DSA, (unlicensed) secondary users (SUs) form a CR network (CRN) and are allowed to opportunistically utilize the spectrum bands of (licensed) primary users (PUs) as long as the SUs do not cause any harmful interference to the PUs. The time period when SUs can reuse a licensed band is called *spectrum opportunity* or *spectrum whitespaces* (WS) [41]. Spectrum agility becomes realizable with the recent progress in wireless communications, such as Software Defined Radios (SDRs) and smart antennas. The concept of spectrum opportunity is illustrated in Fig. 1.1.

1.1 Identification of Spectrum Opportunities

It is crucial for CRNs to identify spectrum opportunities efficiently and correctly, for which *spectrum sensing* is essential. Spectrum sensing is an act of monitoring a spectrum band/channel[1] for a pre-determined amount of time (called sensing-time) to detect PU signals in order to determine its availability to SUs. The sensing-time

[1]The terms *spectrum band* and *channel* are used interchangeably throughout the dissertation.

depends on the characteristics of PU signals as well as the detection method used. A single measurement result is called a sample, indicating whether a channel is busy or idle. Once a channel is sensed idle (i.e., no PU signal is present), it can be utilized by SUs until its PUs return to the channel.

Spectrum sensing can be realized as a two-layer mechanism. The PHY-layer sensing focuses on efficiently detecting PU signals to identify opportunities by properly choosing its detection method. Several well-known PHY-layer detection methods, such as *energy detection*, *matched filter* and *feature detection* [7, 73, 91], have been proposed as candidates for the PHY-layer sensing. On the other hand, the MAC-layer sensing generally focuses on two issues: (1) scheduling of sensing, and (2) collaboration between sensors. Sensing scheduling tries to determine when to sense and which channel to sense. Sensor collaboration implies concurrent sensing, where multiple sensors participate in sensing the same channel simultaneously to enhance the detectability of PU signals.

Sensing can also be categorized into two types: *in-band sensing* performed on in-band channels, and *out-of-band sensing* performed on out-of-band channels. Here, *in-band channels* refer to those channels currently in use by SUs; all others are referred to as *out-of-band channels*. In-band sensing focuses on protecting PUs via fast detection of PUs returning to in-band channels. Since the PUs are given priority in accessing their own channel, SUs must vacate the channel as soon as they detect the PUs (called *channel vacation*). Next, out-of-band sensing focuses on providing enough bandwidth for quality-of-service (QoS) provisioning to SUs, by discovering spectrum opportunities from out-of-band channels. Out-of-band sensing is further divided into two types, periodic and reactive sensing, where the choice of a sensing mode (i.e., periodic vs. reactive) depends on how much demand for opportunities

there exists in CRNs.

The two objectives of spectrum sensing, protecting PUs and promoting QoS of SUs, often conflict. For maximal protection of PUs, it is desirable to perform in-band sensing as frequently as possible, so that latency of detecting the returning PUs can be minimized. Such in-band sensing, however, often incurs high sensing-overhead frequently interrupting data transmission between SUs. Therefore, triggering in-band sensing only if necessary is key to both protect PUs and promote SUs' QoS. On the other hand, out-of-band sensing should not be performed more than necessary, because it forces SUs to reconfigure their antenna frequency to an out-of-band channel and thus interrupts their in-band transmission.

In this dissertation, we propose medium access control (MAC) layer schemes that efficiently schedule in-band and out-of-band spectrum sensing so that PUs can be protected from harmful interference while QoS of SUs can be properly supported. Specifically, we try to address the following two issues in out-of-band sensing: (1) how to maximize the amount of opportunities discovered by sensing, and (2) how to minimize the latency in finding additional opportunities when needed. In terms of in-band sensing, we focus on how to achieve the maximal protection of legacy spectrum users while incurring sensing overhead as minimal as possible.

1.2 Utilization of Spectrum Opportunities

Efficient utilization of the discovered spectrum opportunities is also important since the major objective of DSA is to enhance the overall utilization of legacy spectrum. In particular, we address this issue in the context of *secondary spectrum market*. In a DSA network, the primary license holders may temporarily transfer their spectrum usage rights to CR users [5, 10] via the secondary spectrum market.

The license holders can temporarily lease their channels to the CR users and generate additional revenue by charging for their opportunistic use of paid-but-idle channels. The CR end-users can also benefit from this because they can access the spectrum at a much lower cost than legacy services. However, the CR users are allowed to use the leased channels only when they are not occupied by the licensed (or primary) users because the licensed users are given priority over the CR end-users.

The *Dynamic Spectrum Market* (DSM) is a secondary spectrum market that facilitates the transfer of spectrum rights via an auction mechanism. DSM is composed of three interacting layers/planes: spectrum plane, service plane, and user plane [10,72]. The spectrum is auctioned by a Spectrum Broker (SB) at the top plane where bidders are the *secondary* wireless service providers (WSPs) at the middle plane [6,86]. Here, the SB might be either the regulatory authorities (e.g., FCC in USA and Ofcom in UK) or an authorized third-party. A secondary WSP leases spectrum via auction and subleases a portion of the leased channels to the CR end-users at the bottom plane [44].

This dissertation focuses on two issues in DSM: (1) how a secondary WSP can maximize its profit by user admission and eviction control when the spectrum demand varies with CR users and applications, e.g., audio/video users will need more spectrum bandwidth than text only users, and (2) how co-located WSPs can compete for the price of their service in the customer market and the quality of the leased spectrum in the auction market.

1.3 Overview of Existing Approaches

1.3.1 Discovery of Spectrum Opportunities via Out-of-band Sensing

The following papers are related to the issue of maximal discovery of opportunities. Chou [14] proposed a proactive sensing algorithm with non-adaptive and randomly-chosen sensing periods. Zhao *et al.* [99] introduced a Decentralized Cognitive MAC (DC-MAC) with reactive sensing focusing on slotted-time CSMA-based channel access with synchronized slot information. Sankaranarayanan *et al.* [71] proposed an Ad-hoc Secondary system MAC (AS-MAC) which is a proactive scheme with slotted-time-based channel access.

In the context of fast discovery of opportunities, Jiang *et al.* [45] investigated the optimal sensing sequence in a multi-channel cognitive MAC protocol, and Shu and Krunz [81] studied the problem of sequential sensing for throughput efficiency along with finding the optimal sensing time. Lai *et al.* [53] considered a scenario in which SUs can sense more than one channel simultaneously and utilize all discovered idle channels for their transmission.

1.3.2 Incumbent User Protection via In-band Sensing

There have been many proposals to protect incumbent users via PHY-layer signal detection schemes such as energy detection [35, 77, 90] and feature detection [13, 18, 36, 78]. However, such numerous existing studies are based on the single-time signal detection, which can be greatly enhanced by the MAC-layer support such as sensing scheduling and sensor clustering.

Scheduling of sensing in-band channels is to immediately detect returning PUs to the in-band channels. For example, Cordeiro *et al.* [18] evaluated the performance of fast sensing in 802.22 by scheduling it (1 ms) every 40 ms, but they did not optimize

the sensing-time and sensing-period. Hoang and Liang [42] introduced an adaptive sensing scheduling method to capture the tradeoff between SUs' data-transmission and spectrum-sensing.

There have also been continuing discussions on use of clustered sensor networks. Chen *et al.* [13] proposed a mechanism to form a cluster among neighboring nodes and then interconnect such clusters. Pawelczak *et al.* [62] proposed cluster-based sensor networks to reduce the latency in reporting sensor measurements by designating the cluster head as a local decision maker. Sun *et al.* [88] enhanced performance by clustering sensors where the benefit comes from cluster and sensor diversities.

1.3.3 Utilization of Spectrum Opportunities for Profit Maximization

Once spectrum sensing discovers spectrum opportunities, they can be utilized by CRNs for various purposes. In particular, this dissertation discusses the economic aspects of the whitespace utilization in terms of profit maximization of WSPs. The profit maximization can be achieved by considering two necessary techniques: CR user control in terms of customer admission and eviction, and the competition between co-located WSPs.

The following papers are related to the admission and eviction control of CR users, although none of them have discussed both types of control in the same context. Ishibashi *et al.* [43] considered multi-homed primary users, where a primary user is either classical or cognitive. However, the classical primaries are assumed not to have priority over the cognitive primaries, thus unaccounting for channel eviction. Wang *et al.* [95] proposed a primary-prioritized Markov approach where primary users have exclusive rights to access their own channels, without considering the admission control. Ross and Tsang [66] addressed the problem of optimal admission control

on user arrivals with various spectrum demands, in the framework of traditional networks where the channels are always available without any time-varying patterns.

In the DSM, co-located WSPs compete for leasing the spectrum with the best quality to run their service and enticing more customers by providing a competitive service tariff. Jia and Zhang [44] studied price and capacity competition in a duopoly DSA market, assuming that the customer arrival rate is determined by a quadratic utility function, not by price. Duan *et al.* [23] studied a similar problem with consideration to physical-layer characteristics of heterogeneous end-users and derived threshold-type pricing rules, assuming a constant spectrum leasing cost. Kasbekar *et al.* [46] considered a hierarchical game of quantity–price competition, with a two-level prioritized service available to the end-users. None of the mentioned papers, however, considered time-varying spectrum availability, which is one of the key contributions of this dissertation.

1.4 Main Contributions

The objective of this dissertation is to provide an efficient framework for spectrum sensing and whitespace utilization, where its main contributions are:

- **Maximal discovery of spectrum opportunities via periodic out-of-band sensing.** We address the problem of supporting QoS for SUs by discovering as many spectrum opportunities as possible, so that the overall utilizable bandwidth can be maximized to achieve a higher throughput. In our proposed scheme, spectrum opportunities in out-of-band channels are discovered by periodic sensing. These sensing-periods are optimized to strike a balance between the discovered spectrum opportunities and the sensing overheads, since periodic sensing of out-of-band channels will interrupt SUs utilizing in-band channels.

- **Fast discovery of spectrum opportunities via sequential out-of-band sensing.** We address the problem of finding additional spectrum opportunities whenever an in-band channel is vacated due to the returning PUs. We focus on minimizing the delay in finding the necessary amount of opportunities, since it can help promote seamless service provisioning. To minimize the delay, we propose an optimal sensing sequence found by dynamic programming (DP) by considering the heterogeneous channel characteristics. To alleviate the computational complexity of DP, we also propose a suboptimal sequence with polynomial-time complexity that yields a near-optimal performance.

- **Optimal scheduling of in-band sensing for protection of PUs.** We address the problem of protecting PUs against harmful interference from SUs by optimally scheduling in-band spectrum sensing, where we propose an optimal in-band sensing with optimal sensing-time and sensing-frequency. We also compare simple energy detection with complicated feature detection, and propose a better detection method in terms of the incurred sensing overhead according to the given sensing environment.

- **Profit maximization of secondary WSPs via optimal admission and eviction control.** We propose an optimal admission and eviction control of CR users to maximize the profit of a secondary WSP. The optimization problem is modeled as a semi-Markov decision process and a linear programming (LP) algorithm is formulated to derive the optimal actions to be taken upon each user arrival and channel vacation. The two constraints on the user QoS, the probabilities of user blocking and dropping, are also considered for user satisfaction.

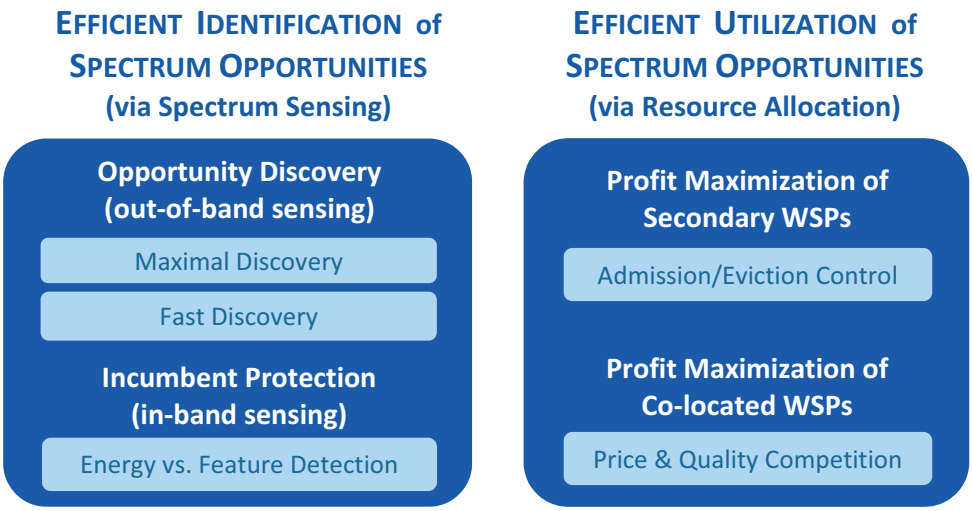

Figure 1.2: An overview of the dissertation.

- **Profit maximization of co-located WSPs via price and quality competition.** We consider co-located WSPs competing against each other to lease the spectrum with the best quality at the spectrum auction and to entice customers with competitive service pricing. The problem is modeled and analyzed using game theory where two WSPs try to find the Nash Equilibrium of their service tariffs and the quality of channels to lease in terms of channel utilization.

Fig. 1.2 shows an overview of the dissertation.

1.5 System Model

This section describes the channel and sensing models used throughout the dissertation, to facilitate understanding of our approaches in the following technical chapters.

1.5.1 Channel Model

In this dissertation, we model a channels as an ON-OFF source where the channel is ON (or busy) if PU signals are present and the channel is OFF (or idle) if PU

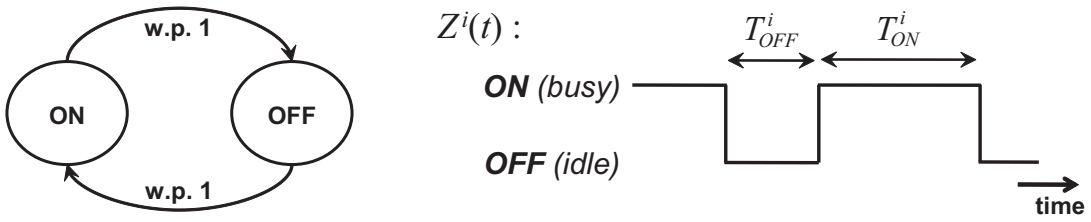

Figure 1.3: Channel model in terms of an ON/OFF alternating renewal process

signals are absent. Hence, SUs can utilize the channel when it is in the OFF state without causing any harmful interference to PUs. This type of channel model has been introduced in [32, 50, 57] where its potential for modeling the channel-usage pattern of PUs was demonstrated.

More formally, we model channel i as an ON-OFF alternating renewal process [20, 68] as illustrated in Fig. 1.3, where we reserve i as the channel index throughout the dissertation. Then, let $Z^i(t)$ denote the state (ON or OFF) of channel i at time t which is given as:

$$Z^i(t) = \begin{cases} 1, & \text{if channel } i \text{ is ON at } t, \\ 0, & \text{otherwise.} \end{cases}$$

The sojourn times of ON and OFF states are represented by random variables T^i_{ON} and T^i_{OFF} with probability density functions (pdfs) $f_{T^i_{ON}}(t)$ and $f_{T^i_{OFF}}(t)$, $t > 0$, respectively. Note that $f_{T^i_{ON}}(t)$ and $f_{T^i_{OFF}}(t)$ can be any distribution functions. In addition, ON (or OFF) periods are independent and identically distributed, and ON and OFF periods are independent of each other.

In addition, we define *channel utilization*, denoted by $u^i \in [0, 1]$, as the fraction of time in which channel i is in ON state, which is determined as

$$u^i = \frac{E[T^i_{ON}]}{E[T^i_{ON}] + E[T^i_{OFF}]}.$$

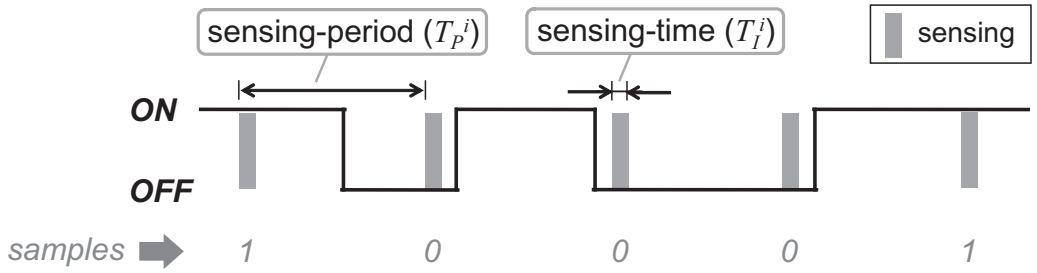

Figure 1.4: Spectrum sensing model with sensing-period T_P^i and sensing-time T_I^i

1.5.2 Sensing Model

Spectrum sensing is akin to the sampling procedure of a given channel process $\{Z^i(t), t \geq 0\}$ since it measures the channel's state at the sensing moment to discover its availability to SUs. Each sensing monitors a channel for a pre-defined amount of time, called *sensing-time* denoted by T_I^i, and detects the presence of PU signals during the moment.

The value of T_I^i is determined to achieve the desired detection performance. For example, in the IEEE 802.22 CR standard [18], spectrum sensing must achieve the false-alarm and mis-detection probabilities less than 0.1 in PU signal detection, for which the minimum duration of T_I^i can be derived. More details on deciding a proper value of T_I^i will be discussed in Chapter IV.

Figure 1.4 illustrates spectrum sensing on an ON/OFF channel with an example of periodic sensing with sensing-period T_P^i. Note, however, that sensing is not necessarily scheduled periodically. As seen in the figure, sensing produces a binary random sequence for each channel because the ON/OFF channel states correspond to the value of $Z^i(t) = 1/0$.

1.6 Organization of the Dissertation

The rest of the dissertation is organized as follows. Chapter II presents maximization of opportunity discovery via out-of-band sensing with optimal sensing-periods, along with ML estimation of ON/OFF channel-usage patterns by PUs. Chapter III proposes an optimal sensing sequence of out-of-band channels to minimize the latency in discovery the necessary amount of opportunities at needed. Chapter IV presents an in-band sensing schedule algorithm with optimal choice of sensing-time and sensing-period, which also selects the better of energy and feature detection. Chapter V presents the problem of maximizing a WSP's profit by using a Semi-Markov Decision Process (SMDP) to derive the optimal admission/eviction control of CR users. Chapter VI discusses price and quality competition between co-located WSPs according to the time-varying spectrum availability. Finally, Chapter VII concludes the dissertation with possible future research directions.

CHAPTER II

OUT-OF-BAND SENSING PART I: MAXIMAL DISCOVERY OF SPECTRUM OPPORTUNITIES

2.1 Introduction

Spectrum sensing is a key building block of the cognitive radio (CR) technology that enables dynamic spectrum access (DSA) in wireless networks by discovering spectrum opportunities and protecting primary users (PUs) from secondary users (SUs) via various signal detection methods. Sensing can be enhanced by the MAC-layer scheduling methods that are essential to enhancing the quality-of-service (QoS) of CR networks (CRNs) and protection of PUs. Therefore, important MAC-layer sensing scheduling issues will be discussed in the first three technical chapters, starting from this chapter. This chapter, in particular, focuses on an important issue of sensing scheduling: how to maximally discover opportunities residing in the licensed channels for a CRN.

When a CRN has a limited bandwidth requirement, it would suffice to discover a necessary number of idle channels and stay with the channels without searching for more idle channels until one of the in-band channels is re-claimed by its PUs. In this case, sensing is performed on demand only when channel vacation occurs, and thus

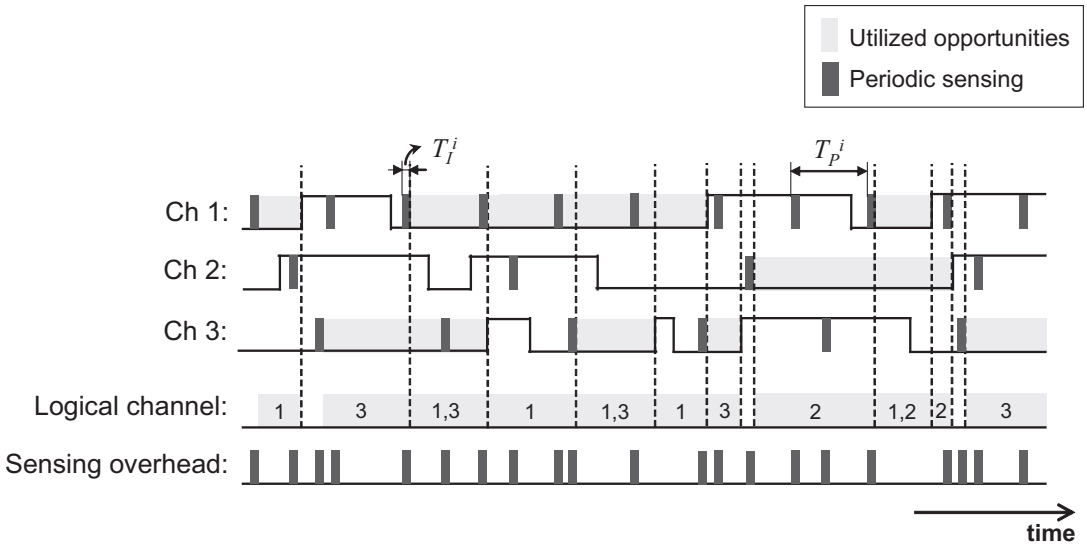

Figure 2.1: An example of periodic sensing

this type of sensing is called *reactive sensing*. On the contrary, a CRN may want to seek more bandwidth than just staying with a few in-band channels. By discovering as many in-band channels as possible, the SUs in a CRN may transmit packets at a higher data rate due to the larger capacity. To discover more idle channels, sensing is performed proactively even without channel vacation, which is called *proactive sensing*. In this chapter, we study proactive sensing with an emphasis on how we can maximize discovery of opportunities by sensing out-of-band channels. However, the issues in reactive sensing will be also discussed later in Chapter III.

To discover more idle channels, we consider periodic sensing of out-of-band channels where each channel has its own sensing-period T_P^i. Any idle channel discovered by the periodic sampling becomes a new in-band channel which then can provide more bandwidth. Although the periodic sensing is performed on every channel independently, the concurrent sensing of N channels must be scheduled in such a way that there would be no other scheduled sensing while a measurement on channel i is being performed for T_I^i seconds. An example of periodic sensing is shown in

Figure 2.1.

In general, more frequent sensing discovers more opportunities. However, one has to account for the fact that each sensing costs a SU T_I^i time units without any packet transmission on the discovered opportunities since there is only a single antenna for both sensing and transmission. Hence, there is a tradeoff between *sensing-time overhead* and *discovery of opportunities*. In Section 2.4, we propose a sensing-period optimization for the proactive sensing by making the tradeoff between the discovered opportunities and the sensing overhead.

The sensing-period optimization approach depends on the underlying channel-usage patterns which we model as ON-OFF alternating processes. Hence, the key is to estimate distribution parameters of ON/OFF periods to formulate our objective functions. Section 2.5 introduces a maximum likelihood (ML) estimation procedure that can estimate and track time-varying channel parameters.

2.1.1 Contributions

Our contribution in this chapter is two-fold. First, we propose in Section 2.4 an optimal sensing-period mechanism that maximizes the discovered and utilized amount of spectrum opportunities by considering the tradeoff between discovery of opportunities and interruption of discovered opportunities. Exploiting the properties of the renewal process, the optimal sensing-periods are derived for generally-distributed ON/OFF periods. Second, we introduce in Section 2.5 an ML estimation technique of the unknown and time-varying channel parameters based on the channel-state samples produced by sensing. Confidence intervals of the proposed estimators are also derived and the impact of the length of ON/OFF periods is discussed.

2.1.2 Organization

The rest of the chapter is organized as follows. Section 2.2 briefly overviews related work, and Section 2.3 presents our network model and assumptions. Section 2.4 presents the sensing-period optimization technique to achieve maximum discovery of opportunities. Section 2.5 introduces the channel-usage pattern estimation method. The MATLAB-based simulation results are presented and analyzed in Section 2.6. Example deployment scenarios of the proposed schemes are discussed in Section 2.7. Finally, we conclude the chapter in Section 2.8.

2.2 Related Work

There have been a limited number of publications on the MAC-layer sensing. The authors of [14] proposed a proactive sensing algorithm with non-adaptive and randomly-chosen sensing periods, in which they did not consider how to maximize discovery of opportunities. [99] proposed a Decentralized Cognitive MAC (DC-MAC) with reactive sensing focusing on slotted-time CSMA-based channel access with synchronized slot information. [71] proposed an Ad-hoc Secondary system MAC (AS-MAC) which is a proactive scheme with slotted-time-based channel access. [99] and [71], however, did not consider the inherent tradeoff between sensing overhead and discovery of opportunities. Although [54] pointed out the impact of number of samples on confidence of estimation, it did not recognize the importance of the upper-bound approach in adapting sensing-periods as discussed in Section 2.5.

2.3 System Model

2.3.1 Network Topology

A group of SUs is assumed to form a single-hop CRN within the transmission range of which there are no other CRNs interfering or cooperating with that CRN. In a practical CRN, however, such as an IEEE 802.22 network [1], the interference among adjacent CRNs should be dealt with in the context of inter-network coordination of channel sensing and allocation. Although the coordination issue is not the main focus of this chapter, our proposed scheme can coexist with any coordination scheme by dynamically adapting the pool of available channels for a CRN in such a way that those channels are not used simultaneously by other CRNs.

Every SU in the CRN is assumed to be equipped with a single identical antenna which can be tuned to any combination of N consecutive licensed channels. This can be done by the Orthogonal Frequency Division Multiplexing (OFDM) technique with adaptive and selective allocation of OFDM sub-carriers to utilize any subset of N licensed channels at the same time [14, 47, 64]. Note that equipping each SU with more than one antenna might cause severe interference among its antennas, thus degrading the SU's performance [49]. We, therefore, focus on SUs, each equipped with a single antenna. Each SU works as a transceiver as well as a sensor in its CRN.

2.3.2 Channel and Sensing Model

We follow the channel and sensing model introduced in Chapter I. Each sensing performs signal detection to identify signals from PUs, where energy and feature detections are two prominent PHY-sensing schemes. It is assumed that all SUs in a CRN should participate in sensing a channel at the same time for each scheduled measurement, which is known as *collaborative sensing*. Collaborative sensing exploits

location diversity of multiple nearby sensors and enhances detection performance of PU signals in terms of mis-detection and false-alarm probabilities [31,34,94] even in fading/shadowing environments. Since collaborative sensing itself is not our major focus, we will use a simple collaboration policy of letting all SUs participate in simultaneously sensing a channel, as a baseline study.

In collaborative sensing, the sample of a channel collected by a SU must be shared/synchronized with other SUs so that each SU can decide on the channel's availability. The authors of [34] introduced a simple rule (OR-rule) in which a channel is considered ON if at least one SU reports that the channel is busy. Since the cooperation among SUs is not a focus of this chapter, we assume the sensing-time T_I^i includes both PHY-layer detection time (e.g., 1 ms for energy detection [18]) and data synchronization time in collaborative sensing.

2.3.3 Opportunity-Usage Model

Whenever sensing is performed on a channel and an opportunity on the channel is discovered, the channel is merged into a pool of available channels where the pool is called a *logical channel*. Therefore, a logical channel can include $0 \sim N$ licensed channels depending on their availability at that instant. The logical channel is treated as if it were a single channel whose capacity is equal to the sum of all licensed channels merged into it. This can be done by using the OFDM technique with selective allocation of sub-carriers to the channels to be utilized [14,47,64]. In this way, more than one (possibly non-adjacent) channels in the logical channel can be simultaneously utilized by SUs.

Return of PUs to an in-band channel should be detected promptly to minimize interference on them. This can be done by in-band sensing which will be actively

discussed in Chapter IV. Hence, we assume returning PUs can be detected within a reasonably small amount of time so that the channel can be vacated by SUs promptly. To vacate the channel due to returning PUs, OFDM should reconfigure sub-carriers to exclude the channel band from usage.

2.4 Maximal Discovery of Opportunities by Optimizing Sensing-Period

When proactive sensing is employed by a CRN and each channel is sensed periodically with its own sensing-period, we would like to optimize the set of N sensing-periods (T_P^i's) to maximize the discovery of opportunities.

Since sensing is nothing but a sampling process, it is not possible to exactly identify each state transition between ON and OFF periods. Hence, the time portion of a discovered OFF period between the start-time and the discovery-time of the OFF period cannot be utilized. In addition, some OFF periods may remain undiscovered at all if sensing is infrequent. However, blindly increasing the sensing frequency is not desirable, as it will increase the sensing overhead, which is proportional to the sum of (T_I^i/T_P^i). Note that the sensing overhead is the time-overhead during which all data traffic among SUs must be suspended to measure a channel's availability. This tradeoff must be captured in the construction of an equation to find the optimal sensing frequencies/periods. So, for each channel i we define two mathematical terms, $UOPP^i(T_P^i)$ (*Unexplored Opportunity*) and $SSOH^i(\mathbf{T_P})$ (*Sensing Overhead*) where $\mathbf{T_P} = (T_P^1, T_P^2, \ldots, T_P^N)$. $UOPP^i(T_P^i)$ is defined as the average fraction of time during which channel i's opportunities are not discovered, in case the channel i is being periodically sensed with its sensing-period T_P^i. On the other hand, $SSOH^i(\mathbf{T_P})$ is defined as the average fraction of time during which channel i's discovered op-

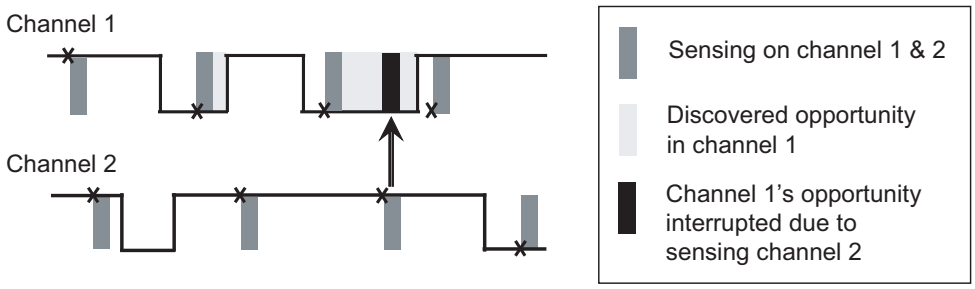

Figure 2.2: The concept of $SSOH^i$: channel 1's discovered opportunity cannot be utilized during sensing of channel 2

portunities are interrupted and not utilized due to sensing of one of N channels. An already-discovered opportunity within a channel will be interrupted by sensing because we assumed: (i) a SU is equipped with a single antenna, and (ii) all SUs in the CRN must participate in sensing a channel. That is, the SUs must suspend use of a discovered channel when it senses other channels, since data transmission and sensing cannot take place at the same time with one antenna. This situation is depicted in Figure 2.2.

Since u^i is defined as the average fraction of time channel i is busy, the average sum of opportunities per unit time is given as $(1 - u^i)$. Our objective function is then to find optimal sensing-periods of N channels, such that

$$\begin{aligned} \mathbf{T_P}^* &= \arg\max_{\mathbf{T_P}} \left\{ \sum_{i=1}^{N} \{(1-u^i) - SSOH^i(\mathbf{T_P}) - UOPP^i(T_P^i)\} \right\} \\ &= \arg\min_{\mathbf{T_P}} \left\{ \sum_{i=1}^{N} \{SSOH^i(\mathbf{T_P}) + UOPP^i(T_P^i)\} \right\} \end{aligned} \tag{2.1}$$

where $\mathbf{T_P}^* = (T_P^{1*}, \ldots, T_P^{N*})$ is a vector of optimal sensing-periods. As a boundary condition of T_P^i, $\sum_{i=1}^{N} \frac{T_I^i}{T_P^i} < 1$ should be satisfied, providing a lower-bound of T_P^i.

2.4.1 Analysis of $UOPP^i(T_P^i)$

We define $T_d^i(t)$ $(d = 0, 1)$ as the average of opportunities (measured in time units) on channel i during $(t_s,\ t_s + t)$, provided a sample d is collected at time t_s.

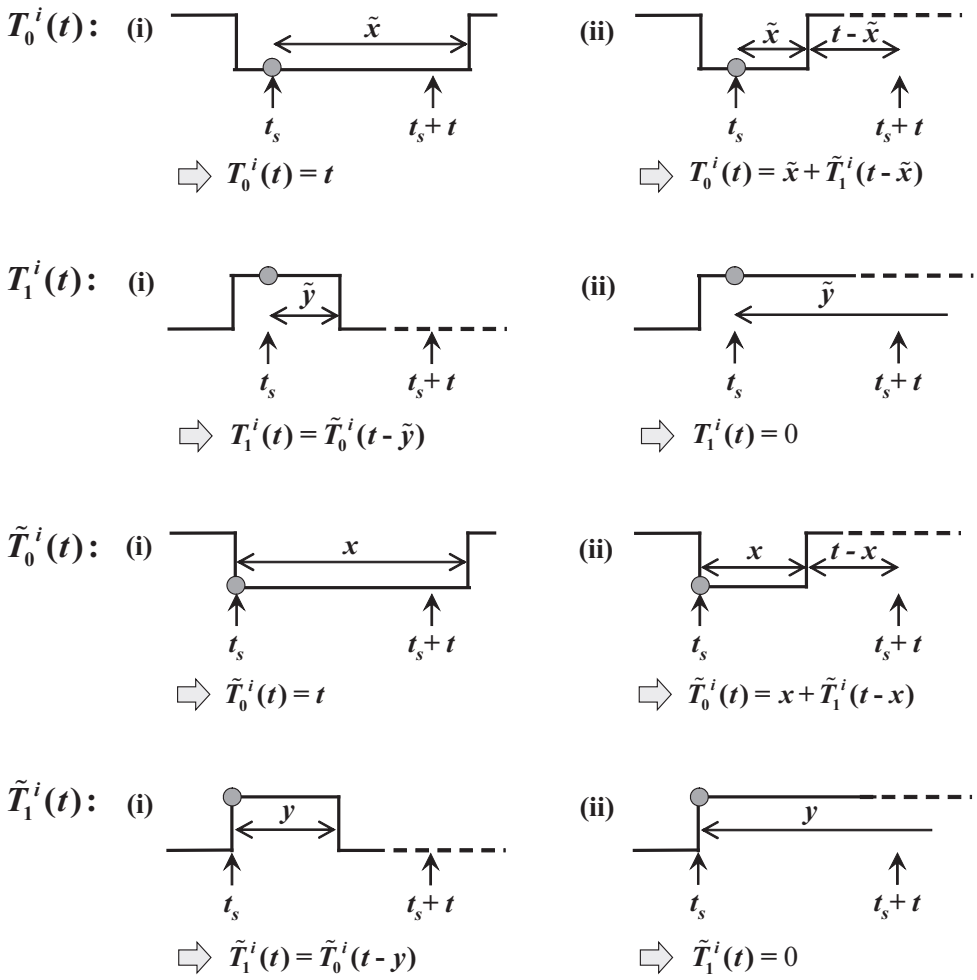

Figure 2.3: Illustration of $T_0^i(t)$, $T_1^i(t)$, $\tilde{T}_0^i(t)$ and $\tilde{T}_1^i(t)$ - $\tilde{x}/\tilde{y}$ denotes the remaining time in the current OFF/ON period starting from t_s. In case the state transition occurs at t_s, x/y is used instead of $\tilde{x}/\tilde{y}$.

In case the state transition (ON→OFF or OFF→ON) occurs at t_s, $\tilde{T}_d^i(t)$ (instead of $T_d^i(t)$) is used to denote the same metric. Possible scenarios of those four functions $T_0^i(t)$, $T_1^i(t)$, $\tilde{T}_0^i(t)$ and $\tilde{T}_1^i(t)$ are illustrated in Figure 2.3. Note that $T_d^i({T_P}^i)$ implies the average amount of channel availability between two consecutive samples in case the first sample is d.

According to the renewal theory, for an alternating renewal process which has been started a long time ago, the remaining time $\tilde{x}$ in the current state (say, OFF

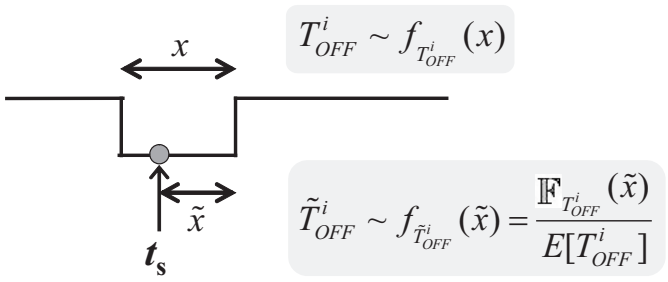

Figure 2.4: The density function of the remaining time in the current OFF period

state) from the sampling time t_s has its p.d.f. of $\mathbb{F}_{T^i_{OFF}}(\tilde{x})/E[T^i_{OFF}],\ \tilde{x} > 0$ [20, 68], where $\mathbb{F}_{T^i_{OFF}}(\tilde{x}) = 1 - F_{T^i_{OFF}}(\tilde{x})$ and $F_{T^i_{OFF}}(\tilde{x})$ is the c.d.f. of the OFF period. This is illustrated in Figure 2.4, where $\tilde{T}^i_{OFF}$ is a random variable of the remaining time in the OFF period. Similarly, the p.d.f. of the remaining time in ON state from t_s is given as $\mathbb{F}_{T^i_{ON}}(\tilde{y})/E[T^i_{ON}],\ \tilde{y} > 0$.

Since these are asymptotic pdfs, application of the pdfs produces approximate solutions. However, using the asymptotic pdfs helps us to analyze the problem even with generally distributed ON/OFF periods, not just for exponentially distributed ones. The impact of such approximation will be evaluated in Chapter V, where it will turn out that our approximation technique is very effective to model the general renewal channels with reasonably small errors.

Using the above facts, we can derive the following equations:

$$
\begin{aligned}
T^i_0(t) &= t\int_t^\infty \frac{\mathbb{F}_{T^i_{OFF}}(x)}{E[T^i_{OFF}]}dx + \int_0^t \frac{\mathbb{F}_{T^i_{OFF}}(x)}{E[T^i_{OFF}]}\left(x + \tilde{T}^i_1(t-x)\right)dx,\\
T^i_1(t) &= \int_0^t \frac{\mathbb{F}_{T^i_{ON}}(y)}{E(T^i_{ON})}\tilde{T}^i_0(t-y)dy,\\
\tilde{T}^i_0(t) &= t\int_t^\infty f_{T^i_{OFF}}(x)dx + \int_0^t f_{T^i_{OFF}}(x)\left(x + \tilde{T}^i_1(t-x)\right)dx,\\
\tilde{T}^i_1(t) &= \int_0^t f_{T^i_{ON}}(y)\tilde{T}^i_0(t-y)dy.
\end{aligned}
$$

By performing the Laplace transform, we get

$$T_0^{i*}(s) = \{\mathbb{F}_{X^i}{}^*(0) - \mathbb{F}_{X^i}{}^*(s)\} / \left\{E[T_{OFF}^i] \cdot s^2\right\} + \mathbb{F}_{X^i}{}^*(s)\tilde{T}_1^{i*}(s)/E[T_{OFF}^i],$$

$$T_1^{i*}(s) = \mathbb{F}_{T_{ON}^i}{}^*(s)\tilde{T}_0^{i*}(s)/E[T_{ON}^i],$$

$$\tilde{T}_1^{i*}(s) = f_{T_{ON}^i}{}^*(s)\tilde{T}_0^{i*}(s),$$

$$\tilde{T}_0^{i*}(s) = \left\{f_{T_{OFF}^i}{}^*(0) - f_{T_{OFF}^i}{}^*(s)\right\} / s^2 + f_{T_{OFF}^i}{}^*(s)\tilde{T}_1^{i*}(s).$$

Hence it leads to:

$$T_0^{i*}(s) = \frac{1}{E[T_{OFF}^i] \cdot s^2} \cdot \left[\mathbb{F}_{T_{OFF}^i}^*(0) - \mathbb{F}_{T_{OFF}^i}^*(s) \cdot \frac{1 - f_{T_{OFF}^i}^*(0) f_{T_{ON}^i}^*(s)}{1 - f_{T_{OFF}^i}^*(s) f_{T_{ON}^i}^*(s)}\right],$$

$$T_1^{i*}(s) = \frac{\mathbb{F}_{T_{ON}^i}^*(s)}{E(T_{ON}^i) \cdot s^2} \cdot \frac{f_{T_{OFF}^i}^*(0) - f_{T_{OFF}^i}^*(s)}{1 - f_{T_{OFF}^i}^*(s) f_{T_{ON}^i}^*(s)}.$$

Now, we develop an expression of $UOPP^i(T_P^i)$ in terms of $T_0^i(t)$ and $T_1^i(t)$.[1] A new term $UOPP_{(d)}^i(T_P^i)$ is defined as the average fraction of time during which usable opportunities are not discovered between two consecutive samples in case the first sample is d. Then, $UOPP^i(T_P^i) = (1 - u^i) \cdot UOPP_{(0)}^i(T_P^i) + u^i \cdot UOPP_{(1)}^i(T_P^i)$.[2]

In case $d = 1$ is collected at time t_s, opportunities existing in $(t_s, t_s + T_P^i)$ cannot be discovered since there is no more sensing between two sampling times t_s and $t_s + T_P^i$. Since the amount of opportunities in $(t_s, t_s + T_P^i)$ is given as $T_1^i({T_P}^i)$,

$$UOPP_{(1)}^i(T_P^i) = \left[\frac{T_1(T_P^i)}{T_P^i}\right].$$

In case $d = 0$ is collected at time t_s, the opportunity discovered at t_s starts to be utilized until PUs' return. If the OFF period lasts more than T_P^i after t_s, there will not be any unexplored portion of opportunities in $(t_s, t_s + T_P^i)$. On the contrary, if PUs emerge at t_e $(t_s < t_e < t_s + T_P^i)$, any opportunities in $(t_e, t_s + T_P^i)$ could not be

[1] Note that $\tilde{T}_d^i(t)$ can be derived from $T_d^i(t)$.

[2] Note that a channel is assumed to be in its equilibrium state, and in such a case, u^i is the probability that a sample 1 is collected from channel i at a random time point [20, 68].

explored since the next sampling time is $t_s + T_P^i$. Hence,

$$UOPP_{(0)}^i(T_P^i) = \frac{1}{T_P^i}\int_0^{T_P^i} \frac{\mathbb{F}_{T_{OFF}^i}(x)}{E[T_{OFF}^i]} \tilde{T}_1^i(T_P^i - x)dx$$

which completes the derivation of $UOPP^i(T_P^i)$.

Two examples of $UOPP^i(T_P^i)$ are introduced here. In case channel i's ON/OFF periods are Erlang-distributed, we have

$$\begin{aligned} &f_{T_{OFF}^i}(x) = xe^{-x}, \;\; f_{T_{ON}^i}(y) = ye^{-y} \;\; (x, y > 0), \\ &UOPP^i(T_P^i) = \frac{1}{2} - \frac{3}{4T_P^i} + \frac{e^{-T_P^i}}{4}\left(\frac{3}{T_P^i} + 1\right). \end{aligned} \tag{2.2}$$

On the other hand, for exponentially-distributed ON/OFF periods, we have

$$\begin{aligned} &f_{T_{OFF}^i}(x) = \lambda_{T_{OFF}^i} e^{-\lambda_{T_{OFF}^i} x} \;\; (x > 0), \;\; f_{T_{ON}^i}(y) = \lambda_{T_{ON}^i} e^{-\lambda_{T_{ON}^i} y} \;\; (y > 0), \\ &UOPP^i(T_P^i) = (1 - u^i) \cdot \left\{1 - \frac{1 - e^{-\lambda_{T_{OFF}^i} {T_P}^i}}{\lambda_{T_{OFF}^i} {T_P}^i}\right\}. \end{aligned} \tag{2.3}$$

These results are reasonable in the sense that $\lim_{{T_P}^i \to \infty} UOPP^i(T_P^i) = 1 - u^i$. As ${T_P}^i \to \infty$, no opportunity is discovered since no sensing will be performed. Therefore, $UOPP^i(T_P^i)$ becomes $(1 - u^i)$.

2.4.2 Analysis of $SSOH^i(\mathbf{T_P})$

As defined earlier, $SSOH^i(\mathbf{T_P})$ is the average fraction of time during which channel i's discovered opportunities cannot be utilized due to sensing of N channels. To express $SSOH^i(\mathbf{T_P})$ mathematically, we introduce a concept of *observed channel-usage pattern*. Since a channel's ON-OFF usage pattern is partially observed by SUs via sensing at discrete-time points, the exact renewal times (i.e., state transition times such as ON $\rightarrow$ OFF or OFF $\rightarrow$ ON) cannot be observed by SUs. Instead, we use *observed* ON-OFF pattern of channel i to derive $SSOH^i(\mathbf{T_P})$. In the observed ON-OFF model, a channel's OFF period starts when the OFF period is discovered.

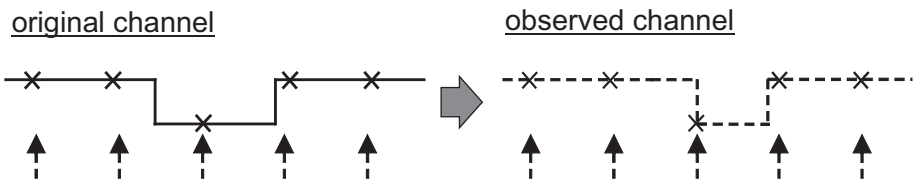

Figure 2.5: The observed channel-usage pattern model

Once an OFF period is discovered, however, the next state transition to the following ON period is assumed to be recognized via the Listen-before-Talk policy. Figure 2.5 illustrates the concept of the new model. This model's channel utilization is called *modified* channel utilization, denoted by $\tilde{u}^i$, which is given as $\tilde{u}^i = u^i + UOPP^i(T_P^i)$.

Using the new model, $SSOH^i(\mathbf{T_P})$ can be derived as

$$SSOH^i(\mathbf{T_P}) = (1 - \tilde{u}^i) \sum_{j=1}^{N} \left(\frac{T_I^j}{T_P^j} \right).$$

In the above equation of $SSOH^i(\mathbf{T_P})$, $(1 - \tilde{u}^i)$ implies the time fraction in which channel i's opportunities are discovered. The reason for using $\tilde{u}^i$ instead of u^i is that $SSOH^i$ is only concerned with the *discovered* portion of OFF periods by its definition. The second term $\sum_{j=1}^{N} \left(\frac{T_I^j}{T_P^j} \right)$ means the cumulative sensing overhead due to sensing on N channels.

2.4.3 Sensing-Period Optimization Algorithm

Based on the derived expressions of $UOPP^i(T_P^i)$ and $SSOH^i(\mathbf{T_P})$, the optimal sensing periods can be determined by solving Eq. (2.1).

2.5 Channel-Parameter Estimation

The estimation of the underlying channel-usage patterns is important to the proposed sensing-period optimization approach, since its solution is expressed with the unknown channel parameters. Therefore, we introduce an ML estimation technique

to estimate the time-varying distribution parameters of an ON/OFF alternating renewal channel.

2.5.1 Maximum Likelihood (ML) Estimators

Suppose we have a vector of r^i samples from channel i, $\mathbf{Z^i} = (Z^i_{t_1}, Z^i_{t_2}, \ldots, Z^i_{t_{r^i}})$, where t_j $(j = 1, \ldots, r^i)$ denotes the timestamp of sample $Z^i_{t_j}$. Suppose the density functions of ON and OFF periods are m-variate, then a total of $2m$ parameters should be estimated. On the other hand, the joint probability mass function of r^i samples can be expressed with 4 types of transition probabilities (0→0, 0→1, 1→0, 1→1) as follows:

$$\begin{aligned}
\theta^{\mathbf{i}} &= (\theta^i_1, \ldots, \theta^i_{2m}), \\
L(\theta^{\mathbf{i}}) &= P(\mathbf{Z^i}; \theta^{\mathbf{i}}) = \Pr(Z^i_{t_1} = z_1; \theta^{\mathbf{i}}) \cdot \prod_{k=2}^{r^i} \Pr(Z^i_{t_k} = z_k | Z^i_{t_{k-1}} = z_{k-1}; \theta^{\mathbf{i}}) \\
&= \Pr(Z^i_{t_1} = z_1; \theta^{\mathbf{i}}) \prod_{k=2}^{r^i} P^i_{z_{k-1} z_k}(t_k - t_{k-1}; \theta^{\mathbf{i}})
\end{aligned}$$

where the Markovian property has been applied. $P^i_{z_{k-1} z_k}(t_k - t_{k-1})$ denotes the probability that a sample z_{k-1} is followed by a sample z_k and the inter-sample-collection time is $t_k - t_{k-1}$. Then, the estimates of parameters of ON/OFF density functions can be found by maximum likelihood estimation, such as

$$\frac{\partial ln L(\theta^{\mathbf{i}})}{\partial \theta^i_l} = 0, \;\; l = 1, \ldots, 2m.$$

Now, the remaining task is to express the likelihood function in a mathematical form. The first component of the likelihood function is given as $\Pr(Z^i_{t_1} = z_1; \theta^{\mathbf{i}}) = (u^i)^{z_1}(1 - u^i)^{1 - z_1}$ since u^i is the probability that channel i is busy (i.e., ON) at a random time (t_1 in this case). Note that the estimator of u^i is simply given as the sample mean of r^i samples.

Another part of the likelihood function is $P^i_{z_{k-1}z_k}(t_k - t_{k-1}; \theta^{\mathbf{i}})$, which is one of four transition probabilities: $P^i_{00}(t_k - t_{k-1}), P^i_{01}(t_k - t_{k-1}), P^i_{10}(t_k - t_{k-1})$ and $P^i_{11}(t_k - t_{k-1})$. The renewal theory [20] suggests that $P^i_{11}(\Delta)$, $\Delta = t_k - t_{k-1}$, is expressed as

$$P^i_{11}(\Delta) = \int_{\Delta}^{\infty} \frac{\mathbb{F}_{T^i_{ON}}(u)}{E[T^i_{ON}]} du + \int_0^{\Delta} h^i_{10}(u) \mathbb{F}_{T^i_{ON}}(\Delta - u) du \tag{2.4}$$

where $h^i_{10}(u)$ is the renewal density of OFF state given that the renewal process started from ON state. It is proven in [20] that $h^{i*}_{10}(s)$ is expressed as

$$h^{i*}_{10}(s) = \frac{f^*_{T^i_{OFF}}(s) \left\{1 - f^*_{T^i_{ON}}(s)\right\}}{E[T^i_{ON}] \cdot s \left\{1 - f^*_{T^i_{ON}}(s) f^*_{T^i_{OFF}}(s)\right\}}.$$

By applying the Laplace transform, Eq. (2.4) becomes

$$P^{i*}_{11}(s) = \frac{1}{s} - \frac{\left\{1 - f^*_{T^i_{ON}}(s)\right\} \left\{1 - f^*_{T^i_{OFF}}(s)\right\}}{E[T^i_{ON}] \cdot s^2 \left\{1 - f^*_{T^i_{ON}}(s) f^*_{T^i_{OFF}}(s)\right\}}.$$

Similarly, $P^i_{00}(\Delta)$ can be easily derived by switching the role of state ON and OFF such as

$$P^{i*}_{00}(s) = \frac{1}{s} - \frac{\left\{1 - f^*_{T^i_{OFF}}(s)\right\} \left\{1 - f^*_{T^i_{ON}}(s)\right\}}{E[T^i_{OFF}] \cdot s^2 \left\{1 - f^*_{T^i_{OFF}}(s) f^*_{T^i_{ON}}(s)\right\}}.$$

Finally, $P^i_{10}(\Delta)$ and $P^i_{01}(\Delta)$ can be derived by using the following relationship: $P^i_{10}(\Delta) = 1 - P^i_{11}(\Delta)$ and $P^i_{01}(\Delta) = 1 - P^i_{00}(\Delta)$.

For example, for a channel with exponentially-distributed ON/OFF periods as shown in Eq. (2.3), transition probabilities are given as

$$\begin{aligned}
P^i_{00}(t) &= (1 - u^i) + u^i \cdot e^{-(\lambda_{T^i_{OFF}} + \lambda_{T^i_{ON}})t}, \\
P^i_{01}(t) &= u^i - u^i \cdot e^{-(\lambda_{T^i_{OFF}} + \lambda_{T^i_{ON}})t}, \\
P^i_{11}(t) &= u^i + (1 - u^i) \cdot e^{-(\lambda_{T^i_{OFF}} + \lambda_{T^i_{ON}})t}, \\
P^i_{10}(t) &= (1 - u^i) - (1 - u^i) \cdot e^{-(\lambda_{T^i_{OFF}} + \lambda_{T^i_{ON}})t}.
\end{aligned} \tag{2.5}$$

Then, there are two parameters to be estimated: $\lambda_{T^i_{OFF}}$ and $\lambda_{T^i_{ON}}$. Since $u^i = \frac{E[T^i_{ON}]}{E[T^i_{ON}]+E[T^i_{OFF}]} = \frac{\lambda_{T^i_{OFF}}}{\lambda_{T^i_{ON}}+\lambda_{T^i_{OFF}}}$, we can estimate $\lambda_{T^i_{OFF}}$ and u^i, instead of $\lambda_{T^i_{OFF}}$ and $\lambda_{T^i_{ON}}$.

As already discussed, the estimator of u^i is given as

$$\hat{u}^i = \frac{1}{r^i}\sum_{k=1}^{r^i} Z^i_{t_k}.$$

On the other hand, the estimator of $\lambda_{T^i_{OFF}}$ can be derived by solving the equation $\partial lnL(\theta)/\partial\lambda_{T^i_{OFF}} = 0$, yielding

$$\hat{\lambda}_{T^i_{OFF}} = -\frac{u^i}{T^i_P} ln\left[\frac{-B+\sqrt{B^2-4AC}}{2A}\right],$$

where

$$\begin{cases} A = (u^i - (u^i)^2)(r^i - 1), \\ B = -2A + (r^i - 1) - (1-u^i)n_0 - u^i \cdot n_3, \\ C = A - u^i \cdot n_0 - (1-u^i)n_3. \end{cases}$$

Note that $n_0/n_1/n_2/n_3$ indicates the number of 0→0/0→1/1→0/1→1 transitions from the total of $(r^i - 1)$ transitions among r^i samples. For instance, in case a sequence of samples is given as (0,1,1,1,0,1,1,0), $r^i = 8$, we have $n_0 = 0, n_1 = 2, n_2 = 2, n_3 = 3$.

2.5.2 Confidence Interval of Estimators

It is also important to understand how much one can have confidence in the derived estimators. The confidence interval is an efficient measure to determine the level of confidence. In most cases, however, it is not easy, or sometimes impossible to derive the confidence interval in a closed form with generally-formed density functions of ON/OFF periods. Here, we show derivation of confidence intervals with exponentially-distributed ON/OFF periods.

Confidence interval of $\hat{u}^i$

When channel i is periodically sensed at an interval T_P^i, the difference between any two timestamps $Z_{t_{k_1}}$ and $Z_{t_{k_2}}$ ($k_1, k_2 \in \{1, 2, \ldots, r^i\}$) is an integer multiple of T_P^i. In such a case, the correlation coefficient of any two samples $Z_{t_{k_1}}$ and $Z_{t_{k_2}}$ ($k_1 > k_2$) is found to be

$$\begin{aligned} E[Z_{t_{k_1}} Z_{t_{k_2}}] &= \Pr(Z_{t_{k_1}} = 1 | Z_{t_{k_2}} = 1) \Pr(Z_{t_{k_2}} = 1) = P_{11}^i(|k_1 - k_2| \cdot T_P^i) \cdot u^i \\ \Rightarrow \rho_{k_1 k_2} &= \frac{E[Z_{t_{k_1}} Z_{t_{k_2}}] - (u^i)^2}{u^i - (u^i)^2} = e^{-(\lambda_{T_{OFF}^i}/u^i) \cdot |k_1 - k_2| T_P^i}. \end{aligned} \tag{2.6}$$

This shows that the correlation is decaying fast (exponentially) as the separation of two sampling times becomes large. Since the rate of decrease is proportional to $(\lambda_{T_{OFF}^i}/u^i)T_P^i$, r^i samples can be assumed to be weakly-correlated as r^i are large unless $(\lambda_{T_{OFF}^i}/u^i)T_P^i$ is close to 0. Using this fact, we can derive the confidence interval. When $(\lambda_{T_{OFF}^i}/u^i)T_P^i$ is not close to 0, $\frac{\overline{Z^i} - E[\overline{Z^i}]}{\sqrt{\text{var}[\overline{Z^i}]}} \to N(0,1)$ as $r^i \to \infty$ by the Central Limit Theorem.[3] Hence, $100(1-\alpha)(\%)$ confidence interval is given as

$$\left[\overline{Z^i} - \sqrt{\text{var}[\overline{Z^i}]} \cdot N^{-1}(1 - \alpha/2), \overline{Z^i} + \sqrt{\text{var}[\overline{Z^i}]} \cdot N^{-1}(1 - \alpha/2) \right].$$

where $\text{var}[\overline{Z^i}]$ is a function of r^i. If $\beta \equiv \sqrt{\text{var}[\overline{Z^i}]} \cdot N^{-1}(1 - \alpha/2)$, r^i can be related to the level α of confidence with the interval length of 2β. In general, we need more samples (i.e., bigger r^i) to achieve a higher level of confidence (i.e., smaller α or β).

Confidence interval of $\hat{\lambda}_{T_{OFF}^i}$

The ML estimator of $\lambda_{T_{OFF}^i}$ has already shown. Unfortunately, the high non-linearity of $\hat{\lambda}_{T_{OFF}^i}$ makes it difficult to find its exact confidence interval. Instead, an upper bound of T_P^i could be derived to ensure a reasonable level of confidence. Note that each of four transition probabilities tends to converge to a constant (u^i or

[3] $\overline{Z^i}$ is the sample mean of $\mathbf{Z^i} = (Z_{t_1}^i, Z_{t_2}^i, \ldots, Z_{t_{r^i}}^i)$.

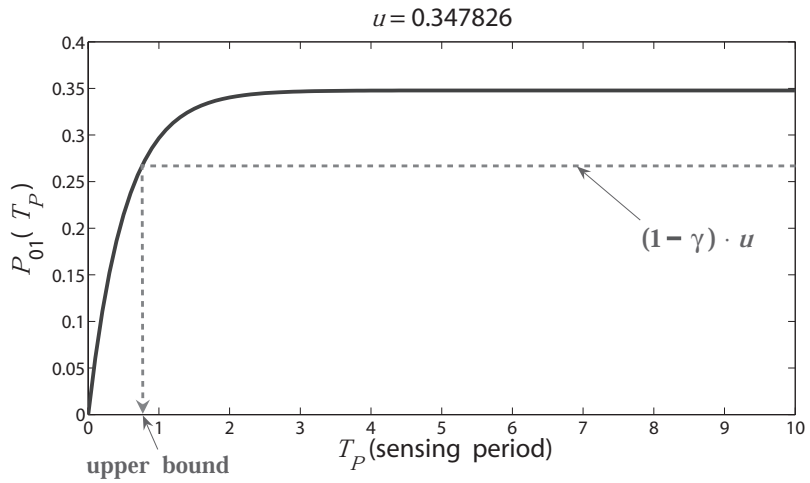

Figure 2.6: The graph of $P_{01}^i(T_P^i)$ and upper bound of T_P^i

$1-u^i$), as T_P^i goes to infinity. Since $lnL(\theta^{\mathbf{i}})$ is expressed with transition probabilities, an ML estimator cannot guarantee accurate estimation with a large T_P^i with which the likelihood function tends to be a constant. Hence we will bound the value of $P_{01}^i(T_P^i)$ below a certain threshold $(1-\gamma)u^i$ to ensure the probability would not be too close to its limit. This concept is shown in Figure 2.6. Then, an upper bound of T_P^i can be derived as

$$|u^i - P_{01}^i(T_P^i)| \geq \gamma \times u^i \;\; \Rightarrow \;\; T_P^i \leq \frac{u^i}{\lambda_{T_{OFF}^i}} ln\left(\frac{1}{\gamma}\right).$$

Hence, the optimal sensing-period in Section 2.4 should be determined subject to the constraint of the upper bound of T_P^i given here.

Discussion

We can apply the same intuition derived from the case of exponentially-distributed ON/OFF periods to general distributions. First, upon estimation of channel utilization u^i, the more samples are given, the more accurate estimates. On the other hand, if we want to estimate $E[T_{OFF}^i]$ and $E[T_{ON}^i]$, it is important to upper-bound T_P^i so that a sufficient number of samples would be collected within each OFF/ON period.

If T_P^i increases, both $E[T_{OFF}^i]$ and $E[T_{ON}^i]$ will be over-estimated, as many OFF/ON periods would be missed by the sensing. So, the number of samples and sensing frequency are two important factors that control the confidence level of estimation.

2.5.3 Estimation on Time-Varying Channels

The ON-OFF patterns of licensed channels are often time-varying, implying that the parameter estimation must be adaptive in time. Here we assume that the channel parameters of ON/OFF periods are slowly time-varying so that the SUs can track their variations by using a moving time-window in collecting samples and making estimation. That is, channel i's sensing results (binary samples) are preserved for those whose sampling timestamps are no older than T_{window}^i, where T_{window}^i indicates the time-window size of channel i. The estimation procedure must be executed frequently enough to track the variation of parameters. As an extreme case, new estimates might be produced every time when a new sample is collected from a channel, although it may incur high processing cost. Therefore, in Section 2.6, we compute estimates once every $T_{estimation}$ seconds, which is much smaller than T_{window}^i. Note that whenever new estimates are computed, the optimal sensing periods derived in Section 2.4 must be re-calculated and adapted accordingly.

2.6 Performance Evaluation

2.6.1 Simulation Setup

To measure the effectiveness of the proposed schemes, we define a performance metric called *Achieved Opportunity Ratio* (AOR). AOR measures the ratio of the total discovered spectrum availability to the total existing availability. This metric will show the efficiency of the proposed sensing-period optimization in terms of the percentage of total opportunities it can discover. Ideally, if all estimates are perfect,

AOR will be as high as

$$AOR_{max} = \frac{\sum_{i=1}^{N} \left\{(1-u^i) - SSOH^i(\mathbf{T}_\mathbf{P}^*) - UOPP^i(T_P^{i\,*})\right\}}{\sum_{i=1}^{N}(1-u^i)}$$

where the numerator comes from Eq. (2.1). In practice, however, AOR_{max} cannot be achieved since estimates are not perfect. We will show how much the actual simulation results deviate from AOR_{max}.

In addition to the above, we also study how close the estimation results would be to the actual channel-parameters, and how well estimates track time-varying channels.

We conducted simulation using MATLAB, and all N channels are assumed to have exponentially-distributed ON/OFF periods. A total of 9 heterogeneous channels have been used ($i = 1, 2, \ldots, 9$), where $(\lambda^i_{T_{OFF}}, \lambda^i_{T_{ON}})$ are independently chosen. We tested different channel conditions by changing the number of channels to be sensed such as: (1) 3 channels (channel 1,2,3), (2) 6 channels (channel 1,2,...,6), and (3) 9 channels (channel 1,2,...,9). For each case, a simulation ran for 5,000 seconds and AOR was measured. To observe the average behavior, the simulation under the same condition was repeated 10 times.

To emulate time-varying channel conditions, the channel parameter $\lambda^i_{T_{OFF}}/\lambda^i_{T_{ON}}$ decreases/increases its value by 10% once every 1,000 seconds. This allows us to show the efficiency of parameter tracking of our estimation with a moving time-window.

The proposed sensing-period optimization scheme is comparatively evaluated against a *reference scheme* without sensing-period optimization. Since there is no sensing-period adaptation in the reference scheme, it starts with a randomly-chosen initial sensing-period which will not be adapted. The reference scheme is tested with four different initial T_P^i: 0.05, 0.1, 0.5, and 1.0 seconds ($\forall i$). For the pro-

γ	T^i_{window} $(\forall i)$	$T_{estimation}$	T^i_I $(\forall i)$
0.2	200(sec)	20(sec)	2(ms)

Table 2.1: General evaluation parameters

AOR test	Proposed	Reference
Initial T^i_P	0.5(sec)	0.05/0.1/0.5/1.0 (sec)

Table 2.2: AOR test parameters

	Ch 1	Ch 2	Ch 3	Ch 4	Ch 5	Ch 6	Ch 7	Ch 8	Ch 9
$E[T^i_{OFF}]$	1.50	0.50	1.00	3.00	1.00	3.50	4.00	0.50	0.75
$E[T^i_{ON}]$	0.80	2.50	1.00	2.50	2.00	0.50	1.00	5.50	2.00

Table 2.3: Channel-usage pattern parameters

posed scheme, the algorithm starts with the initial T^i_P of 0.5 (seconds), and is then adapted and optimized gradually. This comparison will clearly show the importance of sensing-period optimization to efficient collection of more opportunities.

The parameters used for the simulation are shown in Tables 2.1, 2.2, and 2.3, where $E[T^i_{OFF}]$ and $E[T^i_{ON}]$ are in seconds.

2.6.2 The Simulation Results

Achieved Opportunity Ratio

Figure 2.7 plots the AOR of the proposed and reference schemes. The x-axis represents the number N of licensed channels and y-axis presents AOR in %. 100% indicates that a scheme can discover/utilize all existing opportunities of $\sum_{i=1}^{N}(1-u^i)$, which is in practice impossible to achieve due to the sensing overhead ($SSOH^i$) and the missed portion of opportunities ($UOPP^i$). Thus, it is more meaningful to consider the analytical maximum of utilizable opportunities (AOR_{max}).

The results in the figure show the superiority of the proposed algorithm. The sensing-period optimization offers more than 98% of the analytical maximum of

discovered spectrum availability regardless of the tested conditions ($N = 3, 6$, or 9). The small deviation of the performance from AOR_{max} comes from three factors: (1) the time for estimates to converge to the time-varying parameters, (2) the time for sensing-periods to be adapted to optimal ones, and (3) small deviation of estimates from the actual parameters. It also discovers up to 22% more opportunities than the reference schemes which do not offer sensing-period optimization. This improvement may become greater as the initial T_P^i is chosen smaller than 0.05 second, or larger than 1.0 second. In fact, no reference scheme can outperform the proposed scheme. As initial T_P^i is chosen farther away from the optimal one, the performance of the reference scheme degrades greatly for two reasons. First, if T_P^i grows, $SSOH^i$ gets smaller but $UOPP^i$ becomes larger and dominant, resulting in many missed OFF periods. In contrast, if T_P^i decreases, $UOPP^i$ gets smaller and more OFF periods are discovered, but $SSOH^i$ becomes larger, resulting in frequent interrupts in utilizing discovered opportunities on a channel due to sensing channels. Hence, in either case the reference scheme cannot reach AOR_{max}.

One may claim that in some cases (e.g., initial $T_P^i = 0.1$ at $N = 3$) the reference scheme nearly achieved AOR_{max}. The reference scheme, however, chooses initial T_P^i randomly and does not optimize it. Therefore, it would be just a pure luck if the reference scheme chooses its initial T_P^i close to the optimal one. In addition, non-adaptive T_P^i cannot track time-varying channel environments and will eventually yield poor performance if the simulation was run long enough. On the other hand, the sensing periods in the proposed scheme are adapted to the optimal values in a few cycles and they also track changing optimal values as shown in Figure 2.8, where adaptation is performed every $T_{estimation}$ (sec). Dashed lines indicate analytically-derived target optimal sensing-periods.

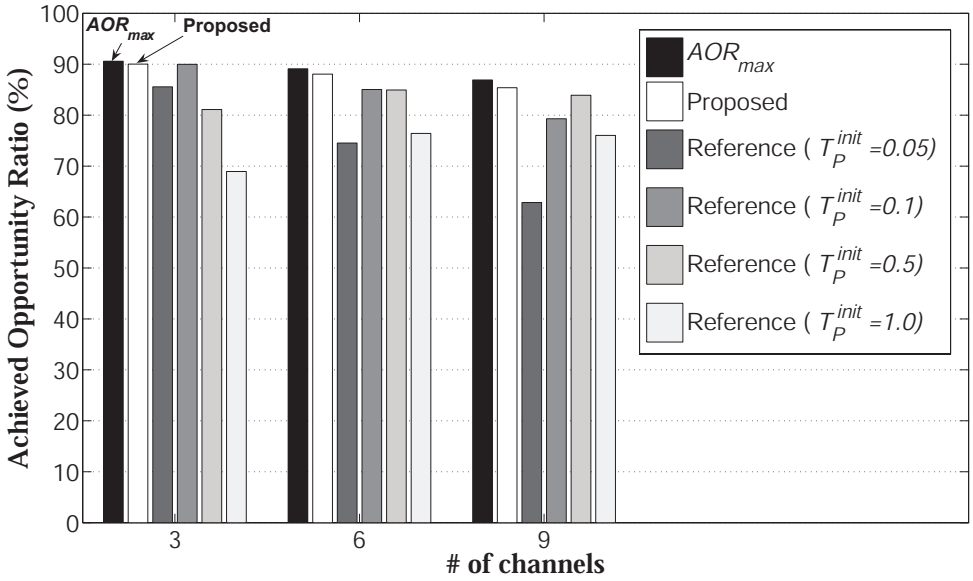

Figure 2.7: Achieved opportunity ratio (AOR)

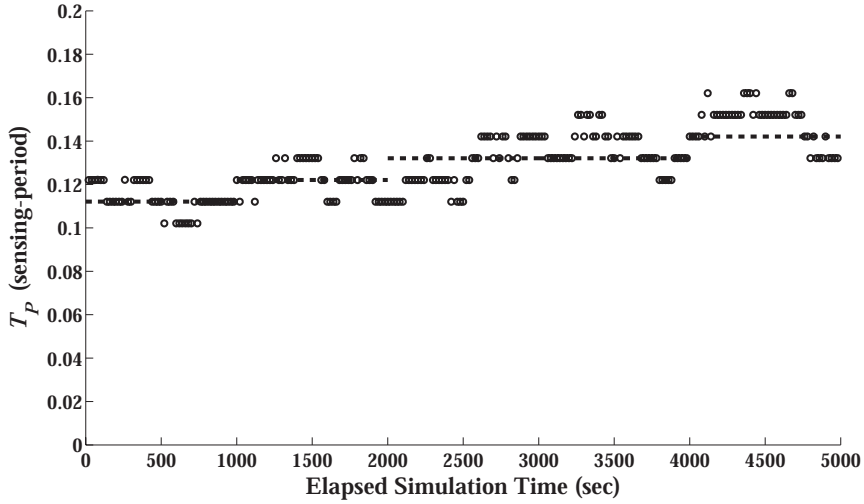

Figure 2.8: Adaptation of sensing-periods (N=3 case: channel 1)

Channel-Parameter Estimation Accuracy

Figure 2.9 shows the accuracy of our channel-usage pattern estimation. Each point in the figure indicates the estimate produced within an estimation cycle, $T_{estimation}$. Dashed lines represent the actual target channel parameters. The plot of $\hat{u}^i$ as well as $\hat{\lambda}_{T^i_{OFF}}$ follow the actual channel parameters very closely even when they are time-varying. The difference between estimates and target values can be

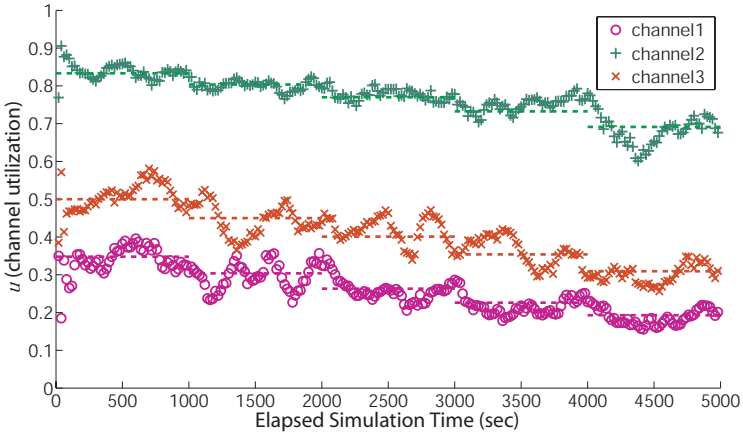

(a) u^i

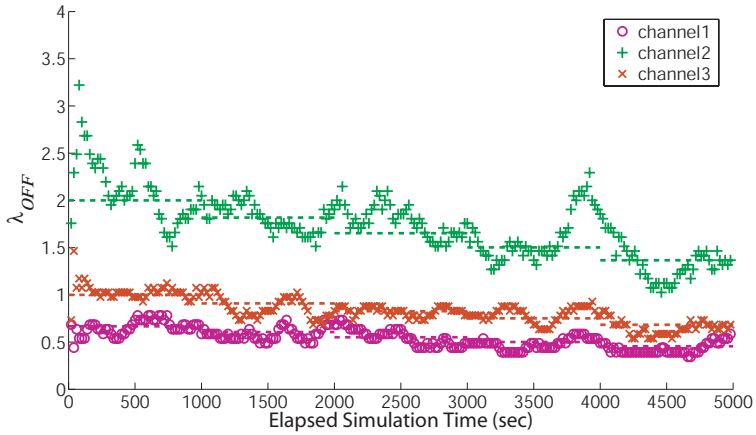

(b) λ^i_{OFF}

Figure 2.9: Estimation of unknown channel parameters: N=3 case

controlled by adapting γ and T^i_{window}, which are related to the number of samples and confidence intervals of estimators.

2.7 Deployment Scenarios

This section discusses how our proposed schemes can be applied to IEEE 802.11 systems as well as other licensed bands.

2.7.1 Application to IEEE 802.11

First, due to limitations in CSMA, 802.11 cannot be directly used as a platform of the proposed schemes. The Clear Channel Assessment (CCA) in CSMA uses energy detection to determine if there is any signal activity in each time slot, and hence, cannot differentiate SU signals from PU signals. As a result, all SUs could be backed off in case there is a PU signal within a contention period, since every SU may think the channel is occupied by another SU, not by PUs. It is, however, not desirable because all SUs have to vacate the channel if there exists any PU.

Hence, the current CCA of 802.11 should be modified in such a way that during a quiet period, no random back-off or data transmission is performed. In addition, the measurement result (busy or idle) of every slot during the quiet period must be reported to the MAC layer, and the MAC should also be modified so that the sensing results can be distributed to and shared by SUs.

To support periodic sensing scheduling on in-band and out-of-band channels, 802.11 MAC should introduce a new feature to reserve quiet periods. It can be done by using beacons or regular packets exchanged among SUs.

One example of using the 802.11 platform/protocol to implement sensing functionalities is described in [49] where an incumbent detection mechanism has been implemented using a commercial WLAN device (Atheros) and its open source device driver, MadWifi. In terms of sensing-periods, a in-band channel is regularly monitored once every frame (100 ms) to detect returning PUs (emulated by a signal generator emitting signals on one of WiFi bands). The sensing-period adaptation, however, can also be implemented by reserving a quiet period (at MAC level) every n frames and adapting n accordingly.

2.7.2 Application to licensed bands

The proposed sensing-period optimization scheme is designed to be adaptive to time-varying channel environments in order to track diverse channel-usage behavior of heterogeneous applications (e.g., voice, video streaming, web browsing, etc.). For example, if there exists a long ON period on a TV band, the proposed adaptive estimation technique with a moving time-window will accumulate 1 (ON) samples and its estimates of mean ON/OFF periods will eventually converge to the maximum/minimum values. As a result, the channel's sensing-period is adapted to a larger value since the channel is not likely to be available.

In case a licensed band has very short ON/OFF periods, spectrum agility may not bring much benefit due to high sensing overhead to track the fast ON/OFF state transitions. Our goal in this chapter, however, is to provide a general sensing framework which can be applied to any application on any band, by providing an adaptive sensing method and estimation technique.

2.8 Conclusion

In this chapter, we have proposed a sensing-period adaptation scheme used to discover spectrum opportunities more efficiently. The proposed scheme strives to discover as many utilizable spectrum opportunities as possible. Channel-usage pattern estimation was also proposed by deriving ML estimators and their confidence intervals. The simulation results demonstrated the advantages of the proposed schemes, such as a larger amount of discovered opportunities and robust parameter estimation.

CHAPTER III

OUT-OF-BAND SENSING PART II: FAST DISCOVERY OF SPECTRUM OPPORTUNITIES

3.1 Introduction

Opportunity discovery is an act of sensing out-of-band channels to locate an enough amount of whitespaces to meet the total spectrum demand of a cognitive radio network (CRN), which may be achieved by a few high-capacity idle channels or by many low-capacity idle channels by combining their capacities. In this chapter, we consider opportunity discovery in multi-channel CR communications where a CRN can simultaneously utilize multiple (idle) in-band channels. In such a scenario, opportunity discovery is triggered when the CRN experiences a shortage of whitespaces due to the return of primary users (PUs) at one of the in-band channels. The appearance of PUs incurs channel vacation which, in turn, reduces the amount of whitespaces the CRN can utilize. Note that the return of PUs is detected by in-band sensing [51], which will be discussed in Chapter IV.

Fast opportunity discovery is essential to seamless service provisioning for the secondary users (SUs) in a CRN, because the CRN may not provide its service in full strength while it experiences a shortage of bandwidth and the discovery of additional

opportunities incurs a non-trivial delay. Therefore, it is desired to derive an optimal way of searching out-of-band channels that minimizes the delay in discovering a necessary amount of additional bandwidth via out-of-band sensing.

3.1.1 Contributions

Our contribution in this chapter is three-fold. First, we propose an optimal sensing sequence that minimizes the latency of discovering available out-of-band channels to achieve the target amount of opportunities. We consider heterogeneous channel characteristics in terms of signal detection time, channel capacity, and the probability θ_i that a channel to be idle, and discuss the difference between offline and online sequences to show that the optimal sequence is an online sequence. Then, we derive the optimal online sequence using dynamic programming (DP), and show that the optimal sequence takes a simple form when channels have homogeneous capacities. To overcome the computational complexity of the DP algorithm, we also propose a suboptimal sequence algorithm that shows a near-optimal performance while incurring insignificant overhead.

Next, we categorize out-of-band channels as *backup* or *candidate* channels, as introduced in IEEE 802.22 [1]. To promote faster discovery of idle channels, we sort and search backup channels at the time of opportunity discovery where the backup channels are specially chosen among those that are more probable to have whitespaces; out-of-band channels other than backup channels are called *candidate channels*, and they are not sensed until they are designated as backup channels. Using this concept, we propose an efficient mechanism that constructs a backup channel list (BCL) and dynamically updates its entries. The proposed scheme maintains a moderate size of the BCL and updates its entries by importing/exporting channels

from/to the candidate channel list (CCL) with a small computational overhead.

Finally, we propose a strategy that estimates ON/OFF channel-usage patterns to predict channel availability, by selectively applying ML and Bayesian estimation. We capture the tradeoff between two estimation techniques: the former is simple but its performance degrades greatly with infrequent samples; the latter requires more computation but performs better with a small number of samples [4]. In addition, our scheme considers imperfect sensing with nonzero probabilities of miss detection (P_{MD}) and false alarms (P_{FA}) in predicting θ_i.

3.1.2 Organization

The rest of the chapter is organized as follows. We first overview related work in Section 3.2, and introduce our system models and assumptions in Section 3.3. Section 3.4 describes the opportunity discovery mechanism via sequential sensing. In Section 3.5, we derive the optimal sensing-sequence and a suboptimal sensing-sequence that achieves a near-optimal performance with small computational overhead. Section 3.6 presents construction of the initial BCL and an BCL-update algorithm to keep the list up-to-date. Section 3.7 introduces a strategy to estimate ON/OFF channel-usage patterns using ML and Bayesian inference. The performance of the proposed schemes are evaluated in Section 3.8, and then the chapter concludes in Section 3.9.

3.2 Related Work

Among a number of studies on spectrum sensing, several notable bodies of work are found to be related to fast opportunity discovery. Chang and Liu [9] proposed a strategy that optimally determines which channel to probe and when to transmit, but they focused on the case of single channel transmission only. Kim and Shin

[50] introduced a sensing-sequence that sorts channels in descending order of the probability θ_i, which we call a *probabilistic* sequence. However, such a sequence only maximizes the chance of finding an idle channel, instead of minimizing the overall discovery-delay. Jiang *et al.* [45] investigated the optimal sensing sequence in a multi-channel cognitive MAC protocol, and Shu and Krunz [81] studied the problem of sequential sensing for throughput efficiency along with finding the optimal sensing time, but both work focused on the case of single channel transmission and identical sensing time over all channels. In contrast, this chapter considers the case where CR-to-CR transmission occurs on a multi-channel environment via channel bonding, and also takes account for heterogeneous channel characteristics with different sensing times and channel capacities. On the other hand, Ahmad *et al.* [2] derived an optimal myopic policy in finding the best channel to sense per each time slot, but their approach was limited to the single channel sensing per slot and thus different from our multi-channel sequencing problem. Lai *et al.* [53] considered a scenario in which SUs can sense more than one channel simultaneously and utilize all discovered idle channels for their transmission, but the problem is not based on the specific target amount of bandwidth to discover as in our case.

On the other hand, Motamedi and Bahai [57] used Bayesian learning to predict the availability of a channel, where the learning process is simplified by assuming a geometric distribution for channel-usage patterns. In this chapter, we use a general alternating renewal process and develop a multi-stage iterative Bayesian inference.

3.3 System Model

3.3.1 Network Model

In this chapter, we focus on a single-hop CRN with a central controller (e.g., an Access Point) and a group of SUs (i.e., CR end-terminals) where the CRN utilizes a set of M licensed channels from which it harvests the necessary amount of spectrum opportunities. The M licensed channels are assumed to be determined and given *a priori* through an inter-CRN coexistence mechanism such as IEEE SCC 41 [96] and the coordinated channel allocation schemes [15, 60]. The inter-CRN coexistence scheme coordinates resource allocation between neighboring CRNs which is necessary to avoid collision by simultaneous channel access, through which the licensed channels can be assigned to the CRNs in a non-overlapping fashion. Since such schemes are beyond the scope of this chapter, we focus on selecting backup channels from the given M channels and optimally sequencing them at opportunity discovery.

Each SU is assumed to have been equipped with a single antenna, widely-tunable to any combination of M channels. That is, a SU can utilize possibly non-contiguous multiple idle channels at the same time, which is made possible by using signal processing techniques such as NC-OFDM [64]. Having one antenna per SU may help reduce the size of a secondary device and avoid potential interference between co-located antennas due to their close proximity [49]. A SU is assumed to act as either a spectrum sensor or a secondary transceiver, by dynamically reconfiguring itself.

We assume the central controller coordinates inter-SU transmission, spectrum sensing, and channel switching. The SU coordination is performed by a CR MAC protocol such as C-MAC [19] and OS-MAC [39], which is beyond the scope of this paper. Using the proposed sensing sequence in Section 3.5, the controller can assign as many SUs/sensors as necessary to achieve the PU protection requirements (e.g.,

P_{MD} and P_{FA}). Note that the optimality of the proposed sensing sequences is intact regardless of which MAC protocol is employed.

3.3.2 Channel and Sensing Model

We follow the channel model introduced in Chapter I. We also assume channel i has a capacity of C_i which is a physical bandwidth or Shannon capacity, taken as a long-term average considering time-varying channel conditions (e.g., fading). Although instantaneous capacity can also be used in view of fast fading statistics at each instant, we avoid using such fast-changing channel conditions in achieving the target amount of opportunities because we do not want overly-sensitive channel switching due to the short-term degradation of channel quality.

In addition, we use the sensing model introduced in Chapter I. When a SU acts as a spectrum sensor, it monitors channel i during *sensing-time* T_I^i, and determines the channel state between ON and OFF. T_I^i is assumed small relative to $E[T_{OFF}^i]$ and $E[T_{ON}^i]$ such that channel i's state remains unchanged during the sensing-time. The value of T_I^i is determined by the underlying detection method (e.g., energy or feature detection) and the type of PU signals [18], and thus it varies with channels.

3.3.3 Notation Table

We summarize the frequently used notations in Table 3.1.

3.4 Sequential Sensing Mechanism

In this section, we overview the sequential sensing mechanism for opportunity discovery, to enhance the understanding of our proposed schemes in the later sections.

M	number of licensed channels
N	number of backup channels ($N \leq M$)
i	channel index
$Z^i(t) \in \{0, 1\}$	channel state at time t (0:OFF, 1:ON)
$u^i \in [0, 1]$	channel utilization factor
T_I^i	sensing-time
C_i	channel capacity
θ_i	channel idle probability at opportunity discovery

Table 3.1: Summary of notations

3.4.1 Opportunity Discovery Procedure

Let B_{req} denote the total amount of bandwidth a CRN requires, which is the sum of spectrum demands of all SUs in the CRN. B_{req} may be achieved by utilizing just one idle channel with $C_i \geq B_{req}$ or by simultaneously utilizing multiple idle channels whose combined capacity exceeds B_{req}. Therefore, there exist one or more in-band channels the CRN currently utilizes.

Opportunity discovery is triggered whenever one of the in-band channels has to be vacated due to the returning PUs. At opportunity discovery, the CRN needs to find a set of new idle channels whose collective capacity achieves B_{target}, which is given as

$$B_{target} = \max\{B_{req} - B_{in-band}, 0\},$$

where $B_{in-band}$ is the sum capacity of the remaining in-band channels after the channel vacation.

New idle channels are discovered by sequentially sensing backup channels such that SUs synchronously tune to one backup channel at a time following a given sensing-sequence. Once a backup channel is detected idle, it becomes an in-band

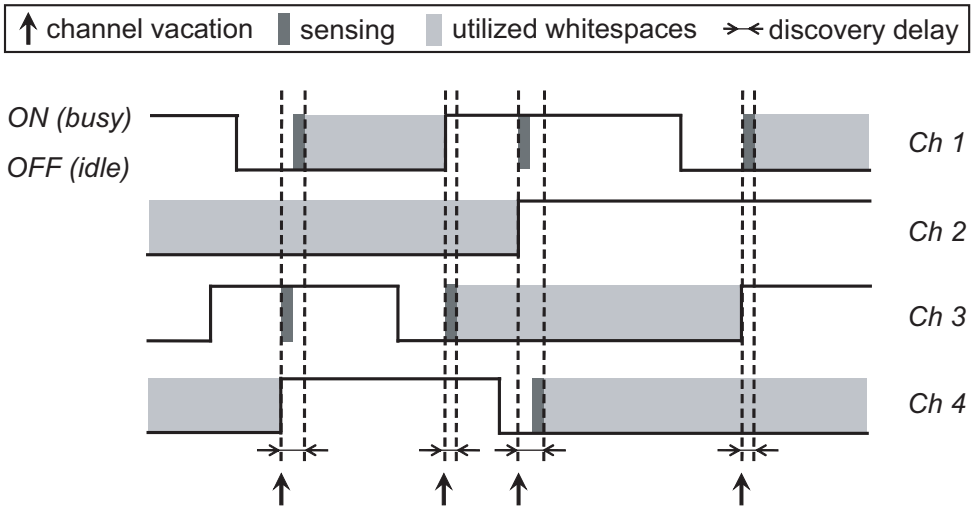

Figure 3.1: An illustration of opportunity discovery when a CRN requires two idle channels for its operation.

channel and merged into the "logical" channel whose capacity equals the combined capacity of all in-band channels. Opportunity discovery completes when the logical channel's capacity reaches or exceeds B_{req}. Note that the concept of logical channel is introduced to help the CRN's central controller instantly see how much more bandwidth is required at each channel vacation.

Fig. 3.1 shows an example where all four channels have the same capacity and the CRN requires two idle channels to meet its B_{req}. In the figure, the delay of each opportunity discovery is also shown, which is the sum of sensing-times spent to sequentially sense the backup channels until B_{req} is achieved by the newly found idle channel. Although in this example it suffices to find just one more idle channel per discovery, we will consider more general cases in the next section where achieving B_{req} may require to find more than one idle channel.

Discussion

This chapter focuses on the sequential sensing of backup channels assuming that all SUs in the CRN participate in sensing an out-of-band channel at each sensing. In

reality, however, the CRN may be able to sense more than one channel simultaneously if it has a sufficient number of SUs in its network. Since each sensing requires participation of 10–20 collaborative sensors to enhance the performance of detecting PUs by exploiting location diversity [31, 34, 56], the number of backup channels that can be simultaneously sensed depends on the total number of terminals in the CRN. For example, if we have 20 SUs and need 10 sensors per channel for collaborative sensing, then we can sense two channels at the same time. Even in such a case, however, the sequential sensing still plays a significant role in minimizing the opportunity discovery delay, since we can first optimally sort all channels and group them according to the number of channels that can be sensed at the same time.

3.4.2 Channel Idle Probability Prediction

In this chapter, we characterize a channel by a tuple of $\{T_I^i, C_i, \theta_i\}$ where T_I^i is the sensing-time, C_i the channel capacity, and θ_i the probability that channel i would be idle if the channel is sensed at opportunity discovery. Although derivation of θ_i for alternating renewal channels is described in Chapter II, we briefly overview the procedure here for completeness of the presentation.

θ_i varies with channels and time since it depends on the ON/OFF usage pattern and the history of sensing results (or samples). Therefore, calculation of θ_i first requires estimation of channel parameters. In Chapter II, an ML estimator and its confidence interval was derived when a set of samples from channel i is given as $\boldsymbol{Z}^i = (Z^i(t_1), Z^i(t_2), \ldots, Z^i(t_r))$ where $t_1 < t_2 < \ldots < t_r$. The r samples can be collected at any time, i.e., they are not necessarily periodic, since they are produced by (1) sequential sensing at opportunity discovery (if the channel is selected and sensed), and/or (2) extra sampling scheduled by the central controller who assigns

some *idle* SUs (i.e., SUs with no transmission) to sense out-of-band channels (even when no opportunity discovery is necessary). The extra sampling is to enhance the accuracy of estimation but is outside of the scope of this chapter.

Then, Chapter II showed that having t as the opportunity discovery time, θ_i of the renewal processes is given as

$$\theta_i = Pr(Z^i(t) = 0 | Z^i(t_1), \ldots, Z^i(t_r)) = Pr(Z^i(t) = 0 | Z^i(t_r))$$

where $Pr(Z^i(t) = 0|Z^i(t_r))$ is the transition probability between the most recent sample at time t_r and an imaginary sample 0 at time t. The transition probability is expressed with the estimated channel parameters. For example, exponentially-distributed ON/OFF periods lead to the following

$$\theta_i = \begin{cases} (1-u^i) + u^i \cdot e^{-(\psi^i_{OFF}+\psi^i_{ON})(t-t_r)}, & \text{if } Z^i(t_r) = 0, \\ (1-u^i)\left\{1 - e^{-(\psi^i_{OFF}+\psi^i_{ON})(t-t_r)}\right\}, & \text{otherwise,} \end{cases}$$

which correspond to $P^i_{00}(t-t_r)$ and $P^i_{10}(t-t_r)$ in Eq. (2.5) in Chapter II. Here, two channel parameters ψ^i_{ON} and ψ^i_{OFF} are from

$$\begin{aligned} f_{T^i_{OFF}}(t) &= \psi^i_{OFF} e^{-\psi^i_{OFF} t}, \\ f_{T^i_{ON}}(t) &= \psi^i_{ON} e^{-\psi^i_{ON} t}, \end{aligned} \tag{3.1}$$

where $E[T^i_{ON}] = 1/\psi^i_{ON}$ and $E[T^i_{OFF}] = 1/\psi^i_{OFF}$.

One can notice that $\theta_i \neq (1-u^i)$ since u^i is a long-term average utilization of channel i while θ_i is the *instantaneous* channel idle probability considering the past channel samples. This also implies that θ_i reflects the correlation between the samples. For example, if $Z^i(t_r) = 0$ and $(t-t_r)$ is small, it is likely that the channel is still in its OFF state, thus making θ_i very close to 1. On the contrary, if $Z^i(t_r) = 1$ and $(t-t_r)$ is small, it is likely that the channel is still in its ON state, thus making

θ_i very close to 0. In addition, once a channel with a long ON period enters the ON state, the channel's θ_i becomes very small until enough time passes.

Sensing Error Compensation

Although the derivation of θ_i is exact, its correctness relies on how accurately the samples reflect the actual channel state. In reality, spectrum sensing is imperfect since P_{MD} and P_{FA} are nonzero. Since the impact of imperfect sensing on θ_i was not considered in Chapter II, we introduce here Bayesian state estimation that can compensate for the sensing error [82]. For the ease of notation, we will omit i in this subsection.

Suppose $\tilde{Z}(t_k) \in \{0, 1\}$ denotes the actual state of a channel at time t_k. Assuming the pdf of the initial state $\tilde{Z}(t_0)$ is known, the estimator is

$$f(\tilde{Z}(t_0)|\mathbf{Z}_0) = f(\tilde{Z}(t_0)),$$

where $\mathbf{Z}_k = \{Z(t_1), Z(t_2), \ldots, Z(t_k)\}$ for $k \geq 1$ and $\mathbf{Z}_0 = \emptyset$. For each $k \geq 1$, we evaluate

$$\begin{aligned} f(\tilde{Z}(t_k)|\mathbf{Z}_{k-1}) &= \sum_{\tilde{Z}(t_{k-1})} f(\tilde{Z}(t_k)|\tilde{Z}(t_{k-1}))f(\tilde{Z}(t_{k-1})|\mathbf{Z}_{k-1}), \\ f(\tilde{Z}(t_k)|\mathbf{Z}_k) &= \frac{f(Z(t_k)|\tilde{Z}(t_k))f(\tilde{Z}(t_k)|\mathbf{Z}_{k-1})}{\sum_{\tilde{Z}(t_k)} f(Z(t_k)|\tilde{Z}(t_k))f(\tilde{Z}(t_k)|\mathbf{Z}_{k-1})}, \end{aligned}$$

where $f(\tilde{Z}(t_k)|\mathbf{Z}_{k-1})$ is the prior pmf of $\tilde{Z}(t_k)$ before observing $Z(t_k)$ and $f(\tilde{Z}(t_k)|\mathbf{Z}_k)$ is the posterior pmf of $\tilde{Z}(t_k)$ after observing $Z(t_k)$.

Prior and posterior pmfs are updated whenever a new sample $Z(t_k)$ is obtained. Then, when opportunity discovery is triggered at time t, θ can be estimated as

$$\theta = f(\tilde{Z}(t_k)|\mathbf{Z}_{k-1})\Big|_{t_k=t, \tilde{Z}(t_k)=0}.$$

In the above procedure, $f(\tilde{Z}(t_k)|\tilde{Z}(t_{k-1}))$ and $f(Z(t_k)|\tilde{Z}(t_k))$ are yet to be determined. $f(\tilde{Z}(t_k)|\tilde{Z}(t_{k-1}))$ is the transition probability between two consecutive samples at times t_{k-1} and t_k, which has been fully derived in Chapter II. On the other hand, $f(Z(t_k)|\tilde{Z}(t_k))$ is easily determined according to the definition of P_{MD} and P_{FA} such as

$$f(Z(t_k)|\tilde{Z}(t_k)) = \begin{cases} 1 - P_{FA}, & \text{if } (\tilde{Z}(t_k), Z(t_k)) = (0,0), \\ P_{FA}, & \text{if } (\tilde{Z}(t_k), Z(t_k)) = (0,1), \\ 1 - P_{MD}, & \text{if } (\tilde{Z}(t_k), Z(t_k)) = (1,0), \\ P_{MD}, & \text{if } (\tilde{Z}(t_k), Z(t_k)) = (1,1). \end{cases}$$

3.5 Optimal Sensing Sequence for Minimal Opportunity-Discovery Latency

In this section, we derive an optimal sensing-sequence of backup channels that incurs the minimal delay in discovering a necessary amount of opportunities, and propose a computationally-efficient sequence algorithm that provides a near-optimal performance. As introduced in Section 3.4, backup channels are characterized by a tuple of $\{T_I^i, C_i, \theta_i\}$ and the opportunity discovery is triggered at channel vacation of an in-band channels where the target amount of bandwidth to discover is denoted by B_{target}. For the notational ease, we will use B to denote B_{target} throughout this section.

3.5.1 Problem Statement

Suppose there are N ($\leq M$) backup channels, and let $S = \{s_1, s_2, \ldots, s_N\} \in \boldsymbol{\mathcal{S}}$ be an *ordered* list of N channels where s_j is the channel index of the j-th channel in the sequence (s_j: positive integer, $1 \leq s_j \leq N$) and $\boldsymbol{\mathcal{S}}$ is the set of all possible

channel-sequences ($|\boldsymbol{\mathcal{S}}| = N!$). Also suppose T_I^i, C_i and θ_i are known a priori.

Our objective is to determine the optimal sensing-sequence S^* that minimizes the average delay in finding idle channels whose cumulative capacity exceeds B. This can be stated formally as:

$$\textbf{Find} \qquad S^* = \underset{S \in \boldsymbol{\mathcal{S}}}{\operatorname{argmin}} E_{\boldsymbol{\theta}} \left[\sum_{i=1}^{N} T_I^{s_i} \cdot I_{\left\{\sum_{j=1}^{i-1} C_{s_j} \cdot (1 - Z^{s_j}) < B\right\}} \right]$$

where

$$\begin{aligned} \boldsymbol{\theta} &= (\theta_1, \theta_2, \ldots, \theta_N), \\ I_{\{\star\}} &= \begin{cases} 1, & \text{if the statement } \star \text{ is true,} \\ 0, & \text{otherwise.} \end{cases} \end{aligned} \tag{3.2}$$

In the above problem statement, the indicator function $I_{\left\{\sum_{j=1}^{i-1} C_{s_j} \cdot (1 - Z^{s_j}) < B\right\}}$ implies that once B is achieved, the sequential sensing stops.[1]

3.5.2 Offline vs. Online Sensing Sequences

To find the optimal sensing sequence, we need to consider two types of sensing sequence: *offline* and *online* sequences. In what follows, we will introduce the concept of the two sequences and discuss the reason why the online sequence must be considered to find the optimal sensing sequence.

Offline Sequence

An offline sensing sequence is a static sequence which strictly follows the initially determined sequence regardless of the channel states observed during the sequential

[1] In practice, $\boldsymbol{\theta}$ must be updated after sensing each channel by re-calculating θ_i's based on the elapsed time due to sensing of the last chosen channel. Although updating $\boldsymbol{\theta}$ is always possible by following the procedure in [50], here we assume T_I^i's are small enough to make the impact of adjusting θ_i's negligible, for the purpose of easier illustration. In fact, this assumption is applicable in most practical scenarios because T_I^i is usually in the order of milliseconds (or even less) while the ON/OFF periods are typically in the order of seconds or minutes.

sensing. The optimal offline sensing sequence is built by considering $\boldsymbol{\theta}$ while ignoring the actual channel states to be observed, and the average discovery delay $\mathcal{D}$ of a given offline sequence $S = \{s_1, s_2, \ldots, s_N\}$ is given as

$$\begin{aligned}\mathcal{D} &= \sum_{z_1=0}^{1}\sum_{z_2=0}^{1}\cdots\sum_{z_N=0}^{1}\left\{\prod_{v=1}^{N}(\theta_{s_v})^{1-z_v}(1-\theta_{s_v})^{z_v}\right. \\ &\quad \left.\times\left(T_I^{s_1}+\sum_{v=2}^{N}T_I^{s_v}\cdot I_{\{\sum_{w=1}^{v-1}C_{s_w}(1-z_w)<B\}}\right)\right\}. \end{aligned} \tag{3.3}$$

Then, the optimal offline sequence is determined as the sequence that minimizes Eq. (3.3) among $N!$ possible sequences.

As an example, let us consider the following scenario:

$$\begin{aligned} &N=3, \quad B=2.0, \quad (C_1,C_2,C_3)=(0.5,1.5,2.0), \\ &(T_I^1,T_I^2,T_I^3)=(1,2,3), \quad (\theta_1,\theta_2,\theta_3)=(0.5,0.3,0.1). \end{aligned} \tag{3.4}$$

By defining $\tilde{\theta}_{s_j} := 1-\theta_{s_j}$, Eq. (3.3) becomes

$$\begin{aligned}\mathcal{D} &= \tilde{\theta}_{s_1}\tilde{\theta}_{s_2}\tilde{\theta}_{s_3}(T_I^{s_1}+T_I^{s_2}+T_I^{s_3}) \\ &+ \tilde{\theta}_{s_1}\tilde{\theta}_{s_2}\theta_{s_3}(T_I^{s_1}+T_I^{s_2}+T_I^{s_3}) \\ &+ \tilde{\theta}_{s_1}\theta_{s_2}\tilde{\theta}_{s_3}(T_I^{s_1}+T_I^{s_2}+T_I^{s_3}\cdot I_{\{C_{s_2}<B\}}) \\ &+ \tilde{\theta}_{s_1}\theta_{s_2}\theta_{s_3}(T_I^{s_1}+T_I^{s_2}+T_I^{s_3}\cdot I_{\{C_{s_2}<B\}}) \\ &+ \theta_{s_1}\tilde{\theta}_{s_2}\tilde{\theta}_{s_3}(T_I^{s_1}+T_I^{s_2}\cdot I_{\{C_{s_1}<B\}}+T_I^{s_3}\cdot I_{\{C_{s_1}<B\}}) \\ &+ \theta_{s_1}\tilde{\theta}_{s_2}\theta_{s_3}(T_I^{s_1}+T_I^{s_2}\cdot I_{\{C_{s_1}<B\}}+T_I^{s_3}\cdot I_{\{C_{s_1}<B\}}) \\ &+ \theta_{s_1}\theta_{s_2}\tilde{\theta}_{s_3}(T_I^{s_1}+T_I^{s_2}\cdot I_{\{C_{s_1}<B\}}+T_I^{s_3}\cdot I_{\{C_{s_1}+C_{s_2}<B\}}) \\ &+ \theta_{s_1}\theta_{s_2}\theta_{s_3}(T_I^{s_1}+T_I^{s_2}\cdot I_{\{C_{s_1}<B\}}+T_I^{s_3}\cdot I_{\{C_{s_1}+C_{s_2}<B\}}). \end{aligned} \tag{3.5}$$

Then, by comparing all 3! sequences, the optimal offline sequence that minimizes Eq. (3.5) is found to be $\{1,2,3\}$.

Online Sequence

An online sensing sequence, on the other hand, is a dynamic sequence which can update itself each time it sense a channel in the sequence such that the remaining unsensed channels are re-ordered to form an updated sub-sequence according to the observed channel states. Such a dynamic sequence is necessary to derive the optimal sensing sequence since the optimality condition changes whenever we sense a new channel and observe its actual state.

To show the impact of online observation of channel states, let us consider again the example in Eq. (3.4). Once the first channel in the optimal offline sequence (i.e., channel 1) is sensed, the capacity-to-go (i.e., the remaining capacity to achieve at the subsequent sensing) is updated as

$$B' = \begin{cases} B - C_{s_1}, & \text{if channel 1 is sensed idle,} \\ B, & \text{otherwise.} \end{cases} \tag{3.6}$$

Then, we need to find the best channel to sense next to minimize the subsequent sensing delay $\mathcal{D}'$ in sensing $S' = \{s_2, s_3\}$, where

$$\begin{aligned} \mathcal{D}' &= \tilde{\theta}_{s_2}\tilde{\theta}_{s_3}(T_I^{s_2} + T_I^{s_3}) + \tilde{\theta}_{s_2}\theta_{s_3}(T_I^{s_2} + T_I^{s_3}) \\ &+ \theta_{s_2}\tilde{\theta}_{s_3}(T_I^{s_2} + T_I^{s_3} \cdot I_{\{C_{s_2} < B'\}}) + \theta_{s_2}\theta_{s_3}(T_I^{s_2} + T_I^{s_3} \cdot I_{\{C_{s_2} < B'\}}). \end{aligned}$$

Using B' and $\mathcal{D}'$ and comparing all $(N-1)!$ possible subsequences, it can be seen that the optimal choice of s_2 minimizing $\mathcal{D}'$ is given as

$$s_2 = \begin{cases} 2, & \text{if channel 1 is sensed idle,} \\ 3, & \text{otherwise.} \end{cases}$$

Therefore, the optimal offline sequence $\{1, 2, 3\}$ is no longer optimal if the first channel is sensed busy. Intuitively speaking, when channel 1 is idle, we have $B' = 1.5$

and thus, we may still want to sense channel 2 next since $C_2 = 1.5$ is large enough to fulfill B'. When channel 1 is busy, however, we have $B' = 2.0$ and we may want to sense channel 3 instead since channel 2 cannot fulfill B' while channel 3 can (since $C_3 = 2.0$). That is, if $s_2 = 2$, the subsequent delay always becomes $(T_I^2 + T_I^3)$ regardless of the state of channel 2, whereas the delay might become T_I^3 if $s_2 = 3$ and channel 3 is sensed idle.

3.5.3 Optimal Online Sensing Sequence Algorithm

As shown in Section 3.5.2, we need to find the optimal *online* sequence to minimize the opportunity discovery delay. To find the optimal online sequence, we propose a dynamic-programming-based search algorithm. We will also show the optimal sequence takes a simple form for the special case of homogeneous channel capacities.

Let us define an N-stage decision problem where at stage k we have $(N - k + 1)$ channels to choose from and $(k - 1)$ channels already sensed. Our objective is then, at stage k, to make an optimal decision on which channel to sense next, to minimize the overall delay in achieving the target amount of bandwidth, based on the already-discovered idle channels. For this, we define *control* u_k as the chosen channel to sense at stage k. We also define $x_k = (U_k, B_k)$ as the state at stage k where U_k is the set of remaining channels to choose from and B_k is the accumulated bandwidth achieved from the idle channels among the already-sensed. Finally, we define $g_k(x_k, u_k)$ as the cost incurred at stage k by the chosen control u_k, which is in fact the sensing time $T_I^{u_k}$ of the chosen channel u_k because our goal is to minimize the overall sensing time.

$B :=$ the total amount of bandwidth to discover;
$U_1 := \{1, 2, \ldots, N\}$;
$B_1 := 0$;
$k := 1$;

For all possible combinations of $x_N = (U_N, B_N)$,
derive $J_N(x_N)$ and $u_N(x_N)$ by Eq. (3.7);

Using $J_N(x_N)$, derive all preceding $J_k(x_k)$ and $u_k(x_k)$
according to Eq. (3.7), for $k = N-1, N-2, \ldots, 1$;

while $(k \leq N)$ {
    $S_k^* := u_k(x_k)$;
    Sensing sequence $S^* := \{S_1^*, S_2^*, \ldots, S_k^*\}$;
    Sense S_k^* and discover its channel state Z;
    if $(Z == 0)$ **then**
        $B_{k+1} := B_k + C_{S_k^*}$;
    else $B_{k+1} := B_k$;
    if $(B_{k+1} \geq B)$ **then**
        Stop the sequential sensing;
        return;
    $U_{k+1} := U_k \setminus \{S_k^*\}$;
    $k := k + 1$;
}
return;

Figure 3.2: Pseudo-code of the dynamic programming (DP) search algorithm (S^*: optimal sequence)

Now, the DP algorithm for the optimal online sequence is formulated as follows.

$$\begin{aligned} J_N(x_N) =& g_N(x_N), \\ J_k(x_k) =& \min_{u_k \in U_k} \{E_{\boldsymbol{\theta}}[g_k(x_k, u_k) + J_{k+1}(x_{k+1})]\}, \\ u_k(x_k) =& \arg\min_{u \in U_k} \{E_{\boldsymbol{\theta}}[g_k(x_k, u) + J_{k+1}(x_{k+1})]\}, \end{aligned} \tag{3.7}$$

where

$$g_k(x_k, u_k) \quad = \quad T_I^{u_k} \cdot I_{\{B_k < B\}}.$$

Eq. (3.7) can be further analyzed using the following relationship,

$$\begin{aligned} U_{k+1} =& U_k \setminus \{u_k\}, \\ B_{k+1} =& \begin{cases} B_k + C_{u_k}, & \text{if channel } u_k \text{ is idle,} \\ B_k, & \text{otherwise,} \end{cases} \end{aligned} \tag{3.8}$$

such as

$$J_k(x_k) \quad = \quad \min_{u_k \in U_k} \{T_I^{u_k} \cdot I_{B_k < B} + \theta_{u_k} \cdot J_{k+1}(U_{k+1}, B_k + C_{u_k}) + (1 - \theta_{u_k}) \cdot J_{k+1}(U_{k+1}, B_k)\}.$$

As an initial condition, we have

$$U_1 = \{1, 2, \ldots, N\}, \quad B_1 = 0.$$

Fig. 3.2 presents the pseudo-code of the proposed DP algorithm.

Algorithm Complexity Analysis

Once $J_N(x_N)$ is computed for every possible x_N's, $J_k(x_k)$ for $k \leq N-1$ can be iteratively derived. Therefore, the complexity of the algorithm depends on the number of possible combinations of U_N and B_N. Since U_N is a set of a single element, there are N possible choices of U_N. For a given U_N, B_N is determined by considering all possible combinations of the channel states (i.e., idle or busy) of the preceding $N-1$ channels—that is, 2^{N-1}. As a result, there are $N \cdot 2^{N-1}$ possible choices of $x_N = (U_N, B_N)$ which gives us the complexity of $O(N \cdot 2^N)$, and hence the DP algorithm is not a polynomial-time solution. In Section 3.5.4, we propose a computationally-efficient suboptimal algorithm that yields a near-optimal performance.

A Special Case: Homogeneous Channel Capacity

In this section, we will prove that in a special case with homogeneous channel capacities, i.e., $C_i = C$, $\forall i$, the optimal online sensing-sequence takes a much simpler form. In Lemma 3.5.1, we first prove that the optimal offline sensing-sequence takes a trivial form with $C_i = C$, and then in Theorem 3.5.1 we prove that the optimal offline sequence becomes the optimal online sequence under the same condition.

Lemma 3.5.1. *If $C_i = C$, $\forall i$, then the optimal offline sensing-sequence is built by sorting channels in ascending order of T_I^i/θ_i.*

Proof. Let L be the optimal sensing-sequence and L' be its counterpart constructed by switching the order of the k-th and $(k+1)$-th channels in L. That is,

$$\begin{aligned} L &= (l_1, \ldots, l_{k-1},\ l_k, l_{k+1},\ l_{k+2}, \ldots, l_N), \\ L' &= (l_1, \ldots, l_{k-1},\ l_{k+1}, l_k,\ l_{k+2}, \ldots, l_N). \end{aligned}$$

On the other hand, $\mathcal{D}_L^B$ is defined as the average delay in locating idle channels whose cumulative capacity exceeds B, using a sensing-sequence L. $\mathcal{P}_L^B$ is defined as the probability that the sum of capacities of idle channels in a sensing-sequence L may be strictly less than B.

In addition, let us define the following ordered lists:

$$\begin{aligned} L_{k-1} &= (l_1, l_2, \ldots, l_{k-1}), \\ L_k &= (l_1, l_2, \ldots, l_k), \\ L_{k+1} &= (l_1, l_2, \ldots, l_{k+1}), \\ L_{k-1,k+1} &= (l_1, l_2, \ldots, l_{k-1},\ l_{k+1}), \\ L_{k-1,k+1,k} &= (l_1, l_2, \ldots, l_{k-1},\ l_{k+1}, l_k), \\ L_{k+1}^c &= (l_{k+2}, \ldots, l_N). \end{aligned}$$

Since a channel is sensed only when those channels preceding in the list provide less opportunities than B, we can express $\mathcal{D}_L^B$ and $\mathcal{D}_{L'}^B$ as

$$\begin{aligned}\mathcal{D}_L^B &= \mathcal{D}_{L_{k-1}}^B + \mathcal{P}_{L_{k-1}}^B \cdot T_I^{l_k} + \mathcal{P}_{L_k}^B \cdot T_I^{l_{k+1}} + \mathcal{P}_{L_{k+1}}^B \cdot \mathcal{D}_{L_{k+1}^c}^B, \\ \mathcal{D}_{L'}^B &= \mathcal{D}_{L_{k-1}}^B + \mathcal{P}_{L_{k-1}}^B \cdot T_I^{l_{k+1}} + \mathcal{P}_{L_{k-1,k+1}}^B \cdot T_I^{l_k} + \mathcal{P}_{L_{k-1,k+1,k}}^B \cdot \mathcal{D}_{L_{k+1}^c}^B.\end{aligned}$$

Since $\mathcal{D}_L^B \leq \mathcal{D}_{L'}^B$ and $\mathcal{P}_{L_{k+1}}^B = \mathcal{P}_{L_{k-1,k+1,k}}^B$, we have

$$\mathcal{P}_{L_{k-1}}^B \cdot T_I^{l_k} + \mathcal{P}_{L_k}^B \cdot T_I^{l_{k+1}} \leq \mathcal{P}_{L_{k-1}}^B \cdot T_I^{l_{k+1}} + \mathcal{P}_{L_{k-1,k+1}}^B \cdot T_I^{l_k}$$

which reduces to

$$\frac{T_I^{l_k}}{(\mathcal{P}_{L_{k-1}}^B - \mathcal{P}_{L_{k-1}}^{B-C_{l_k}})\theta_{l_k}} \leq \frac{T_I^{l_{k+1}}}{(\mathcal{P}_{L_{k-1}}^B - \mathcal{P}_{L_{k-1}}^{B-C_{l_{k+1}}})\theta_{l_{k+1}}}, \tag{3.9}$$

since $\mathcal{P}_{L_k}^B = \mathcal{P}_{L_{k-1}}^B \cdot (1-\theta_{l_k}) + \mathcal{P}_{L_{k-1}}^{B-C_{l_k}} \cdot \theta_{l_k}$.

By substituting C for C_{l_k} and $C_{l_{k+1}}$ in Eq. (3.9), the inequality condition reduces to:

$$\frac{T_I^{l_k}}{\theta_{l_k}} \leq \frac{T_I^{l_{k+1}}}{\theta_{l_{k+1}}}, \text{ for } 1 \leq k \leq N-1, \tag{3.10}$$

which is a necessary condition for optimality. However, since there exists a single and unique sequence satisfying such a necessary condition,[2] the condition also becomes sufficient. Therefore, the resulting sequence is optimal. □

Now, using Lemma 3.5.1, we present the following theorem on the optimal online sensing sequence.

Theorem 3.5.1. *If $C_i = C$, $\forall i$, then the optimal online sensing sequence is built in the same way as the optimal offline sensing sequence, by sorting channels in ascending order of T_I^i/θ_i.*

[2]Note that since $\theta_i \in [0,1]$, it is not likely to have ties with the same T_I^i/θ_i. If it happens, we can still sort them uniquely in ascending/descending order of channel index i.

Proof. The optimal *online* sequence is built by repeatedly searching for the optimal offline subsequences. Let us denote by S the optimal offline sequence of all N channels. According to Lemma 3.5.1, S is simply constructed by sorting channels in ascending order of T_I^i/θ_i. Then, the first channel in S, say s, becomes the first channel in the optimal online sequence. Now, to find the next channel in the optimal online sequence, we need to sort $S \setminus \{s\}$, again, according to Lemma 3.5.1. However, since Eq. (3.10) does not depend on B, the sorted sequence of $S \setminus \{s\}$ is still the same as $S \setminus \{s\}$. Therefore, the second channel in the optimal online sequence is the second entry of S. By the same argument, S becomes the optimal online sequence, which proves the theorem. □

3.5.4 Efficient Suboptimal Sensing Sequence Algorithm

The proposed DP algorithm suffers from high computational complexity. Therefore, we propose a computationally efficient algorithm that determines a suboptimal sequence in polynomial time while providing a near-optimal performance.

To derive a suboptimal sequence, we utilize the necessary condition for optimality in Eq. (3.9). We first recognize that the first channel in the sequence (i.e., $k = 1$) satisfies $L_{k-1} = \emptyset$, and thus we have $\mathcal{P}^B_{L_{k-1}} = 1$ and

$$\mathcal{P}^{B-C_{l_k}}_{L_{k-1}} = \begin{cases} 0, & \text{if } C_{l_k} \geq B, \\ 1, & \text{otherwise,} \end{cases}$$

by the definition of $\mathcal{P}^B_L$.[3] Then, we get

$$\frac{T_I^{l_k}}{(\mathcal{P}^B_{L_{k-1}} - \mathcal{P}^{B-C_{l_k}}_{L_{k-1}})\theta_{l_k}} = \begin{cases} T_I^{l_k}/\theta_{l_k}, & \text{if } C_{l_k} \geq B, \\ \infty, & \text{otherwise.} \end{cases}$$

[3]Note that the sum capacity of idle channels in an empty set is equal to zero.

Therefore, to satisfy Eq. (3.9), the first channel should be the one with the smallest T_I^i/θ_i among all unsensed channels satisfying $C_i \geq B$. In case all unsensed channels have $C_i < B$, we have $\mathcal{P}_{L_{k-1}}^{B-C_{l_k}} = 1$, and thus the term $\mathcal{P}_{L_{k-1}}^{B} - \mathcal{P}_{L_{k-1}}^{B-C_{l_k}}$ in Eq. (3.9) cancels out. As a result, the first channel in this case (i.e., $C_i < B$ for all unsensed channels) is determined as the one with the smallest T_I^i/θ_i.

Once the first channel is determined, we sense the channel and observe its channel state. Depending on the state, we update B as in Eq. (3.6) and find the next channel to sense. Since the problem becomes identical to the initial problem of finding the first channel except the updated B and the set of unsensed channels (i.e., one less unsensed channels by excluding the one just sensed), we can apply the same procedure described above to find the next channel. Finally, the procedure completes when the updated B satisfies $B \leq 0$.

The pseudo-code of the proposed suboptimal sequence algorithm is described in Fig. 3.3. In Section 3.8, we will show the near-optimal performance of the proposed sequence.

Algorithm Complexity Analysis

The algorithm sorts $(N - k + 1)$ channels at stage k, where $k = 1, 2, \ldots, N$. Therefore, the number of computations required is $N + (N-1) + \ldots + 1 = N(N+1)/2$, and thus we have $O(N^2)$. Therefore, the suboptimal algorithm is solvable in polynomial time, significantly reducing the computational overhead compared to the DP algorithm.

3.5.5 Discussion

A CRN may sometimes fail to find the necessary amount of opportunities (i.e., B) after searching all N channels. In such a case, the CRN must *retry* opportunity

```
B := the total amount of bandwidth to discover;
U := {1, 2, ..., N};
k := 1;

while (k ≤ N) {
    U' := {channels in U with C_i ≥ B};
    if (U' == ∅)    then
            U' := U;
    S*_k := the channel in U' with smallest T^i_I/θ_i;
    Sensing sequence S* := {S*_1, S*_2, ..., S*_k};
    Sense S*_k and discover its channel state Z;
    if (Z == 0)    then
            B := B − C_{S*_k};
    else    B := B;
    if (B <= 0)    then
        Stop the sequential sensing;
        return;
    U := U \ {S*_k};
    k := k + 1;
}
return;
```

Figure 3.3: Pseudo-code of the proposed suboptimal sensing sequence algorithm (S^*: near-optimal sequence)

discovery after waiting for a certain amount of time, and it should keep retrying until enough opportunities are discovered. The reason for waiting is that the channels sensed busy may still be in the same state if the CRN performs an instant retry. We denote the period of such retries by *tRETRY*, which is a design parameter.

Once the first opportunity discovery fails, the total discovery delay to accomplish B depends more on *tRETRY* due to the subsequent retries. Therefore, it is desirable

to have an enough number of 'good' channels in BCL to promote successful opportunity discovery at the first trial. The construction of such a BCL will be discussed in Section 3.6.

An idle channel discovered by sequential sensing could become busy again before the sequential sensing completes, because there is a gap between the moment the channel is sensed and the time the sequential sensing completes. However, such state transition is detected by in-band sensing as shown in [51], and the detected channel is vacated immediately triggering opportunity discovery once more. However, the effectiveness of the proposed channel sequence is still valid since it can also minimize the delay in finding additional idle channels by such subsequent opportunity discovery.

3.6 Backup Channel List Management

The objective of BCL is to find and maintain 'good' channels among the excessively many licensed channels, e.g., 68 TV channels in the VHF/UHF bands [17], to achieve the following two goals: (1) increase the chance of finding spectrum opportunities as much as necessary at each opportunity discovery, and (2) mitigate an overhead in ordering channels by keeping a minimal number of backup channels. To achieve both objectives, we propose a BCL management strategy that constructs an initial BCL and periodically updates its entries via importing, exporting, and swapping channels between BCL and CCL.

Fig. 3.4 illustrates how a channel changes its association among in-band, backup and candidate channels, according to our BCL management strategy. A backup channel becomes an in-band channel if it is sensed idle during opportunity discovery, and channel vacation of an in-band channel makes it a backup channel again.

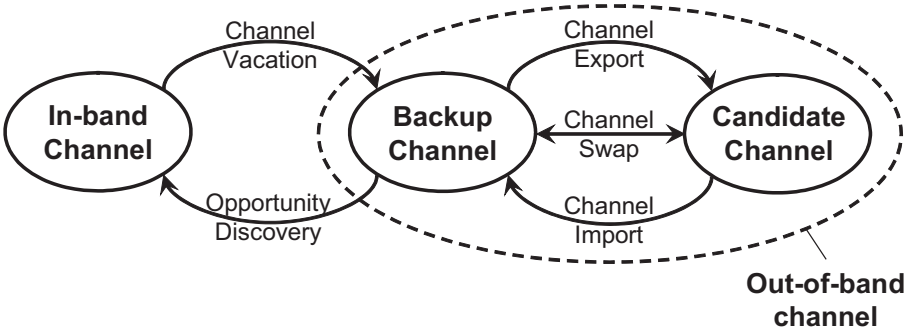

Figure 3.4: Transition of channel association

Channel exports/imports/swaps are triggered to update the entries of BCL: (1) if the BCL contains backup channels more than necessary, the backup channels with 'poor' quality can be exported to CCL, (2) if the BCL needs more channels to provide enough spectrum opportunities, a set of candidate channels can be imported to BCL, and (3) a channel swap exchanges the worst backup channel with the best candidate channel.

3.6.1 Construction of Initial BCL

Initially, we assume there are M licensed channels with no prior knowledge on their channel availability (i.e., θ_i), because samples are not yet collected from those channels. Without knowing θ_i, we contruct the initial BCL by randomly selecting N channels from the M channels. From the thus-chosen N channels, the CRN finds in-band channels to start its network with by performing an initial scan. Then, the remaining $(M - N)$ channels are placed in the initial CCL. Note that we define BCL as a combination of in-band channels and (out-of-band) back-up channels, and thus N will henceforth be used to denote the number of in-band channels plus the number of back-up channels.

One may want to restrict N within some range such as $N_{lower} \leq N \leq N^{upper}$, where N_{lower} and N_{upper} are design parameters. N_{lower} helps reserve a minimal num-

ber of backup channels so that opportunity-discovery may be successful. On the other hand, N^{upper} upper-bounds the computational overhead in sorting backup channels.

3.6.2 Periodic BCL Update

The entries of BCL must be constantly updated for the following reasons. First, as the sensing accumulates samples of backup channels,[4] channel parameters are estimated more accurately, and thus, θ_i can be predicted more reliably. Second, the channel parameters of the ON/OFF distribution may vary with time.

Our goal is to maintain 'good' N channels so that they may contain opportunities more than B_{req} with probability *thPOTENTIAL*, which is a pre-defined threshold (e.g., *thPOTENTIAL*= 0.9). More formally, we build a sequence of channels $L_N = \{l_1, l_2, \ldots, l_N\}$ where in-band channels are placed first (in any order) and the backup channels are placed last in descending order of $C_i \cdot \theta_i$ which is called *effective capacity* of channel i. Then, we calculate $\mathcal{C}_{L_N}^{B_{req}}$, *capacity potential of* B_{req} *in* L_N, representing the probability that L_N may contain more opportunities than B_{req}, such that

$$\mathcal{C}_{L_N}^{B_{req}} := \sum_{z_1=0}^{1}\sum_{z_2=0}^{1}\cdots\sum_{z_N=0}^{1}\left\{\prod_{v=1}^{N}(\theta_{l_v})^{1-z_v}(1-\theta_{l_v})^{z_v} \times \left(I_{\{\sum_{w=1}^{N} C_{l_w}(1-z_w)\geq B_{req}\}}\right)\right\} = 1 - \mathcal{P}_{L_N}^{B_{req}}.$$

Using $\mathcal{C}_{L_N}^{B_{req}}$, we propose an efficient and light-weight BCL update strategy that sorts BCL or CCL separately and only when necessary. In this strategy, BCL is updated periodically every *tUPDATE* seconds, and at BCL update $\mathcal{C}_{L_N}^{B_{req}}$ is calculated using the most recent channel estimates. According to $\mathcal{C}_{L_N}^{B_{req}}$, one of the following actions is taken: channel *export* (BCL $\rightarrow$ CCL), channel *import* (BCL $\leftarrow$ CCL), and channel *swap* (BCL $\leftrightarrow$ CCL).

[4] As discussed in Section 3.4.2, the samples are collected via opportunity discovery (if the channel is a backup channel) and/or extra sampling scheduled by the central controller.

Channel export

If $\mathcal{C}_{L_N}^{B_{req}} > thPOTENTIAL^{upper}$, we export a certain number of least preferred channels from BCL since it contains more channels than necessary. We use $thPOTENTIAL^{upper} = thPOTENTIAL + \epsilon_1$ ($\epsilon_1 > 0$) to avoid any impetuous channel export. To export channels, we find the optimal $N = N^*$ using the sequence L_N such that

$$N^* = min\left\{N | \mathcal{C}_{L_N}^{B_{req}} \geq thPOTENTIAL\right\}.$$

Then, we export the last $\min\{N - N^*, N_{backup}\}$ channels in the sequence to CCL, where N_{backup} implies the number of backup channels. Here the term N_{backup} is necessary to avoid exporting current in-band channels.

Channel import

If $\mathcal{C}_{L_N}^{B_{req}} < thPOTENTIAL_{lower}$, a number of candidate channels are imported from CCL to satisfy $\mathcal{C}_{L'_N}^{B_{req}} \geq thPOTENTIAL$, where L'_N is an extended BCL after importing the CCL channels. We use $thPOTENTIAL_{lower} = thPOTENTIAL - \epsilon_2$ ($\epsilon_2 > 0$) to avoid impetuous channel import. To import channels, candidate channels are sorted in descending order of $C_i \cdot \theta_i$ and are imported to BCL one by one to augment L_N by adding the imported channels at the end, until $\mathcal{C}_{L'_N}^{B_{req}} \geq thPOTENTIAL$ is met. In case the imported channel has never been sensed, we assume it has $\theta_i = 1/2$.

Channel swap

When N_{lower} and N^{upper} are used, channel export (or import) cannot be processed if $N^* = N_{lower}$ (or N^{upper}). In such a case, we *swap* the least preferred backup channel with the most preferred candidate channel if the swap helps decrease/increase $\mathcal{C}_{L_N}^{B_{req}}$

as desired.

3.7 Channel-Parameter Estimation

In Section 3.4, we described how to predict θ_i, an element indispensable to the formulation of the optimal sensing sequence. There we also showed that θ_i is a function of the ON/OFF distribution parameters, and thus, the estimation of the channel parameters' accuracy is a key to the performance of the optimal sensing sequence.

In [50] we introduced an ML estimator of the channel parameters, showing that the sampling period must be proportional to $min\{E[T^i_{ON}], E[T^i_{OFF}]\}$ to maintain a similar level of parameter estimation accuracy over channels. To achieve such sampling rates, the central controller of a CRN needs to perform extra sampling on backup channels in addition to the samples produced from opportunity discovery. However, the extra sampling may not be practical for the channels with short ON/OFF periods due to the high sensing overhead, making the ML estimator an unsuitable choice.

To overcome this problem, we introduce a hybrid estimation technique that utilize both ML and Bayesian estimation. Unlike large-sample asymptotic estimators (e.g., ML) whose estimation accuracy degrades as the channel is less infrequently sampled, Bayesian estimation is known to perform reasonably well even if the number/frequency of samples is limited [4]. Exploiting such features, we propose the following *hybrid* estimation strategy:

- Class-S channels: perform Bayesian estimation, and
- Class-L channels: perform ML estimation,

where *class-S* channels imply the channels with short ON/OFF periods and *class-L* channels imply the channels with long ON/OFF periods.

In what follows, we first introduce single-step Bayesian inference and its extension to multi-stage iterative estimation. We will then discuss how to reduce the computational complexity of the Bayesian estimation.

3.7.1 Single-Step Bayesian Inference

A single-step Bayesian inference [4] is summarized as follows. Suppose we have a vector of samples from channel i such as $\mathbf{Z}_k^i = (Z^i(t_1), Z^i(t_2), \ldots, Z^i(t_k))$, whose joint probability mass function (pmf) is $f(\mathbf{Z}_k^i|\boldsymbol{\psi}^i)$ which depends on the vector $\boldsymbol{\psi}^i \in \boldsymbol{\Psi}^i$ of the channel parameters of $f_{T_{ON}^i}(t)$ and $f_{T_{OFF}^i}(t)$. Denoting by $\pi(\boldsymbol{\psi}^i)$ a prior distribution of $\boldsymbol{\psi}^i$, the posterior distribution of $\boldsymbol{\psi}^i$ after observing $\mathbf{Z}_k^i$, denoted by $\pi(\boldsymbol{\psi}^i|\mathbf{Z}_k^i)$, is given as

$$\pi(\boldsymbol{\psi}^i|\mathbf{Z}_k^i) = \frac{\pi(\boldsymbol{\psi}^i) f(\mathbf{Z}_k^i|\boldsymbol{\psi}^i)}{f(\mathbf{Z}_k^i)} = \frac{\pi(\boldsymbol{\psi}^i) f(\mathbf{Z}_k^i|\boldsymbol{\psi}^i)}{\int_{\boldsymbol{\Psi}^i} \pi(\boldsymbol{\psi}^i) f(\mathbf{Z}_k^i|\boldsymbol{\psi}^i) d\boldsymbol{\psi}^i},$$

where $f(\mathbf{Z}_k^i)$ is the marginal joint pmf of $\mathbf{Z}_k^i$. Then, the estimates of $\boldsymbol{\psi}^i$ are obtained as

$$\hat{\boldsymbol{\psi}}^i = E[\boldsymbol{\psi}^i],$$

where $E[\cdot]$ is taken over the distribution $\pi(\boldsymbol{\psi}^i|\mathbf{Z}_k^i)$.

3.7.2 Iterative Bayesian Inference

We extend the single-step procedure in 3.7.1 to provide an iterative Bayesian process where estimates are produced each time a new sample is collected. Fig. 3.5 illustrates the concept of our iterative Bayesian inference. The process starts with an initial prior distribution $\pi(\boldsymbol{\psi}^i)$, and the first stage begins upon collection of the first two samples. Upon arrival of the $(k+1)$-th sample (i.e., at stage k), the k-th pair

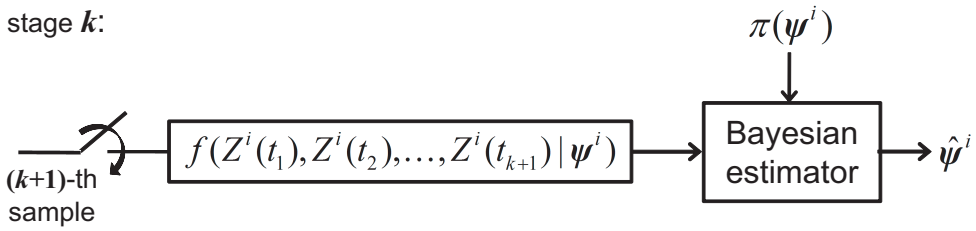

Figure 3.5: Iterative Bayesian inference

of new estimates are computed by using $\pi(\boldsymbol{\psi}^i)$ and $f(\mathbf{Z}_{k+1}^i|\boldsymbol{\psi}^i)$ of $(k+1)$ samples. Note that henceforth the channel index i will be omitted unless it causes ambiguity.

For an illustrative purpose, we use exponentially-distributed ON and OFF periods with pdfs of Eq.(3.1) to present the proposed procedure. Then, channel parameters to estimate are given as

$$\boldsymbol{\psi} = (\psi_{ON}, \psi_{OFF}), \;\; \boldsymbol{\Psi} = \{0, \infty\} \times \{0, \infty\}.$$

It should be noted, however, that the proposed procedure can be applied to any general pdfs of T_{ON} and T_{OFF}.

The initial prior distribution $\pi(\boldsymbol{\psi})$ is usually chosen with subjective reasoning. The criteria in selecting the prior is based on the prior knowledge of $\boldsymbol{\psi}$. For exponentially-distributed ON and OFF periods, $\pi(\boldsymbol{\psi}) = \pi(\psi_{ON}, \psi_{OFF})$ should be chosen to satisfy the following condition:

$$\psi_{ON} > 0, \;\; \psi_{OFF} > 0, \tag{3.11}$$

by the definition of exponential distribution. On the other hand, if some statistics are available on average ON and OFF periods on a large time-scale (e.g., a day or a week), such knowledge can be reflected in the choice of the prior. For example, suppose τ_{ON} and τ_{OFF} are the average ON and OFF periods in a day. Then, the prior knowledge can be used to form $\pi(\boldsymbol{\psi})$ such that

$$\tau_{ON} = 1/E[\psi_{ON}], \;\; \tau_{OFF} = 1/E[\psi_{OFF}], \tag{3.12}$$

since $\psi_{ON} = 1/E[T_{ON}]$ and $\psi_{OFF} = 1/E[T_{OFF}]$.

Here we assume τ_{ON} and τ_{OFF} are given, and the prior distribution is set as

$$\pi(\psi_{ON}, \psi_{OFF}) = \tau_{ON} e^{-\tau_{ON}\psi_{ON}} \cdot \tau_{OFF} e^{-\tau_{OFF}\psi_{OFF}},$$

or equivalently

$$\pi(u, \psi_{OFF}) = \tau_{ON}\tau_{OFF} e^{(\tau_{ON} - \tau_{OFF} - \tau_{ON}/u)\psi_{OFF}},$$

where ψ_{ON} and ψ_{OFF} are assumed to be exponentially-distributed with mean τ_{ON} and τ_{OFF}, respectively.[5] Setting the prior distribution as above can satisfy the conditions (3.11) and (3.12).

Considering the fact that an alternating renewal process is semi-Markov [20], $f(\mathbf{Z}_{k+1}|\boldsymbol{\psi})$ at stage k becomes

$$f(\mathbf{Z}_{k+1}|\boldsymbol{\psi}) = f(Z_{t_1}|\boldsymbol{\psi}) f(Z_{t_2}|Z_{t_1}, \boldsymbol{\psi}) \cdots f(Z_{t_{k+1}}|Z_{t_k}, \boldsymbol{\psi}).$$

The derivation of the transition probability $f(Z_{t_{j+1}}|Z_{t_j}, \boldsymbol{\psi})$, $j = 1, 2, \ldots, k$, for arbitrarily-formed $f_{T_{ON}}(t)$ and $f_{T_{OFF}}(t)$ can be found in [20]. For example, with exponentially-distributed ON and OFF periods, we can show

$$\begin{aligned} f(Z_{t_1}|\boldsymbol{\psi}) &= (1-u)^{1-Z_{t_1}} u^{Z_{t_1}}, \\ f(Z_{t_{j+1}}|Z_{t_j}, \boldsymbol{\psi}) &= (1-u)^{1-Z_{t_{j+1}}} \cdot u^{Z_{t_{j+1}}} + (-1)^{Z_{t_j}+Z_{t_{j+1}}} \cdot \\ &\qquad u^{1-Z_{t_j}} \cdot (1-u)^{Z_{t_j}} \cdot e^{-\psi_{OFF}\Delta_j/u}, \end{aligned} \tag{3.13}$$

where $\Delta_j = t_{j+1} - t_j$.

[5] Note that modeling ψ_{OFF} and ψ_{ON} to be exponentially-distributed has nothing to do with exponentially-distributed ON and OFF periods.

Now, $f_k(\mathbf{Z}_{k+1})$ at stage k is derived as

$$\begin{aligned} f_k(\mathbf{Z}_{k+1}) &= \int_0^\infty \int_0^\infty \pi(\boldsymbol{\psi}) f(\mathbf{Z}_{k+1}|\boldsymbol{\psi}) d\psi_{ON} d\psi_{OFF} \\ &= \int_0^1 \int_0^\infty \pi(u, \psi_{OFF}) \cdot (1-u)^{1-Z_{t_1}} u^{Z_{t_1}} \\ &\quad \cdot \left\{ \prod_{j=1}^{k} f(Z_{t_{j+1}}|Z_{t_j}, \boldsymbol{\psi}) \right\} \cdot \left(\frac{\psi_{OFF}}{u^2} \right) d\psi_{OFF} du, \end{aligned}$$

which provides a closed-form solution by transforming the product of sums with k terms, $\prod_{j=1}^{k} f(Z_{t_{j+1}}|Z_{t_j}, \boldsymbol{\psi})$, into a sum of products with 2^k terms. We then obtain two estimates $\hat{\psi}_{ON}$ and $\hat{\psi}_{OFF}$ at stage k as

$$\begin{aligned} \hat{\psi}_{ON,k} &= \int_0^\infty \int_0^\infty \psi_{ON} \cdot \pi(\boldsymbol{\psi}|\mathbf{Z}_{k+1}) d\psi_{ON} d\psi_{OFF} \\ &= \int_0^1 \int_0^\infty \psi_{OFF} \left(\frac{1}{u} - 1 \right) \frac{\pi(u, \psi_{OFF}) f(\mathbf{Z}_{k+1}|\boldsymbol{\psi})}{f_k(\mathbf{Z}_{k+1})} \cdot \left(\frac{\psi_{OFF}}{u^2} \right) d\psi_{OFF} du, \\ \hat{\psi}_{OFF,k} &= \int_0^\infty \int_0^\infty \psi_{OFF} \cdot \pi(\boldsymbol{\psi}|\mathbf{Z}_{k+1}) d\psi_{ON} d\psi_{OFF} \\ &= \int_0^1 \int_0^\infty \psi_{OFF} \frac{\pi(u, \psi_{OFF}) f(\mathbf{Z}_{k+1}|\boldsymbol{\psi})}{f_k(\mathbf{Z}_{k+1})} \cdot \left(\frac{\psi_{OFF}}{u^2} \right) d\psi_{OFF} du, \end{aligned}$$

where both of which provide closed-form estimators with the same transformation as in $f_k(\mathbf{Z}_{k+1})$. The derived Bayesian estimators work as fast as ML estimators since both are expressed in closed forms.

3.7.3 Complexity Reduction

Despite its simplicity and good performance, Bayesian inference suffers from computational complexity inherent in integration of pdfs to produce $f_k(\mathbf{Z}_{k+1})$ and $\hat{\boldsymbol{\psi}}$. In case there are no closed-form solutions for them, the complexity grows exponentially as the number of stages increases, although the number of samples increases linearly.

To overcome this problem, we make a few adjustments to the proposed scheme. First, *MAX_BS_STAGE*, a design parameter, is introduced such that the process resets to stage 1 whenever the current stage number reaches *MAX_BS_STAGE*. When

it resets, the prior distribution $\pi(\boldsymbol{\psi})$ is updated with the most recent estimates. That is, τ_{ON} and τ_{OFF} in $\pi(\boldsymbol{\psi})$ are replaced by $1/\hat{\psi}_{ON}$ and $1/\hat{\psi}_{OFF}$ respectively, where $\hat{\psi}_{ON}$ and $\hat{\psi}_{OFF}$ are the most recent estimates.

Next, a pre-computed *look-up* table is used to evaluate the integrals. When an integration does not provide an analytical solution, numerical integration (e.g., Simpson's rule) or Monte Carlo integration [4] can be used. Through a series of computations, the estimates of unknown parameters can be pre-computed for each possible pair of sample values and their timestamps. This way, the computational complexity of Bayesian estimation can be bounded reasonably small.

3.8 Performance Evaluation

To demonstrate the efficacy of the proposed schemes, we conducted two types of simulation. The first test in Section 3.8.1 compares the average opportunity-discovery delay of the proposed near-optimal sequence with the optimal DP-based sequence and previously-proposed probabilistic sequences (i.e., sorting channels in descending order of θ_i) in [45, 50]. The second test in Section 3.8.2 demonstrates the performance improvement of the BCL update strategy compared to the case without BCL update.

The simulation parameters for the tests are summarized in Table 3.2. For channel i, we set

$$T_I^i = T_I^{max} - (2 \cdot T_I^{max} - 26) \cdot (i-1)/(M-1) \text{ in msec,}$$

$$u^i = 0.4 \cdot (i-1)/(M-1) + (\bar{u} - 0.2),$$

where T_I^{max} and $\bar{u}$ are shown in Table 3.2.

Channels are simulated as alternating renewal processes with exponentially-distributed ON and OFF periods. The channel parameters ψ_{ON} and ψ_{OFF} are assumed time-

Test 1	Test 2
$M = 12$	$M = 18$
$C_i = 1.0$ for $i \in \{1, 2, 3\}$ $C_i = 2.5$ for $i \in \{4, 5, 6\}$ $C_i = 4.0$ for $i \in \{7, 8, 9\}$ $C_i = 5.5$ for $i \in \{10, 11, 12\}$	$C_i = 1.0$ for $i \in \{1, 2, 3\}$ $C_i = 2.5$ for $i \in \{4, 5, 6, 7\}$ $C_i = 4.0$ for $i \in \{8, 9, 10, 11\}$ $C_i = 5.5$ for $i \in \{12, 13, 14, 15\}$ $C_i = 7.0$ for $i \in \{16, 17, 18\}$
Test 1(a): $B_{req} = 8$, $T_I^{max} = 25$, $\bar{u} = 0.4 - 0.6$ Test 1(b): $B_{req} = 6 - 10$, $T_I^{max} = 25$, $\bar{u} = 0.4$ Test 1(c): $B_{req} = 8$, $T_I^{max} = 14.5 - 25$, $\bar{u} = 0.4$	

Table 3.2: Test-specific simulation parameters, $i \in \{1, \ldots, M\}$

varying and increasing/decreasing by 10% every 100 seconds. In addition, Test 1 sets $1.0 \leq E[T_{ON}^i] \leq 1.45$ (in seconds) and Test 2 uses 12 channels with $1.0 \leq E[T_{ON}^i] \leq 1.45$ and 6 channels with $E[T_{ON}^i] \in \{15, 20\}$.

For every test, a single simulation ran for 1,000 seconds, and the same test was repeated 10 times to take the average performance. Other test parameters are set as follows: $tRETRY = 0.1$, $tUPDATE = 5$, $thPOTENTIAL = 0.9$, $thPOTENTIAL_{lower} = 0.88$, $thPOTENTIAL^{upper} = 0.93$, $N_{lower} = 5$, and $N^{upper} = 10$.

For all tests, we use the average delay as a yardstick in discovering opportunities. The average discovery-delay is captured by considering two different cases: (1) when opportunity discovery completes during the first round of searching backup channels (called *Type-I delay*), and (2) when it completes during the successive retries, provided the first round failed (called *Type-II delay*). The Type-I delay says how efficient a sensing sequence is, whereas the Type-II delay shows how efficiently the BCL is constructed/updated so that opportunity discovery may be successful at early rounds.

In our simulations, we assume perfect estimates and perfect sensing (i.e., $P_{MD} \approx 0$ and $P_{FA} \approx 0$), which helps us focus on the efficacy of the proposed sensing-sequence and BCL update strategies. It should be noted, however, that this assumption is made only for an illustrative purpose, and our schemes can adopt the schemes in Section 3.7 for estimation and Section 3.4.2 for imperfect sensing.

3.8.1 Test 1: Performance of Proposed Sequence

In this test, the proposed suboptimal sensing-sequence is compared with the optimal sequence given by the DP algorithm, along with the probabilistic sequence that sorts channels in descending order of θ_i and a random sequence. We tested three scenarios where either $\bar{u}$, B_{req}, or T_I^{max} varies. The case of varying T_I^{max} corresponds to the standard deviation of T_I^i's varying from 1 to 8. In addition, no BCL update is performed to focus on the performance of the sequences.

Fig. 3.6 plots the simulation results. The proposed suboptimal sequence shows a near-optimal performance in all three scenarios incurring only a 0.16–1.3% (average: 0.5%) longer delay than the optimal performance. Moreover, the proposed scheme is shown to enhance the delay by 19.8–50.1% (average: 41.2%) against the probabilistic sequence and by 15.3–38.0% (average: 30.9%) against the random sequence. Interestingly, the previously-proposed probabilistic sequence performs even worse than the random one in the tested scenario, since the channels with smaller u^i (i.e., lower-indexed channels) incur larger sensing-time while providing smaller capacities. This shows that the optimal sequence can only be derived by considering all three channel characteristics defined by the tuple of (C_i, T_I^i, θ_i).

We have also measured how many times *channel-state conversion* occurs, which is the event where at least one idle channel discovered by sequential sensing becomes

busy again at the completion of the sequential sensing. In the tested scenarios, each sequential sensing senses 4.4 channels on the average, and after sensing the channels channel-state conversion occurs 5.9% of the time on the average. The reason we have such a moderate conversion rate is that each sequential sensing requires to discover only a few idle channels to compensate for the bandwidth of the vacated channel. Even if channel-state conversion occurs, however, in-band sensing detects the event and immediately triggers a subsequent sequential sensing where the proposed (near)optimal sequence still plays a significant role in minimizing the additional delay, as discussed in Section 3.5.5.

3.8.2 Test 2: BCL Update vs. No BCL Update

In this test, the efficiency of the proposed BCL update strategy is evaluated and compared with another scheme with no BCL update. Both schemes initialize their BCL assuming no prior knowledge on the ON/OFF usage patterns. As the simulation progresses, however, the proposed scheme updates BCL via channel import/export/swap and adjusts the BCL size accordingly, whereas the latter scheme always stays with its initial BCL entries. In addition, both schemes use the proposed suboptimal sequence.

In Fig. 3.7, we plot the average 'overall' delay (i.e., Type-I and Type-II combined) with the delay-type ratio between the number of Type-I events and that of Type-II events. The proposed BCL update scheme flexibly adjusts its BCL size from 5 to 10 to maximize the chance of successful opportunity discovery at the first round of sequential sensing, and thus the BCL update case incurs more Type-I events than Type-II events compared to the no-update case (as shown for $\bar{u} \geq 0.45$) reducing the overall delay by 7.7–49.9% (average: 35.7%). This is because the Type-II delay is

more costly due to the huge delays in retrying sequential sensing.

3.9 Conclusion

In this paper, we proposed a DP-based optimal sensing-sequence and a computationally efficient near-optimal sensing-sequence for fast discovery of spectrum opportunities to promote seamless service provisioning of CRNs while minimizing QoS degradation. To support the proposed fast opportunity discovery mechanism, we also proposed an efficient backup channel list (BCL) management algorithm and a hybrid estimation strategy of ML and Bayesian inference for reliable estimation of channel-usage patterns.

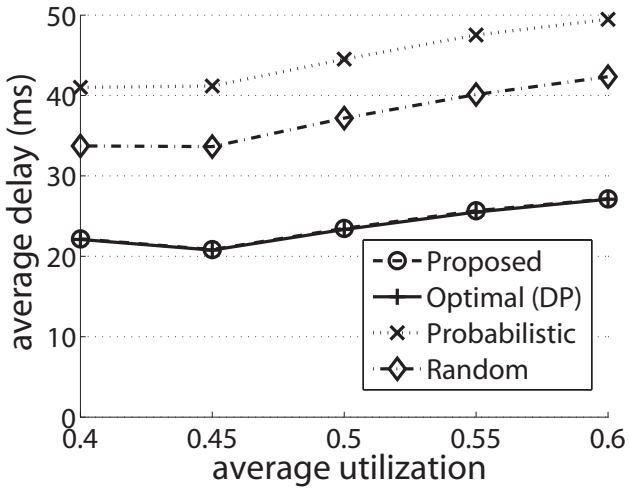

(a) Varying u^i

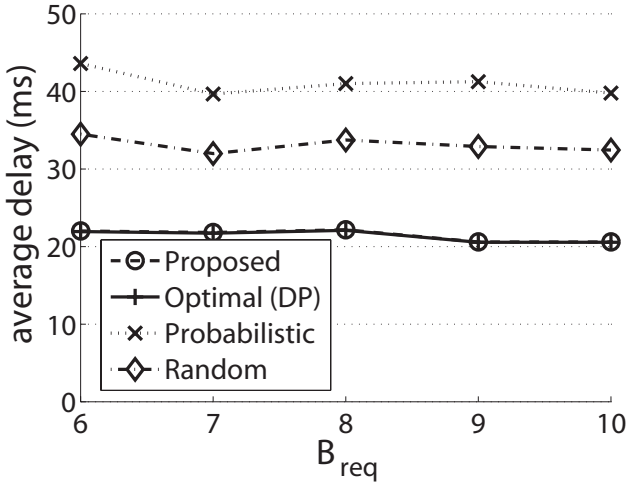

(b) Varying B_{req}

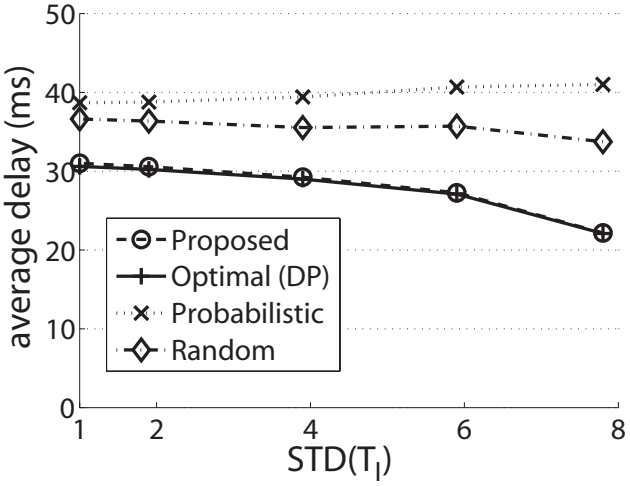

(c) Varying T_I^i

Figure 3.6: Test 1: performance of the proposed sequences

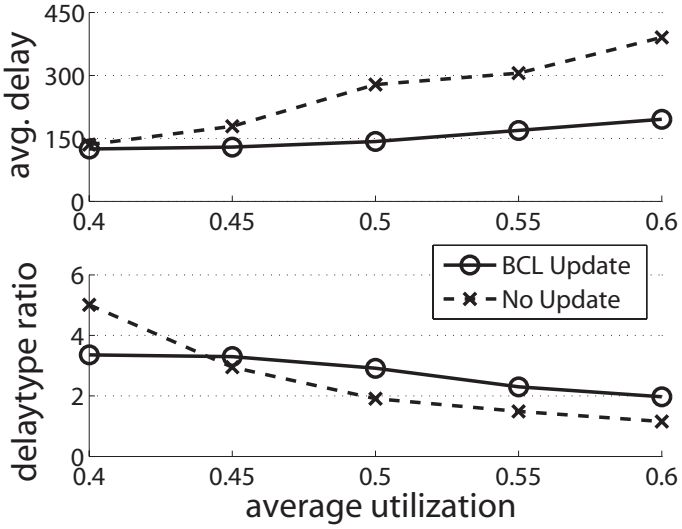

Figure 3.7: Test 2: proposed BCL update vs. no update

CHAPTER IV

IN-BAND SENSING: PROTECTION OF LEGACY SPECTRUM USERS

4.1 Introduction

One of the major challenges in cognitive radio networks (CRNs) is to strike a balance between (1) protection of primary users (PUs) against interference from secondary users (SUs) and (2) efficient reuse of legacy spectrum. For maximal protection of PUs, the FCC has set a strict guideline on in-band sensing. For example, in IEEE 802.22 Wireless Regional Area Networks (WRANs), the world's first international CR standard, PUs should be detected within 2 seconds of their appearance with the probabilities of misdetection (P_{MD}) and false detection (P_{FA}) no greater than 0.1. To meet these requirements, in-band sensing must be run frequently enough (at least once every 2 seconds) and a detection method (e.g., energy or feature detection [18]) that yields the best performance should be selected. The impact of spectrum sensing on SUs' quality-of-service (QoS) impairment should also be considered since sensing is performed during *quiet periods* [1,18], within which communications between SUs are suspended.

In this chapter, we present several techniques for efficient in-band sensing in IEEE 802.22. We first advocate use of clustered sensor networks and identify its unsolved

research issues. We then show how to schedule in-band sensing in order to enhance both sensing performance and SUs' QoS in CRNs. Finally, we investigate how strict detection requirements should be, in order to avoid unnecessary channel-switches due to false detection of incumbents.

4.1.1 Sensor Clustering

Collaborative sensing [31] is known to be essential for accurate detection of PUs as it exploits sensor diversity via simultaneous sensing of a channel at multiple locations. Presence/absence of PUs on a channel is determined by data fusion of the simultaneous measurements, and OR-rule [34] is the most common fusion rule under which a channel is considered occupied by PUs if at least one sensor reports so. Its sensing performance with N cooperative sensors has been shown as

$$P_{MD}(N) = (P_{MD})^N \text{ and } P_{FA}(N) = 1 - (1 - P_{FA})^N \tag{4.1}$$

under the assumption that every sensor has the same P_{MD} and P_{FA} for a given signal.

Eq. (4.1), however, does not hold in a large CRN such as the IEEE 802.22 WRAN in which a base station (BS) covers an area of radius ranging from 33 km (typical) to 100 km [18]. In such a case, the average received signal strength[1] (RSS) of a primary signal at two distant sensor locations (e.g., CPE A and CPE B in Fig. 4.1) may vary greatly. Therefore, the heterogeneity of sensors' P_{MD} and P_{FA} values must be considered in analyzing the performance of collaborative sensing, making it harder to determine how many and which sensors are needed to achieve the target sensing performance.

This problem can be avoided or alleviated by using a *clustered* sensor network, which groups sensors in close proximity into a cluster so that they can acquire a

[1]Note that the average received signal strength is given by *empirical* large-scale path loss in the shadow-fading channel model in [37].

similar average RSS of any primary signal and thus Eq. (4.1) can still hold. Sensor clustering also mitigates the control overhead in data fusion, because each cluster head (CH) makes a local decision based on intra-cluster (i.e., local) measurements and then reports it to the BS.

Contributions — Although there has been considerable research into clustered CR sensor networks [13, 62, 88], two important issues have not yet been addressed: (1) cluster-area size and (2) sensor density. Section 4.4 addresses these two issues as follows. First, we will derive the maximum radius of a cluster's area so as to upper-bound the variation of the average RSS within a cluster by 1 dB. Second, we will derive the maximum sensor density to guarantee near-independent sensor observations, by suppressing the shadow-fading correlation [38] to be below 0.3. With this approach, one-time (collaborative) in-band sensing in a cluster can be effectively captured by Eq. (4.1) with N as the number of sensors within the cluster.

4.1.2 Scheduling of In-band Sensing

IEEE 802.22 provides the *two-stage sensing* (TSS) mechanism that selectively uses energy and feature detection in a quiet period. Although energy detection requires less sensing time (e.g., 1 ms), its susceptibility to *noise uncertainty* [89] limits its usability. By contrast, feature detection is less susceptible to noise uncertainty [90], while it requires a larger sensing time (e.g., 24.2 ms [18]).

The current IEEE 802.22 draft standard, however, does not specify how often to schedule sensing and which detection method to use, and under what condition. Although there have been several studies on the performance of energy and feature detection [11, 36, 77], they were all based on a one-time detection. Hence, we will study how to enhance detection performance by scheduling sensing and investigate

which of energy and feature detection is preferred under what conditions.

Contributions — In Section 4.5, we propose *periodic* sensing scheduling that (1) minimizes sensing overhead by optimizing the sensing period (T_P) and the sensing time (T_I), and (2) chooses the better of energy or feature detection in a given sensing environment. Then, in Section 4.6, we consider SNR_{wall} [89, 90], the minimum SNR threshold *due to noise uncertainty* below which a detector completely fails to detect a signal regardless of the sensing time. Although it has been believed that the SNR_{wall} of energy detection is an absolute barrier, we will show it is true only with the AWGN channel while in reality the barrier becomes obscure with the shadowing channel, making the energy detection still a good candidate due to its small T_I. Finally, two important factors affecting the detection performance—noise uncertainty and inter-CRN interference—will be considered in deriving two SNR thresholds above which energy detection becomes (1) feasible to use and (2) preferred to feature detection. We also derive the minimum number of collaborative sensors required for feasible energy detection.

4.1.3 False Detection vs. Efficient Channel-Reuse

The current 802.22 draft requires the detection performance should satisfy $P_{MD} \leq 0.1$ and $P_{FA} \leq 0.1$, where their purposes on spectrum reuse are vastly different. First, the constraint on P_{MD} focuses on the protection of PUs by encouraging prompt and accurate detection of the returning PUs. On the contrary, the constraint on P_{FA} aims to enhance the QoS of SUs by avoiding impatient channel-switching caused by false detection of PUs.

Despite its importance, the impact of P_{FA} has been received less attention. As P_{FA} becomes larger, a CRN will unnecessarily vacate an in-band channel and switch

to another channel even at PUs' absence. Once a channel is vacated, it is not allowed to be sensed or reused at least for 10 minutes [84], and hence, the pool of idle channels will soon be depleted as the CRN makes such unnecessary channel-switches. This implies that P_{FA} should be set small enough not to impair SUs' operation.

Contributions — In Section 4.7, we investigate if the current upper-bound of 0.1 on P_{FA} is efficient in terms of the expected reuse time of an in-band channel. For this, we express the expected channel-reuse time as a function of P_{FA}, and vary the upper-bound of P_{FA} from 0.001 to 0.1 to evaluate how much we can enhance the channel-reuse time, and at what cost. Based on these results, we will show that P_{FA} needs to be set to be below 0.001, not 0.1, for practically meaningful channel-reuse, and will also show that the new constraint induces similar sensing overhead as in the $P_{FA} \leq 0.1$ case when both achieving $P_{MD} \leq 0.1$.

4.1.4 Organization

The rest of the chapter is organized as follows. Section 4.2 briefly overviews related work, followed by Section 4.3 which reviews IEEE 802.22 and PHY-layer signal detection methods. In Section 4.4, we introduce the concept of sensor clustering, and derive the maximum radius of a cluster as well as the maximum sensor density. Section 4.5 describes the proposed in-band sensing algorithm that can be used in a cluster. Then, in Section 4.6, we study if simple energy detection is feasible to meet the detection requirements in a very low SNR environment and under what condition it becomes more efficient than feature detection, considering two important factors: noise uncertainty and inter-CRN interference. Finally, Section 4.7 investigates how strict detection requirements should be for efficient reuse of an idle channel without incurring too frequent channel-switches, and the chapter concludes in Section 4.8.

4.2 Related Work

There have been continuing discussions on use of clustered networks in CRs. Chen *et al.* [13] proposed a mechanism to form a cluster among neighboring nodes and then interconnect such clusters. Pawelczak *et al.* [62] proposed cluster-based sensor networks to reduce the latency in reporting sensor measurements by designating the cluster head as a local decision maker. Sun *et al.* [88] enhanced performance by clustering sensors where the benefit comes from cluster and sensor diversities. None of these authors, however, mentioned the importance of optimizing cluster size and sensor density.

Despite numerous existing studies on the performance of one-time signal detection in CRs, the optimal scheduling of in-band sensing has not received much attention. Cordeiro *et al.* [18] evaluated the performance of fast sensing in 802.22 by scheduling it (1 ms) every 40 ms, but they did not optimize the sensing-time and sensing-period. Datla *et al.* [21] proposed a backoff-based sensing scheduling algorithm, but their scheme was not designed for detecting returning PUs in an in-band channel. Hoang and Liang [42] introduced an adaptive sensing scheduling method to capture the tradeoff between SUs' data-transmission and spectrum-sensing. Their scheme, however, did not focus on protection of in-band PUs.

4.3 System Model

4.3.1 IEEE 802.22

In this chapter, we consider important issues of in-band sensing in IEEE 802.22 WRANs. The IEEE 802.22 WRAN is an infrastructure-based wireless network where a Base Station (BS) coordinates nodes in a single-hop cell which covers an area of radius ranging from 33 km (typical) to 100 km. End-users of an 802.22 cell are called

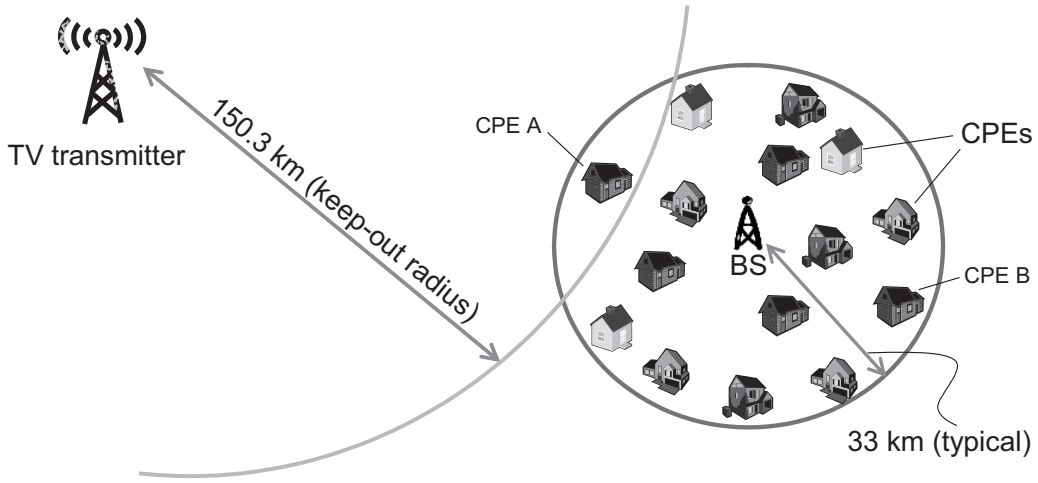

Figure 4.1: Illustration of an IEEE 802.22 WRAN

Consumer Premise Equipments (CPEs) representing households in a rural area (and hence stationary nodes).

802.22 reuses UHF/VHF bands where three types of primary signals present: Analog TV (ATV), Digital TV (DTV), and wireless microphone (WM). Our proposed schemes in this chapter mostly consider DTV transmitters as the major source of primary transmission, and their extension for WMs is also discussed.[2] By considering the minimum D/U (Desired to Undesired) signal ratio of 23 dB and the DTV protection contour of 134.2 km, the keep-out radius of CPEs from the DTV transmitter is given as 150.3 km [77]. CPEs within this keep-out radius are forced to avoid use of the DTV channel. Fig. 4.1 illustrates this scenario.

In 802.22, sensing must be performed during a quiet period within which no CPEs are allowed to transmit so that any signal detected by sensors should originate from PUs. The quiet periods have to be synchronized among sensors in the same cell as well as between neighboring cells, which is achieved by exchanging Coexistence Beacon Protocol (CBP) frames [18].

[2]After ATV to DTV transition, ATV is no more of our interest.

4.3.2 Channel and Sensing Model

We follow the channel and sensing model introduced in Chapter I. In addition, we assume each sensing performs either energy or feature detection. Therefore, we briefly overview the two detection methods used in IEEE 802.22, along with their theoretical performance in terms of P_{MD} and P_{FA}.

Energy Detection

Energy detection is the most popular detection method due to its simple design and small sensing time. Shellhammer *et al.* [77] analyzed the energy detection of a DTV signal using its discrete-time "PHY-layer" samples, where the signal is sampled by its Nyquist rate of 6 MHz.[3] The detection threshold γ to yield P_{FA} is then

$$\gamma = N_d B \left(1 + \frac{Q^{-1}(P_{FA})}{\sqrt{M_s}}\right), \tag{4.2}$$

and P_{MD} with γ is given as

$$P_{MD} = Q\left(\frac{\sqrt{M_s}}{P + N_d B}\left[(P + N_d B) - \gamma\right]\right). \tag{4.3}$$

where M_s is the number of samples,[4] N_d the noise power spectral density (PSD), B the signal bandwidth (6 MHz), P the signal power, and $Q(\cdot)$ the Q function.

Note that the effect of multipath fading is insignificant in detecting a DTV signal due to frequency diversity over the 6 MHz band [77, 90]. Instead, the impact of shadow fading must be considered in the variation of RSS at different sensor locations. Ghasemi and Sousa [35] derived the average performance of energy detection by numerically integrating P_{MD} over the fading statistics.

[3]The DTV signal ranges from -3 MHz to +3 MHz in the baseband.

[4]By 'sample,' we mean a "PHY-layer" sample at the ADC, which has nothing to do with the "MAC-layer" sample indicating 'idle' or 'busy'. That is, the ADC samples a channel M_s times during T_I at each sensing time.

Feature Detection

Feature detection captures a specific signature of a DTV signal, such as pilot, field sync, segment sync, or cyclostationarity [18]. Each feature detector is reviewed briefly for completeness.

ATSC uses 8-VSB to modulate a DTV signal, and an offset of 1.25 is added to the signal which creates a *pilot signal* at a specific frequency location. The authors of [78] introduced pilot energy detection which filters the DTV signal with a 10 KHz narrowband filter at the pilot's frequency location. They showed that the pilot signal's SNR is 17 dB higher than the DTV signal's SNR, making it a strong feature to detect.

A DTV data segment starts with a *data segment sync* of pattern {+5 -5 -5 +5}. A data field consists of 313 data segments, and the first data segment of each data field is called a *field sync segment* which contains special pseudo-random sequences: PN511 and PN63. Therefore, segment sync and field sync can be used as a unique feature to detect. Detectors of such features are introduced in [13,18,74], where P_{MD} and P_{FA} are not analytical derived but evaluated only by simulation.

Since the DTV signal is digitally modulated, it shows the cyclostationary feature. The cyclostationary detection of ATSC and DVB-T DTV signals has been studied in [13, 36, 40], where its performance is investigated by simulation because it is mathematically intractable to derive P_{MD} and P_{FA} of cyclostationary detectors for complex modulation schemes (e.g., 8-VSB) [69].

In this chapter, we use the pilot energy detector (henceforth called simply "pilot detector") as an illustrative example of the feature detectors to evaluate the tradeoffs between energy and feature detection. The pilot detector has an advantage of others since its P_{MD} and P_{FA} have been completely analyzed [78], but other types of feature

detectors can also be considered by evaluating their P_{MD} and P_{FA} via simulation at various detection thresholds for which the real DTV signal capture [92] and the sensing simulation model [80] can be utilized.

In [78], P_{MD} and P_{FA} of the pilot detector are derived similarly to energy detection, using a 70 KHz bandpass filter in capturing the pilot signal to overcome uncertainty in the pilot locations and inaccuracy in the local oscillator (LO). Hence, we will use the sampling frequency of 70 KHz, instead of 10 KHz, in our analysis. Unlike energy detection in a 6 MHz bandwidth, Rayleigh fading becomes a significant factor due to the narrow band of 70 KHz, and we thus consider both Rayleigh and lognormal shadow fading to derive P_{MD} and P_{FA}.

4.4 Spectrum Sensor Clustering

As discussed in Section 4.1, sensor clustering can make the behavior of collaborative sensing more predictable and can achieve scalability in collecting measurements for data fusion by enabling cluster heads (CHs) to make local decisions. The concept of the 2-tiered sensor cluster network is illustrated in Fig. 4.2. In this section, we identify two important but yet-unsolved challenges in sensor clustering: cluster size and sensor density.

4.4.1 Cluster Size

We derive the maximum radius of a sensor cluster such that the variation of the average RSS in the cluster is bounded by 1 dB, to make it possible to use Eq. (4.1) in modeling the performance of a collaborative sensor network. The effect of fading is considered by averaging P_{MD} in Eq. (4.3) over the fading statistics (Rayleigh and/or lognormal) and by substituting it into Eq. (4.1).

In a cluster, the variation of the average RSS is maximized by the two sensors

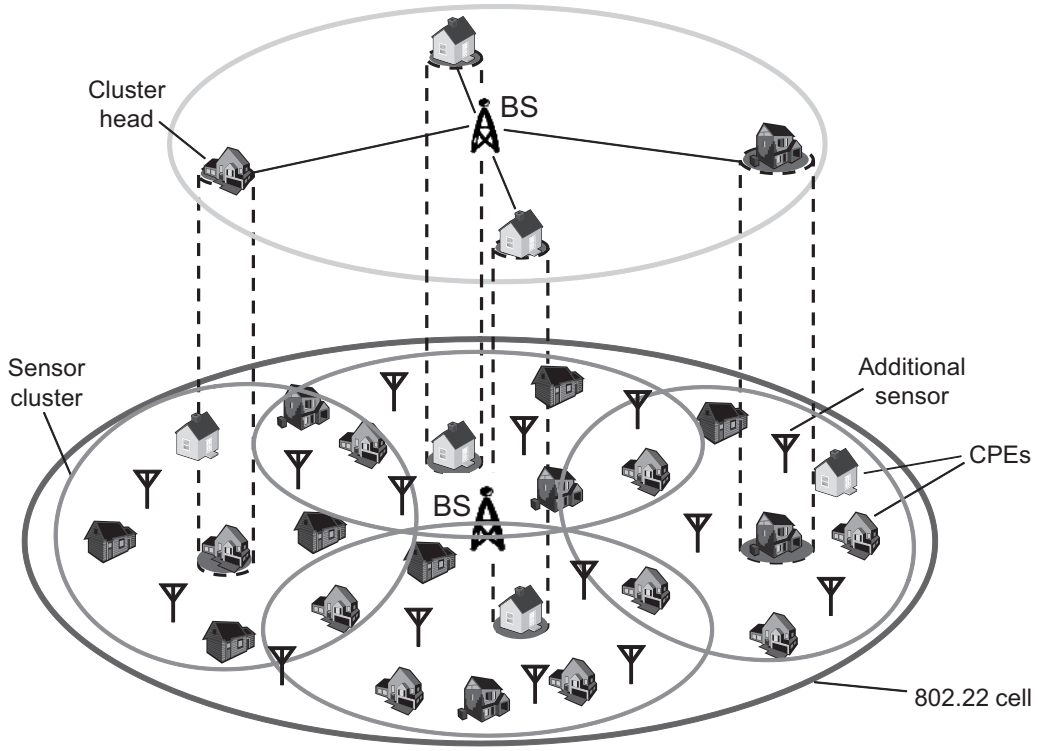

Figure 4.2: An illustration of clustered sensor networks

located at $(R - R_c)$ and at $(R + R_c)$ meters away from a primary transmitter (PT), respectively, where R is the distance between the PT and the center of the cluster, and R_c is the radius of the cluster. Then, using the polynomial power decay path-loss model [70] where the average RSS at a sensor r meters away from the PT is given as $P_1 r^{-\alpha_{12}}$ (P_1 is the PT's transmit power and α_{12} is the path loss exponent), the maximum cluster size is determined as

$$10\alpha_{12} log_{10}\left(\frac{R + R_c}{R - R_c}\right) \leq 1(dB),$$

which gives

$$R_c = \frac{\beta - 1}{\beta + 1} R, \;\; \beta = 10^{0.1/\alpha_{12}}. \tag{4.4}$$

For example, for a cluster at the keep-out radius (i.e., $R = 150.3$ km), R_c is given as 5.76 km, using $\alpha_{12} = 3$ suggested in the Hata model [83].[5]

[5]Although the Hata model is not the best fit for 802.22 since it is designed for signal propagation

4.4.2 Sensor Density

We now explore the maximum sensor density to guarantee enough distance between sensors for near-independent observations to use Eq. (4.1) for a collaborative sensor network. The need for near-independence also comes from the fact that a few tens of independent sensors provide as much collaborative gain as many more correlated sensors whose collaborative gain is limited by geographical correlation in shadowing [56]. That is, a blind increase in sensor density does not yield a linear increase of collaborative gain.

According to the Gudmundson's model [38], the shadow correlation between two locations that are d meters apart is given as $R(d) = e^{-ad}$ ($a = 0.002$ in a suburban area) which decays exponentially fast. Then, we want to suppress the correlation to be, on average, less than 0.3 between any two neighboring sensors such that $R(d) = e^{-0.002d} \leq 0.3$ resulting in $d \geq 602$ meters.

Assuming the hexagonal deployment of sensors as in Fig. 4.3, where the minimum distance between neighbors is d, the density of sensors (D_S) is shown to be

$$D_S = \frac{2}{\sqrt{3}d^2}(\text{sensors/m}^2),$$

and for $d = 602$ m, the maximum sensor density is

$$D_S^{max} = 3.18(\text{sensors/km}^2).$$

The minimum sensor density (D_S^{min}) is determined by the household density, since a household represents a CPE which plays role as both a sensor and a transceiver. According to the WRAN reference model [16], the minimum household density in a

up to 20 km from the transmitter, it works better than the widely-accepted Okumura model [65] which does not deal with rural environments. Here, we consider α_{12} as a design parameter and evaluate our schemes with $\alpha_{12} = 3$ as an example. Determination of α_{12} is outside of the scope of this chapter.

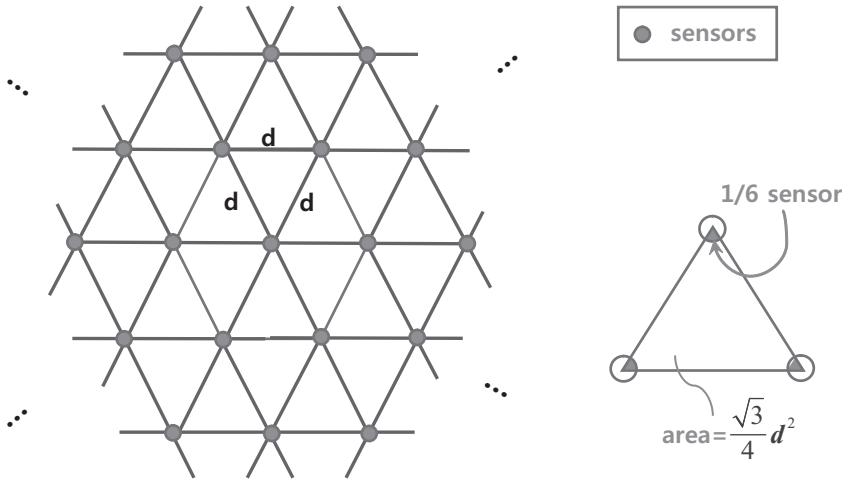

Figure 4.3: An example hexagonal sensor deployment

rural area is 0.6 (houses/km^2), thus giving

$$D_S^{min} = 0.6(\text{sensors/km}^2).$$

The next question is: at D_S^{min}, are there enough (e.g., at least 10) sensors in a cluster for collaboration? Using the above-derived D_S^{min} and D_S^{max}, the number of sensors in a cluster ranges between N_{sensor}^{min} and N_{sensor}^{max} where

$$N_{sensor}^{min} = D_S^{min} \cdot \pi {R_c}^2, \;\; N_{sensor}^{max} = D_S^{max} \cdot \pi {R_c}^2.$$

With $R_c = 5.76km$, this gives 62$\sim$331 sensors per cluster which exceeds the recommendation in [56]. Therefore, the CH can select a subset of sensors at each quiet period such that its area can be covered evenly.

4.4.3 Discussion

Sensor locations

In reality, the location of CPEs may not follow the hexagonal model since they are likely to be cluttered within small areas (e.g., a town or a village) where the actual sensor density is much higher than the average household density (e.g., 0.6 houses/km^2). Moreover, CPEs are rare outside the populated areas. Therefore, we

Analog TV (NTSC)	-94 dBm (at peak of sync of the NTSC picture carrier)
Wireless Microphones	-107 dBm (200 KHz bandwidth)
Digital TV (ATSC)	-116 dBm (6 MHz bandwidth)

Table 4.1: Incumbent detection threshold (IDT) of primary signals

take two approaches: (1) the CHs in a populated area should selectively choose CPEs according to the recommended sensor density to avoid correlated measurements, and (2) additional sensors should be deployed in less-populated areas to achieve D_S^{min} (as shown in Fig. 4.2). In either case, the hexagonal model may be still useful in selecting proper CPEs for sensing or in deploying more sensors.

Sub-clusters

A sensor cluster may be further divided into smaller sub-clusters to detect localized deep shadow fading which is not represented well by the lognormal model. Then, more than N_{sensor}^{max} sensors can be elected in each cluster to utilize their *correlated* measurements for identification of the localized shadowing. Further development of sub-clustering is left as our future work.

Sensor clustering for low-power incumbents

The typical EIRP of wireless microphones (WMs) is 50 mW in VHF bands and 250 mW in UHF bands. Due to their use of low power, the footprints of WMs cover a relatively small area compared to high-power primaries, and hence, it is very difficult to find a sufficient number of collaborative sensors in a cluster with identical and independent observations.

To quantify this difficulty, we consider a sensor cluster whose center is R_u km away from the microphone such that the sensor at its center would experience average

RSS of -107 dBm. Here, -107 dBm is chosen because it is the Incumbent Detection Threshold (IDT) of WMs in IEEE 802.22, where the IDT is the weakest primary signal power (in dBm) above which sensors should be able to detect. IDTs for three types of primary signals (in the US) [1] are shown in Table 4.1. Then,

$$R_u = \left(10^{-10.7}/P_u\right)^{-1/\alpha'_{12}},$$

where P_u is the transmit power of the WM (in mW) and α'_{12} is the path loss exponent. For $P_u = 50$ mW,

$$R_u = \begin{cases} 13.58 \text{ km} , & \text{if } \alpha'_{12} = 3, \\ 1.25 \text{ km} , & \text{if } \alpha'_{12} = 4. \end{cases}$$

Replacing R and α_{12} in Eq. (4.4) with R_u and α'_{12} gives

$$R_c = \begin{cases} 0.52 \text{ km} , & \text{if } \alpha'_{12} = 3, \\ 0.036 \text{ km} , & \text{if } \alpha'_{12} = 4. \end{cases}$$

Finally, applying the maximum sensor density $D_S^{max} = 3.18$ will result in $2.7(\alpha'_{12} = 3)$ and $0.01(\alpha'_{12} = 4)$ sensors per cluster. Hence, sensor collaboration is not practical for detecting low-power primaries due to the limited number of available sensors. Fortunately, however, recent work has shown that even a single sensor can meet the detection requirement of wireless microphones by exploiting their special features [12, 98]. So, we will focus on DTV detection via sensor clustering in the remaining part of the chapter.

4.5 Scheduling of In-band Sensing

In this section, we propose an in-band sensing scheduling algorithm that optimizes sensing-time and sensing-period to achieve detection requirements in IEEE 802.22

with minimal sensing overhead. We first briefly overview the sensing requirements and the two-stage sensing (TSS) mechanism in IEEE 802.22, and then describe the proposed sensing scheduling algorithm with detailed analysis. As mentioned earlier, we will focus on in-band DTV detection.

4.5.1 Sensing Requirements in IEEE 802.22

Channel detection time (CDT) is given to be $\leq$2 seconds, within which the returning PUs must be detected with $P_{MD} \leq 0.1$, regardless of the number of times sensing is performed during CDT. Similarly, $P_{FA} \leq 0.1$ must also be met when the same sensing algorithm used to meet $P_{MD} \leq 0.1$ is run for CDT seconds during which no PUs are present. The requirement on P_{MD} is to guarantee minimal interference to incumbents, whereas the requirement on P_{FA} is to avoid unnecessary channel switching due to the false detection of PUs.

Based on the above interpretation of P_{MD} and P_{FA}, the two performance metrics can be expressed as

$$\begin{aligned} P_{MD} &= \Pr(\text{detect PT within } CDT | H_1) \leq 0.1, \\ P_{FA} &= \Pr(\text{detect PT within } CDT | H_0) \leq 0.1, \end{aligned} \tag{4.5}$$

where H_0 and H_1 are two hypotheses on the presence of PUs in the channel:

$$\begin{aligned} H_0: &\quad \text{No PU exists in the channel,} \\ H_1: &\quad \text{PUs exist in the channel.} \end{aligned}$$

Note that P_{MD} and P_{FA} in Eq. (4.5) have different meanings from those in Eq. (4.1). P_{MD} and P_{FA} in Eq. (4.5) are the probabilities measured by monitoring an in-band channel for CDT seconds during which sensing may be scheduled *multiple times*, whereas P_{MD} and P_{FA} in Eq. (4.1) are the probabilities of *one-time*

sensing. To avoid any confusion, we will henceforth replace P_{MD} and P_{FA} in Eq. (4.5) with P_{MD}^{CDT} and P_{FA}^{CDT}.

4.5.2 TSS mechanism in IEEE 802.22

To support a sensing algorithm to meet the detectability requirements shown in Eq. (4.5), IEEE 802.22 provides the two-stage sensing (TSS) mechanism. With TSS, a sensing algorithm schedules either *fast* or *fine* sensing in each quiet period (QP), where fast sensing employs energy detection while fine sensing uses feature detection.

Although the QPs can be scheduled as many as necessary, there are some restrictions on the sensing period. For example, the QP of fast sensing, usually less than 1 ms, should be scheduled at the end of an 802.22 MAC frame (10 ms) at most once in each frame. Hence, the period of fast sensing becomes a multiple of the frame size (i.e., $n \cdot 10$ ms, $n \in \mathbb{N}$). In addition, in case fine sensing adopts a feature-detection scheme that requires sensing-time longer than one MAC frame (e.g., 24.2 ms for DTV field sync detection), its QP should be scheduled over consecutive MAC frames.

4.5.3 In-band Sensing Scheduling Algorithm

An efficient sensing algorithm must capture the tradeoff between fast and fine sensing, i.e., for one-time sensing, (1) fast sensing consumes a minimum amount of time but its performance is more susceptible to noise uncertainty, and (2) fine sensing usually requires much more time than fast sensing, but its performance is better than fast sensing. Therefore, a sensing algorithm may have to schedule fast sensing at a high frequency, or it may decide to schedule fine sensing at a low frequency. In either case, the scheduling goal is to minimize the overall time spent for sensing (called *sensing-overhead*) while meeting the detectability requirements.

Analysis of In-band Sensing Scheduling

We consider periodic fast or fine sensing. Suppose both fast and fine sensing consume less than 10 ms (i.e., one MAC frame size) for one-time sensing. Then, the sensing-period T_P is given as

$$T_P = n \cdot FS, \;\; 1 \leq n \leq \left\lfloor \frac{CDT}{FS} \right\rfloor, \;\; n \in \mathbb{N},$$

where FS is the MAC frame size. The upper-bound of T_P is necessary since sensing must be performed at least once every CDT seconds.

When the channel transits from OFF to ON due to the returning PUs as shown in Fig. 4.4, periodic sensing will measure the channel M times in CDT seconds, where

$$M = \left\lfloor \frac{CDT - \tau}{T_P} \right\rfloor + 1.$$

Each (one-time) sensing in Fig. 4.4 represents collaborative sensing with N sensors whose performance is described by Eq. (4.1). The value of N lies between N_{sensor}^{min} and N_{sensor}^{max} which were derived in Section 4.4.

We assume that τ/T_P is uniformly distributed in $[0, 1]$ since ON/OFF periods (in the order of hours) are in general much larger than T_P (less than 2 seconds). Under this assumption, the probability mass function (pmf) of M is derived as:

$$\begin{aligned} p(M_1) &= \Pr\left(M = \left\lfloor \frac{CDT}{T_P} \right\rfloor\right) = 1 - \frac{CDT}{T_P} + \left\lfloor \frac{CDT}{T_P} \right\rfloor, \\ p(M_2) &= \Pr\left(M = \left\lfloor \frac{CDT}{T_P} \right\rfloor + 1\right) = \frac{CDT}{T_P} - \left\lfloor \frac{CDT}{T_P} \right\rfloor. \end{aligned}$$

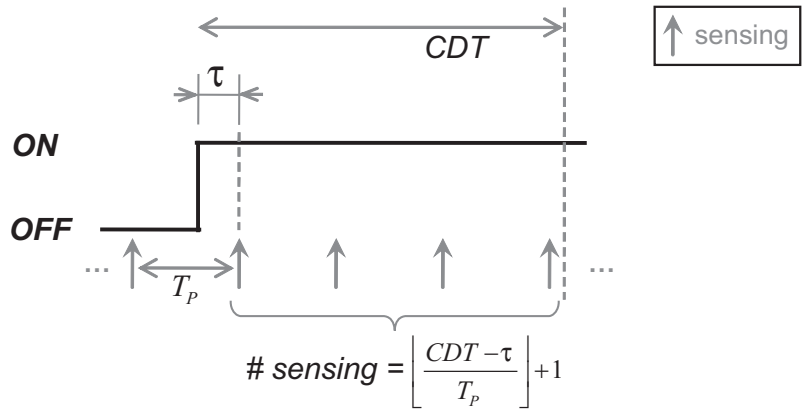

Figure 4.4: An example of periodic sensing when a channel transits from OFF to ON due to the returning PUs

Then, P_{MD}^{CDT} can be expressed as:[6]

$$\begin{aligned} P_{MD}^{CDT} &= \sum_{M} \Pr(M \text{ sensings detect no PU}|H_1)p(M) \\ &= \sum_{M} \left(P_{MD}(N)\right)^{M} p(M) \\ &= \sum_{M} \left(P_{MD}\right)^{NM} p(M) \quad \leq 0.1. \end{aligned} \tag{4.6}$$

Similarly, P_{FA}^{CDT} can be expressed as:

$$\begin{aligned} P_{FA}^{CDT} &= 1 - \sum_{M} \Pr(M \text{ sensings detect no PU}|H_0)p(M) \\ &= 1 - \sum_{M} \left(1 - P_{FA}(N)\right)^{M} p(M) \\ &= 1 - \sum_{M} \left(1 - P_{FA}\right)^{NM} p(M) \quad \leq 0.1. \end{aligned} \tag{4.7}$$

In Eqs. (4.6) and (4.7), P_{MD} and P_{FA} are detection-method specific. They also depend on T_I and the RSS of the primary signal. P_{MD} and P_{FA} of energy and pilot detectors are fully described by Eqs. (4.2) and (4.3).

[6]Here we assume that N sensors experience the same average RSS, thus having the same P_{MD}, since we focus on network planning before deploying sensors without knowledge of actual realization of shadow-fading. In case a network designer prefers to use the actual RSS, however, one can extend our equation by introducing P_{MD}^{s} where s is the sensor index.

The Proposed Sensing Scheduling Algorithm

Our objective is to find the optimal sensing-period T_P for given T_I and RSS, that minimizes the sensing overhead while satisfying two conditions of Eqs. (4.6) and (4.7). The sensing-overhead of a sensing algorithm is defined as the fraction of time in which sensing is performed, i.e.,

$$\text{sensing-overhead} = T_I/T_P$$

for periodic sensing.

The problem of optimizing T_P is identical to that of maximizing n that satisfies Eqs. (4.6) and (4.7). Therefore, the proposed algorithm examines n from its upper bound $\lfloor CDT/FS \rfloor$ and decreases n until the one that meets the condition is found.

Since P_{FA}^{CDT} is a monotonic function[7] of P_{FA} and there is a one-to-one mapping between P_{FA} and P_{MD}, we first want to find the value of P_{FA} that solves the equality of Eq. (4.7). Then, P_{MD} corresponding to P_{FA} can be found from the ROC curve between them. Finally, the feasibility of the tested n can be checked by substituting P_{MD} into Eq. (4.6). If the tested n does not satisfy Eq. (4.6), then n is decreased by 1 and the above procedure is repeated.

If there does not exist any n satisfying both equations, the detection method considered cannot meet the detectability requirements with given T_I and RSS. On the contrary, if the optimal sensing period is found at $n = n_{opt}$, its sensing overhead is determined as: $T_I/(n_{opt} \cdot FS)$.

Finally, to find an optimal pair (T_I, T_P) that gives the minimal sensing-overhead for given RSS, we vary T_I within a possible range of interest so that the proposed algorithm finds the best T_P for each T_I. Then, among multiple pairs of (T_I, T_P),

[7]This can be shown by differentiating P_{FA}^{CDT} with respect to P_{FA}.

$n := \lfloor CDT/FS \rfloor$;
while $(n > 0)$ {
  $P_{FA} := \{x | 1 - \sum_M (1-x)^{NM} p(M) = 0.1\}$;
  $\gamma := N_d B(1 + Q^{-1}(P_{FA})/\sqrt{M})$;
  $P_{MD} := Q([(P + N_d B) - \gamma] \cdot \sqrt{M}/(P + N_d B))$;
  if $(P_{MD}^{CDT}(P_{MD}) \leq 0.1)$ **then** {
    ⟨set sensing-period: $T_P = n \cdot FS$⟩;
    return;
  }
  else $n := n - 1$;
}
⟨mark the current detection method infeasible⟩;
return;

Figure 4.5: The in-band sensing scheduling algorithm

we choose an optimal pair with minimal sensing-overhead. More details on this procedure are provided in Section 4.6.2.

The pseudo-code of the proposed algorithm for energy and pilot detection is given in Fig. 4.5.

Discussion

An important aspect of the proposed algorithm is that it computes the optimal sensing periods offline, and the optimal periods can be looked up from the database with two inputs, T_I and RSS, at runtime. A sensor can create/store one database per detection method, and adaptively choose the best method with optimal (T_I, T_P). In Section 4.6, we will evaluate and compare the performance of energy and pilot detection. The optimal sensing strategy (i.e., optimal detection method, sensing-period, and sensing-time) with the average RSS varying from -120 dBm to -90 dBm will also be proposed.

In practice, the dissemination of sensing results should also be accounted for. The dissemination delay, however, depends on the type of reporting mechanism used. For example, the dissemination delay can be reduced significantly if the cluster head collects 'busy' samples only. Since selecting a reporting mechanism is beyond the scope of this chapter, we focus on the detection overhead, but our scheme can be easily extended to include the additional delay by re-defining the sensing time as the sum of detection and dissemination times. Moreover, such an additional delay is common to both energy and feature detection, hence unchanging the tradeoff between two detection schemes in Section 4.6.

We, therefore, focus on the tradeoff between energy and feature detection, investigating energy-only and feature-only schemes. As a possible extension, one can consider a hybrid of the two schemes or a more complex dynamic scheduling scheme than simple periodic sensing, which are left as our future work.

4.6 Feasibility of Energy Detection

In this section, we study the feasibility of energy detection in achieving the detectability requirements, and investigate the condition under which energy detection is preferred to feature detection. In addition, we derive the minimum number of sensors necessary for feasible energy detection when the average RSS equals IDT.

4.6.1 Two Important Factors in In-band Sensing

We first briefly overview the impact of noise uncertainty and inter-CRN interference in in-band sensing.

Noise Uncertainty

Below SNR_{wall} [89], energy detection in an AWGN channel completely fails to detect a signal regardless of the sensing-time spent. SNR_{wall} is due to the uncertainty in the noise power (called *noise uncertainty*) where their relationship is

$$SNR_{wall} = (\rho^2 - 1)/\rho,$$

when $\rho = 10^{x/10}$ and x is the noise uncertainty in dB. According to [75], noise uncertainty depends on four factors: calibration error, thermal variation, changes in low-noise amplifier (LNA) gain, and interference. For example, the noise uncertainty under 20 °K of temperature variation is given as ± 1 dB.

Therefore, energy detection is often considered unsuitable for CRNs which must detect a very weak signal power (e.g., as low as -116 dBm for DTV signals). However, we found that SNR_{wall} can actually be overcome even when the average SNR (modeled by aRSS) of the collaborative sensors is below SNR_{wall}, since the energy detection of DTV signals will experience a lognormal shadow-fading channel, and thus at some sensor locations, instantaneous SNR may exceed SNR_{wall} due to the location diversity.

Fig. 4.6(a) shows the impact of shadow-fading, where dB-spread of 5.5 dB is assumed as in the ITU propagation model of 802.22 [76]. With noise uncertainty of 1 dB,[8] none of the N sensors overcomes SNR_{wall} of -3.33 dB under the AWGN channel (illustrated as a vertical dotted line at $RSS = -98.5$ dBm) as predicted in [89]. With shadow-fading, however, some sensors under constructive fading[9] may

[8] We followed the worst-case analysis in [79] where the upper (lower) limit of noise PSD is used to calculate P_{FA} (P_{MD}), when noise uncertainty is Δ dB and the range of noise PSD is given as $-163 \pm \Delta$(dBm/Hz).

[9] Constructive fading happens under lognormal shadowing, because the instantaneous RSS (in dB) is modeled as "average RSS (dB) + X (dB)" where X is a zero-mean Gaussian random variable.

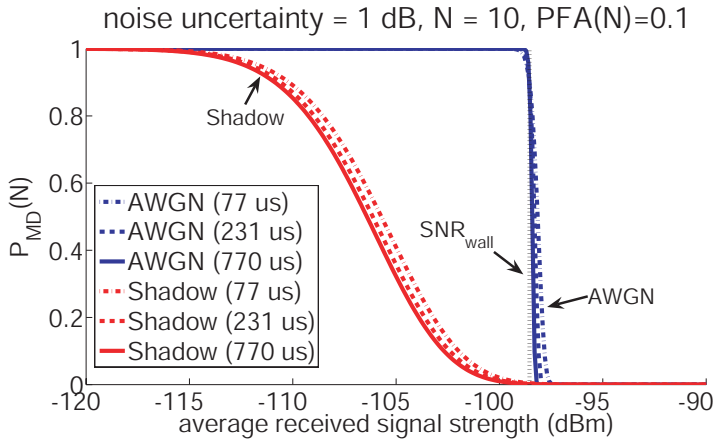

(a) AWGN channel vs. shadow-fading channel

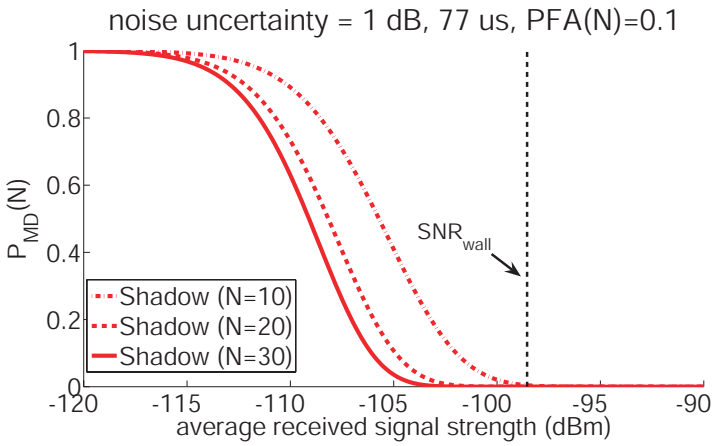

(b) Shadow-fading channel (T_I=77us)

Figure 4.6: Performance comparison (in $P_{MD}(N)$) of energy detection: AWGN channel and shadow-fading channel

experience SNR greater than SNR_{wall} contributing to the performance enhancement, while other sensors under destructive fading does not degrade the performance since their instantaneous RSSs are already below SNR_{wall} under which $P_{MD} = 1$. In addition, Fig. 4.6(b) shows that the performance of collaborative sensing improves as the number of sensors N increases.

Unlike energy detection, SNR_{wall} of feature detection decays as the channel coherence time increases [90], meaning that SNR_{wall} in feature detection is insignificant, since 802.22 CPEs and BSs are stationary devices.

Inter-CRN Co-channel Interference

Although the perfect synchronization of QPs between neighboring 802.22 cells is guaranteed by the CBP protocol, 802.22 cells more than one-hop apart may be assigned the same channel. In such a case, they could introduce non-negligible interference to the CPEs. Moreover, future CRN standards other than IEEE 802.22 may co-exist in the same TV bands, which will cause additional interference to 802.22 cells. We call this type of interference *inter-CRN co-channel interference*.

We first evaluate how much interference is expected between 802.22 cells that are m hops away from each other. Fig. 4.7 shows two scenarios of co-channel interference. In Fig. 4.7(a), cell A's two-hop neighbor cell B uses the same channel 1, which will interfere with the sensor at the border of cell A. According to [16], a BS with coverage radius of 35 km will have a transmit EIRP of 23.5 dBW, when its antenna has a typical height of 75 m [8]. The interference power of cell B's BS to the sensor[10] is then found to be -96.5 dBm since

$$P_{\text{cell B's BS}} \cdot (3R_{cell})^{-\alpha} \;=\; 10^{23.5} \cdot (3 \cdot 33 \times 10^3)^{-3} \;\; W,$$

which is comparable to the noise power of -95.2 dBm in the 6 MHz band [77]. In Fig. 4.7(b), however, the three-hop neighbor cell B's interference power is -103 dBm which is negligible. Hence, we only consider interference from two-hop neighbors. Note that additional noise uncertainty due to this inter-CRN interference can be reduced by letting neighboring CRNs exchange the information on their transmission power.

Fig. 4.8 shows the worst-case scenario of channel assignment for the central 802.22 cell to have maximal inter-CRN interference. There can be up to 6 two-hop interfer-

[10]Note that the CPEs in cell B are not significant interferers as a CPE uses a directional antenna to communicate with its BS which minimizes its emitted power to the outside of its cell.

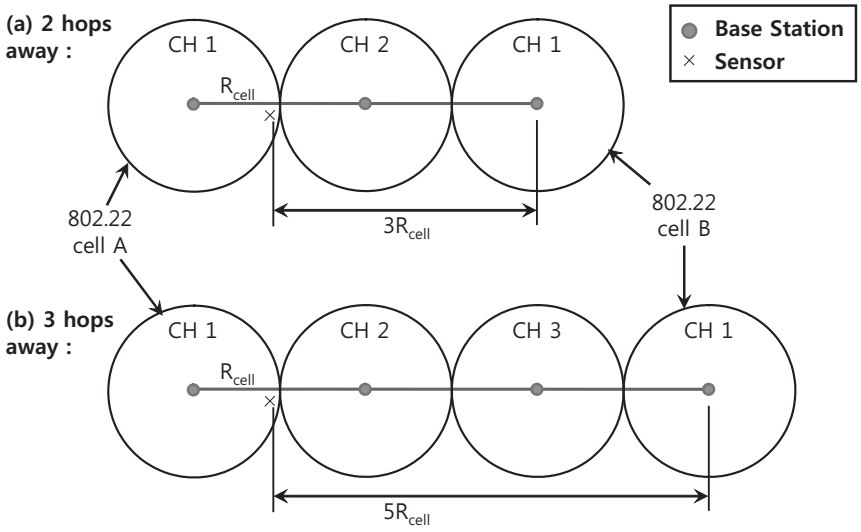

Figure 4.7: Inter-cell interference scenarios in 802.22

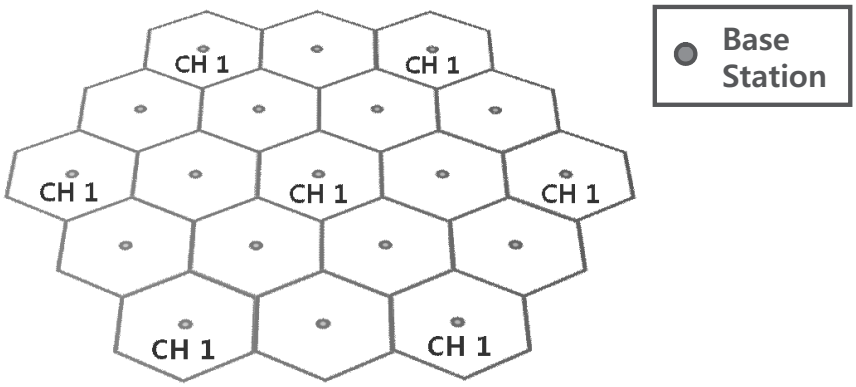

Figure 4.8: The worst-case channel assignment to have maximal inter-cell interference

ing neighbors of a cell. Thus, the interference power will vary from $-\infty$ dBm (i.e., no interference) to -88.7 dBm (6 times more than -96.5 dBm) in our numerical analysis.

4.6.2 Optimal Sensing Time and Frequency

We evaluate energy and pilot detection to find the optimal sensing-time (T_I) and sensing-period (T_P) to minimize the sensing overhead, when they meet the detectability requirements of $P_{MD}^{CDT}, P_{FA}^{CDT} \leq 0.1$.

Each detection scheme is evaluated while varying the average RSS (of the 6 MHz DTV signal) from -120 dBm to -90 dBm in step of 0.1 dBm. This RSS range is chosen because (1) the IDT of DTV signal is -116 dBm, and (2) RSS at the keep-out radius of a DTV transmitter is -96.48 dBm [77]. Therefore, our interest lies in the range between -116 dBm and -96.48 dBm, which is well covered by the simulated RSS range.

We study the impact of noise uncertainty by varying the uncertainty to 0 dB, 0.5 dB, 1 dB, or 2 dB. The effect of inter-CRN interference is also evaluated by changing the number of interfering 802.22 cells to 1, 2, 4, or 6 cells while fixing noise uncertainty at 1 dB. For both tests, the number of cooperative sensors is fixed at $N = 10$.

Energy Detection

Since one data segment of a DTV signal is 77 μs, we tested 10 different sensing-times for energy detection, such as $k \cdot (77\mu s)$, $k = 1, 2, \ldots, 10$. During each sensing-time, the proposed sensing scheduling algorithm searches for the optimal sensing-frequency and the minimal sensing-overhead at every RSS value. After optimizing the sensing-frequency, the sensing overheads from 10 different sensing-times are compared and the best sensing-time at each RSS input is chosen.

First, we show the effects of noise uncertainty. Fig. 4.9(a) compares energy detection under the noise uncertainty of 0 dB vs. 2 dB. For an illustrative purpose, three sensing-times (1, 3, 10 segments) are presented. For the 0 dB case, energy detection performs very well at any RSS with a negligible overhead of less than 0.3%. By contrast, for the 2 dB case, energy detection becomes infeasible for RSS < -111.7 dBm. Note that the blank between -113 dBm and -111.7 dBm implies

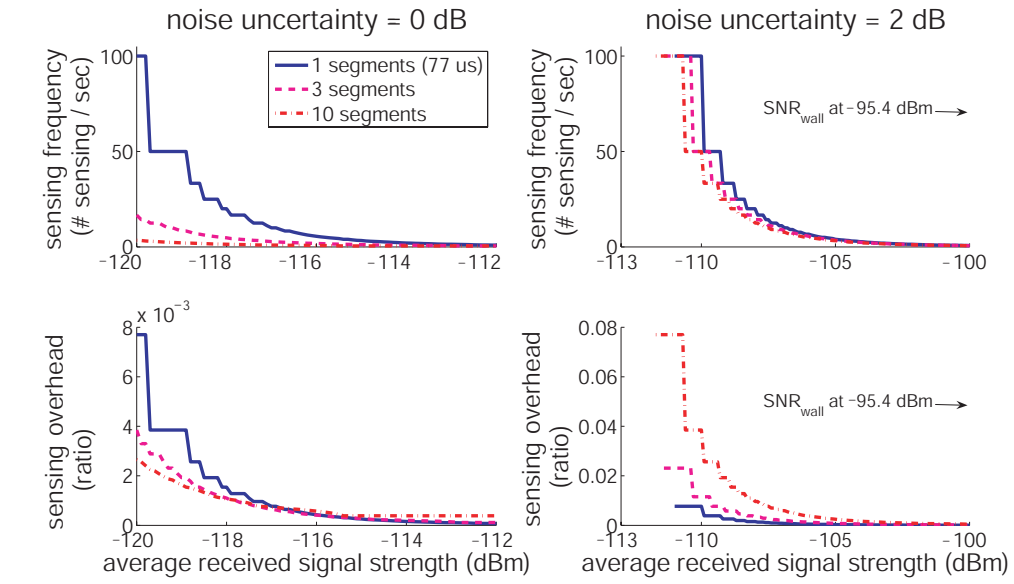

(a) Various noise uncertainty (left: 0 dB; right: 2 dB)

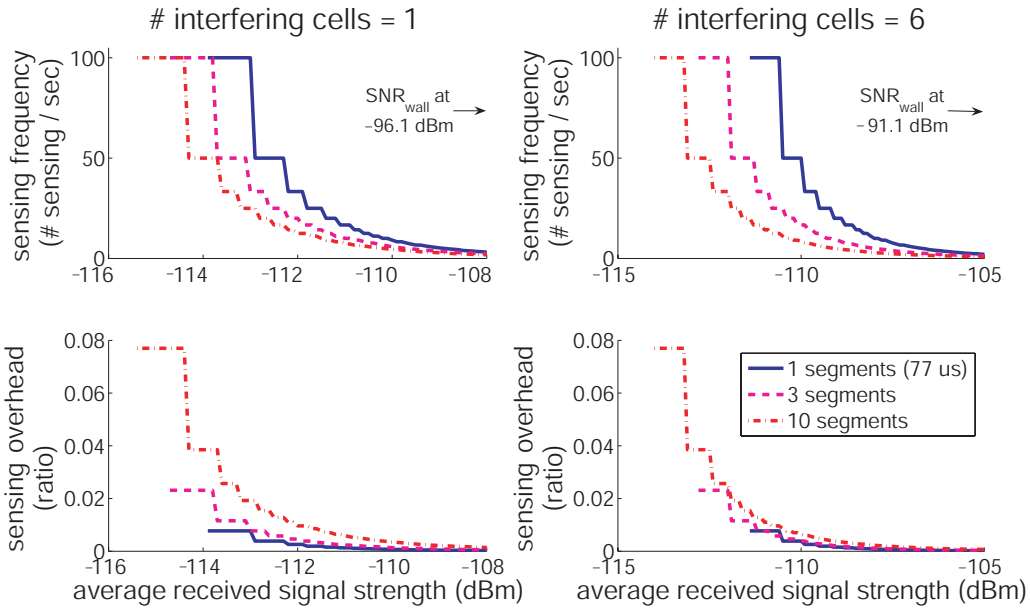

(b) Various inter-CRN interference (left: 1 cell; right: 6 cells)

Figure 4.9: Energy detection: sensing-overhead and sensing-frequency

that there is no T_P satisfying the detectability requirements. However, compared to the AWGN's SNR_{wall} of -95.4 dBm, energy detection's feasibility region is enlarged significantly thanks to the sensor diversity under the shadow-fading. Interestingly, at the 2 dB case, the performance (in terms of sensing overhead) does not get better as the sensing-time grows, since the impact of SNR_{wall} becomes more dominant at

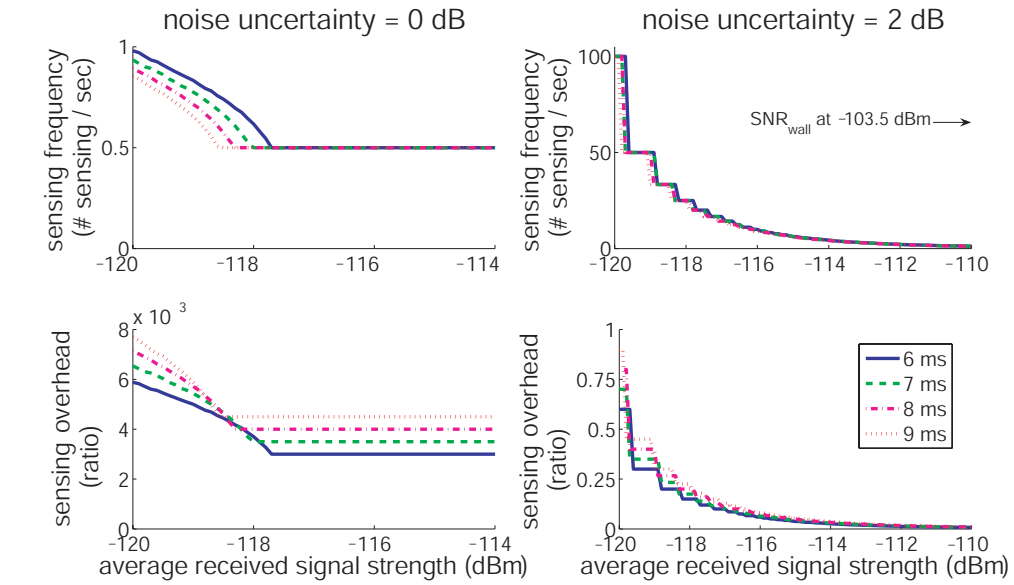

(a) Various noise uncertainty (left: 0 dB; right: 2 dB)

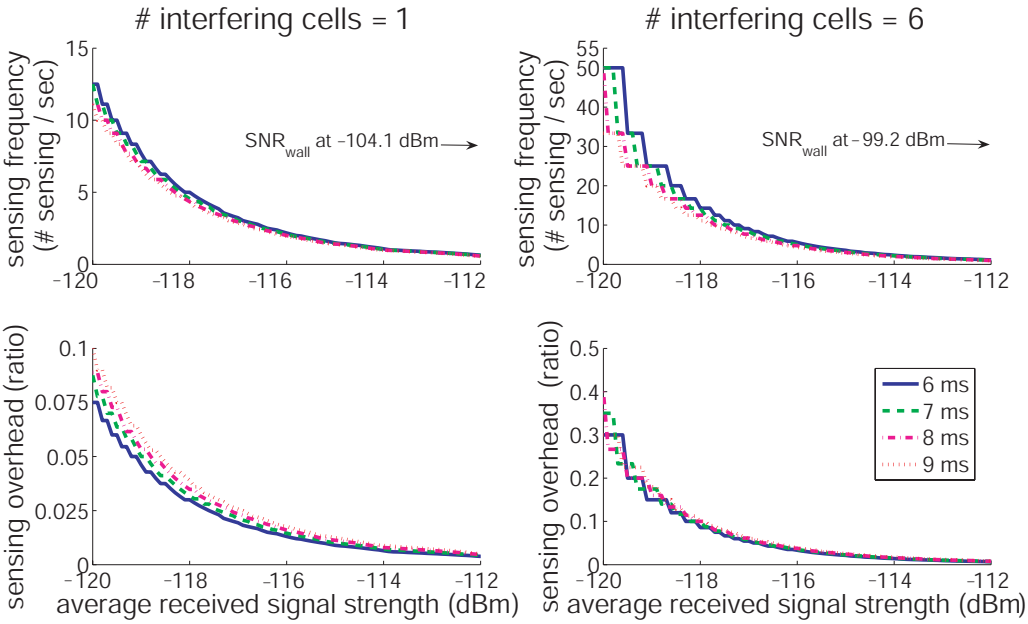

(b) Various inter-CRN interference (left: 1 cell; right: 6 cells)

Figure 4.10: Pilot detection: sensing-overhead and sensing-frequency

a larger noise uncertainty.

Second, we vary the number of interfering 802.22 cells to observe the behavior of energy detection. Fig. 4.9(b) shows two extreme cases: 1 cell vs. 6 cells. As expected, an increase of interfering cells increases the noise plus interference power

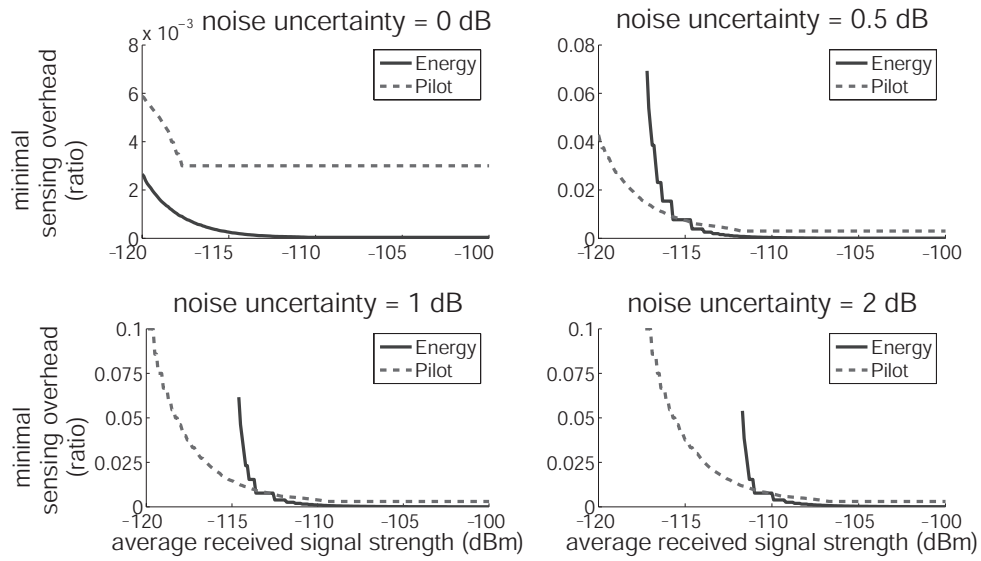

(a) Various noise uncertainty

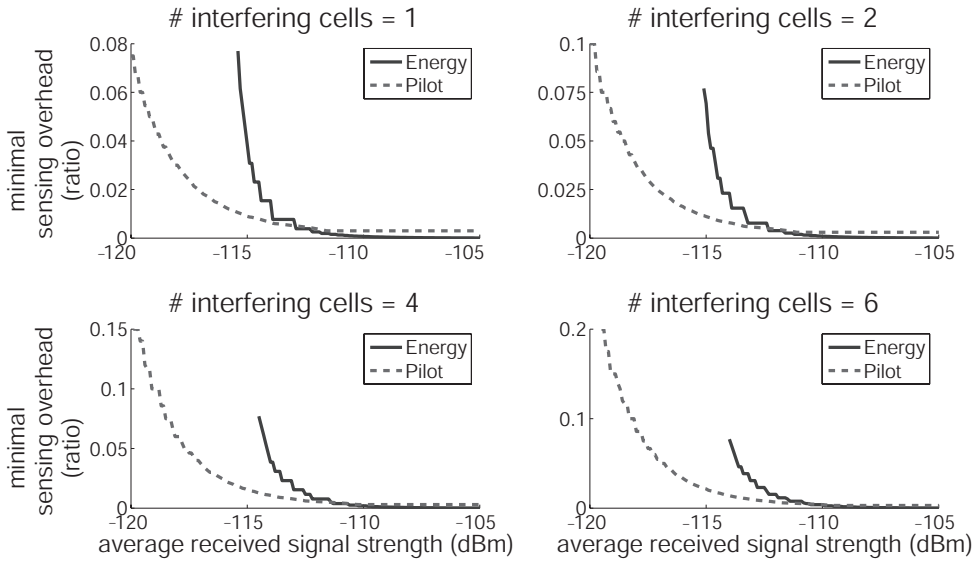

(b) Various inter-CRN interference

Figure 4.11: Energy detection vs. pilot detection: location of $aRSS_{threshold}$

which impairs performance due to degraded SNR.

Feature (Pilot) Detection

Since pilot (energy) detection is based on the energy measurement of a pilot signal, it requires a sufficient number of samples to yield satisfactory results. Due to its lower sampling frequency, sensing-time of pilot detection is chosen to be 85

noise uncertainty	0.5 dB	1 dB	2 dB
$aRSS_{threshold}$ (dBm)	-114.6	-112.5	-109.9
$aRSS_{min}^{energy}$ (dBm)	-117.2	-114.6	-111.7

Table 4.2: RSS thresholds under various noise uncertainty

times longer (6MHz/70KHz=85.7) than that of energy detection to acquire the same number of samples (i.e., M_s) as energy detection.[11] On the other hand, the MAC frame size of 10 ms gives an upper-bound of sensing-time. Based on this observation, we vary the sensing-time of pilot detection to be 6, 7, 8, or 9 ms, considering that $85.7 \times 77\mu s = 6.6$ ms.

Fig. 4.10(a) plots the performance of pilot detection while varying the noise uncertainty. Note that the x-axis represents the average RSS of a 6 MHz DTV signal, not of a pilot signal in the 70 KHz band. The power of pilot signal is 11.3 dB less than the DTV signal power. Unlike energy detection, pilot detection is feasible at every RSS regardless of the level of noise uncertainty, due to its higher SNR at the pilot location.

Fig. 4.10(b) shows the performance of pilot detection while varying the number of interferers. At a given number of interfering cells, the sensing-time does not appear to offer a large performance enhancement.

4.6.3 Energy Detection vs. Feature Detection

Finally, we investigate the location of $aRSS_{threshold}$, below which pilot detection is preferred to energy detection. We also introduce $aRSS_{min}^{energy}$, the minimum aRSS above which energy detection becomes feasible for detection of DTV signals.

Fig. 4.11(a) compares the minimal sensing-overheads of energy and pilot detec-

[11] Since Eqs. 4.2 and 4.3 are approximated performance by applying the Central Limit Theorem [77], their accuracy degrades as M_s decreases. Hence we match M_s by adjusting sensing-time, to compare energy and feature detection under the same condition.

# of interferers	1	2	4	6
$aRSS_{threshold}$ (dBm)	-112.9	-112.3	-111.3	-110.5
$aRSS_{min}^{energy}$ (dBm)	-115.4	-115.1	-114.5	-114

Table 4.3: RSS thresholds under various inter-CRN interference

tion under various noise uncertainty conditions. With no noise uncertainty, energy detection is the best to use. As the noise uncertainty grows, however, pilot detection becomes preferable at a low aRSS and $aRSS_{threshold}$ increases accordingly. The position of $aRSS_{threshold}$ is shown in Table 4.2 along with $aRSS_{min}^{energy}$. With 1 or 2 dB noise uncertainty, pilot detection becomes feasible and preferable even at -120 dBm, but it incurs more than 10% of sensing overhead.

$aRSS_{threshold}$ and $aRSS_{min}^{energy}$ of various inter-CRN interference are also presented in Fig. 4.11(b) and Table 4.3. With 1 or 2 dB noise uncertainty, pilot detection incurs more than 15% of sensing overhead at -120 dBm.

From Tables 4.2 and 4.3, one can see that the feasibility region of energy detection is reduced just by 1.4 dB between 1 cell and 6 cells, whereas the gap is 5.5 dB between noise uncertainty of 0.5 dB and 2 dB. As a result, noise uncertainty seems to have a more significant influence on energy-detection's performance.

Other Feature Detectors

From Figs. 4.11(a) and 4.11(b), one can observe that energy detection, above $aRSS_{threshold}$, incurs *at most* 0.385% of sensing overhead. Here, we compare this overhead with three other types of feature detectors than pilot-energy detection: the pilot-location detection in [19], the PN511 detection in [18], and the cyclostationary detection in [11]. Since sensing-times for such feature detectors are 30 ms, 24.1 ms, and 19.03 ms, respectively, their sensing overheads are given as *at least* 1.5, 1.2, and 0.95 % even when sensing is scheduled only once every CDT seconds. Therefore, en-

noise uncertainty	0	0.5	1	2	# of interferers	1	2	4	6
N_{min}	1	5	24	221	N_{min}	30	38	58	86

Table 4.4: The minimum number of sensor (N_{min}) necessary for energy detection to become feasible at $aRSS = IDT$

ergy detection performs better in its preferred region (i.e., above $aRSS_{threshold}$) than the pilot-energy as well as other three types of feature detectors under consideration.

4.6.4 Minimum Number of Sensors for Feasible Energy Detection at $aRSS = IDT$

As shown in Fig. 4.6(b), the performance of collaborative sensing improves as N grows. Thus, as we increase N, $aRSS_{min}^{energy}$ also becomes smaller. This means that we can find a minimum N, denoted by N_{min}, with which energy detection can be feasible even at $aRSS = IDT$. Here we investigate such N_{min} and its relationship with other optimization parameters, such as T_I and T_P.

Fig. 4.12 illustrates the tradeoff between sensing-overhead and N_{min}. As we allow higher sensing-overhead by introducing longer T_I and smaller T_P, we can achieve the same target detection performance (i.e., $P_{MD}^{CDT} = 0.1$ and $P_{FA}^{CDT} = 0.1$) with smaller N, and vice versa. Therefore, to find N_{min}, we allow maximum possible overhead, $T_I = 770$ μs and $T_P = 10$ ms, in the scenario considered in Section 4.6.2. Then, the corresponding N_{min} becomes the lower bound of all possible N's below which no energy detection becomes feasible at $aRSS = IDT$. Table 4.4 shows the N_{min} for various noise uncertainty and inter-CRN interference. In both cases, the maximum N_{min} (i.e., 221 and 86) does not exceed 331 sensors, which is the maximum number of sensor in a cluster derived in Section 4.4.

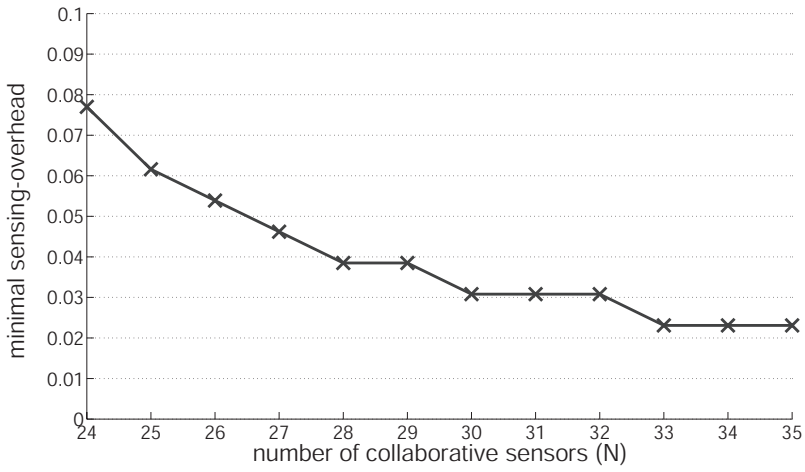

Figure 4.12: Number of sensors (i.e., N) vs. optimal sensing-overhead ($aRSS = IDT$, 1 dB noise uncertainty)

4.7 Effective Channel-Reuse Time

In the current 802.22 draft, the detectability requirements are specified as $P_{MD}^{CDT} \leq 0.1$ and $P_{FA}^{CDT} \leq 0.1$. The upper-bound of 0.1 on P_{MD}^{CDT} is set for the purpose of protecting PUs, i.e., SUs can only cause limited interference to the PUs returning to the channel currently occupied by the SUs. On the other hand, the upper-bound on P_{FA}^{CDT} is set to limit unnecessary channel-switches due to false detection of incumbents.

However, the chosen upper-bound of P_{FA}^{CDT}, denoted by P_{FA}^{max} (i.e., $P_{FA}^{max} = 0.1$ in the current draft), has not been evaluated for its efficiency in reusing idle channels. Here, we measure the efficiency of P_{FA}^{max} in terms of the expected duration, T_{reuse}, of reusing an idle channel until an unnecessary channel-switch takes place due to false detection. We focus on this metric because, according to 802.22, once a channel is vacated due to the detection of PUs in an in-band channel, SUs are not allowed to use the channel again for the *Non-Occupancy Period*, which is set to 10 minutes [84]. That is, frequent unnecessary channel-switches may soon deplete reusable channels

even if there are many idle ones.

Thus, we would like to see if the requirement $P_{FA}^{max} = 0.1$ is strict enough by analyzing T_{reuse} for a given P_{FA}^{max}, and determine a proper P_{FA}^{max} allowing practically long enough reuse of idle channels. For this purpose, we consider periodic in-band sensing, as in Fig. 4.4, on an idle channel during its long OFF period, where we assume that each sensing operation is performed by N cooperating sensors with P_{FA} as the single-sensor's false alarm probability.

First, we denote $P_{FA}(N)$ by P_{FA}^N for notational simplicity, and express Eq. (4.7) as a function of P_{FA}^N, i.e., the false alarm probability of single-time cooperative sensing as given in Eq. (4.1), as follows

$$P_{FA}^{CDT}(P_{FA}^N) = 1 - \sum_M \left(1 - P_{FA}^N\right)^M p(M). \tag{4.8}$$

Then, it is trivial to show that Eq. (4.8) is a monotonic increasing function of P_{FA}^N. Hence, having P_{FA}^{CDT} upper-bounded by P_{FA}^{max} is the same as having P_{FA}^N upper-bounded by $\hat{P}_{FA}^{max}$, where $P_{FA}^{CDT}(\hat{P}_{FA}^{max}) = P_{FA}^{max}$.

Next, the expected channel-reuse duration, T_{reuse}, is derived as

$$\begin{aligned} T_{reuse} &= T_P \cdot (1 - P_{FA}^N) P_{FA}^N + 2T_P \cdot (1 - P_{FA}^N)^2 P_{FA}^N + \cdots \\ &= \sum_{i=0}^{\infty} iT_P \cdot (1 - P_{FA}^N)^i P_{FA}^N = T_P \left(\frac{1 - P_{FA}^N}{P_{FA}^N} \right). \end{aligned} \tag{4.9}$$

Therefore, the smaller P_{FA}^N, the longer an idle channel can be reused without false detection of PUs. This implies that we need to set $\hat{P}_{FA}^{max}$ small enough to make T_{reuse} reasonably large.

We now want to evaluate the efficiency of the current detectability requirement in the 802.22 draft, i.e., $P_{FA}^{max} = 0.1$. While varying P_{FA}^{max} from 0.001 to 0.1, we compute N_{min} for each P_{FA}^{max} value, where N_{min} is defined the same as in Section 4.6.4. Then, for each pair (P_{FA}^{max}, N_{min}), our in-band sensing scheduling algorithm is applied to

determine the optimal sensing-period T_P and sensing-time T_I with minimal sensing overhead. Finally, we calculated T_{reuse} using the chosen P_{FA}^{max}, the derived T_P, and Eq.(4.9). The results are plotted in Fig. 4.13.

As shown in Fig. 4.13(a), T_{reuse} at $P_{FA}^{max} = 0.1$ turns out to be just 20 seconds. That is, with the currently-chosen upper-bound 0.1, a WRAN can reuse an idle channel for an average of only 20 seconds before making an unnecessary channel-switch. This implies that a WRAN may require at least 30 idle channels exclusively assigned for its use to provide a seamless service to CPEs, considering the Non-Occupancy Period of 10 minutes. However, there are only 68 channels in TV bands, and thus, it is unlikely to have 30 concurrently idle channels while there are many active TV stations. In addition, self co-existence between neighboring WRANs will make it harder to find an enough number of idle channels reserved for a certain WRAN.

To resolve this issue, we can impose a much more strict upper-bound on the false alarm probability by reducing P_{FA}^{max} significantly. Fig. 4.13(a) indicates that by using $P_{FA}^{max} = 0.001$, the expected channel-reuse time is enhanced by two orders-of-magnitude (i.e., $E[T_{reuse}] = 2,000$ seconds) which is reasonably long for SUs to operate on an idle channel. Although one may wonder if the new constraint on P_{FA}^{max} might increase N_{min} and the sensing overhead significantly, Figs. 4.13(b) and 4.13(c) show a minimal increase in N_{min} (just 3 more sensors) and a bounded sensing overhead between 0.069 and 0.077 when P_{FA}^{max} varies.

As a result, we recommend $P_{FA}^{max} = 0.001$ as a new requirement on the false-alarm probability. Using this new value of P_{FA}^{max}, combined with the proposed in-band sensing scheduling, we can still meet the detectability requirements with a slight increase in the number of collaborative sensors while enhancing the channel-reuse

time significantly.

4.8 Conclusion

In this chapter, we discussed three important aspects of in-band spectrum sensing in the IEEE 802.22: sensor clustering, sensing scheduling, and detectability requirements. First, we showed the necessity of sensor clustering and derived the maximum sensor cluster size and sensor density. Next, we proposed an in-band sensing scheduling algorithm that minimizes sensing-overhead while meeting the detectability requirements, and evaluated its performance with respect to noise uncertainty and inter-CRN interference. We also derived the SNR threshold above which energy detection is preferred to feature detection and the minimum number of collaborative sensors for feasible energy detection at a given SNR. Finally, we investigated how strict the detectability requirement must be to guarantee efficient channel reuse without incurring unnecessarily often channel-switches.

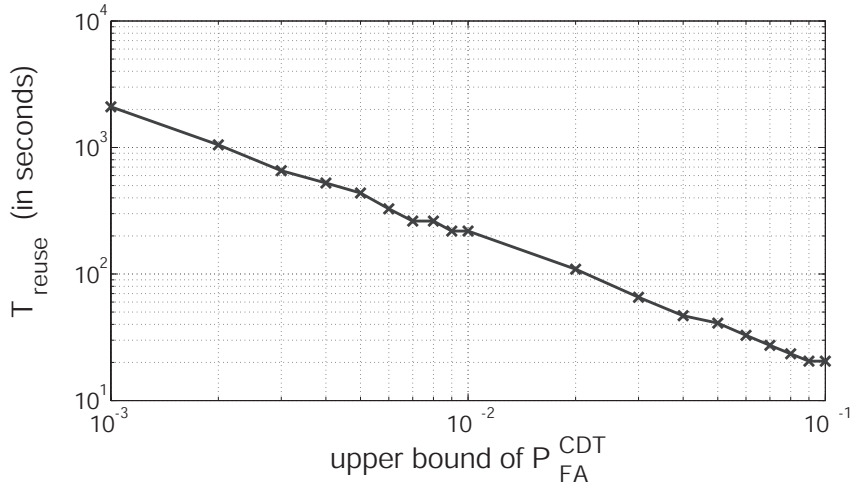

(a) Expected T_{reuse}

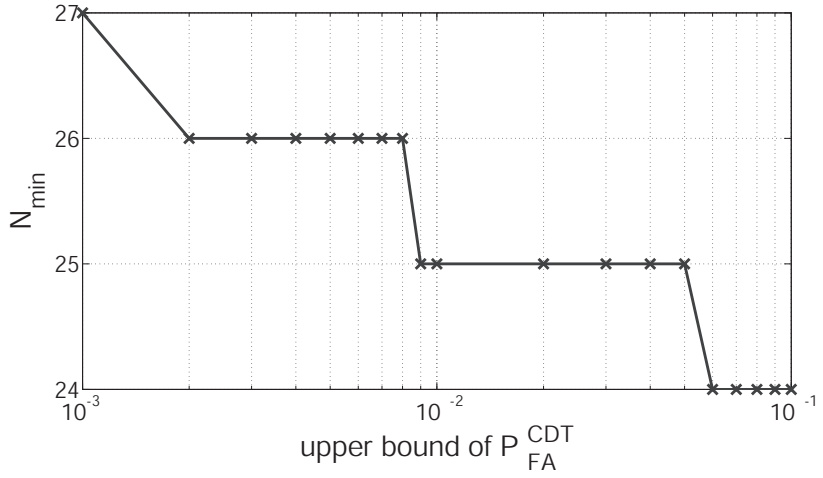

(b) N_{min}

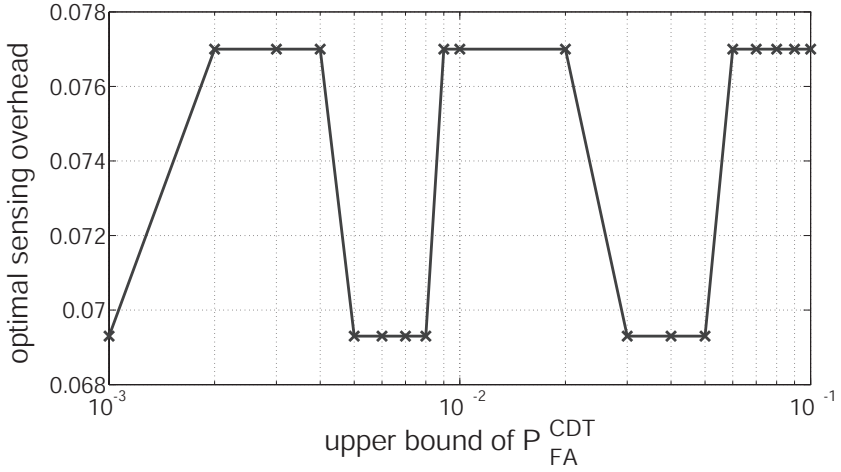

(c) Sensing overhead T_I/T_P

Figure 4.13: T_{reuse}, N_{min}, and sensing overhead T_I/T_P with varying P_{FA}^{max}

CHAPTER V

WHITESPACE UTILIZATION PART I: OPTIMAL CONTROL OF SECONDARY USERS FOR PROFIT MAXIMIZATION AT CR SERVICE PROVIDERS

5.1 Introduction

The application of dynamic spectrum access (DSA) ranges from public to commercial and military networks. In this chapter, we focus on a commercial DSA application, *cognitive radio (CR) Wi-Fi hotspots*, which is an attractive and promising example of DSA. A CR Wi-Fi hotspot (henceforth simply referred to as CR hotspot) consists of a CR access point and CR-enabled customer terminals where a CR wireless service provider (WSP) opportunistically utilizes the licensed spectrum to provide Internet access to the CR customers. The use of spectrum whitespaces for this *Wi-Fi-like* service has been identified as an important step in DSA development, due to its similarity to today's Wi-Fi and more favorable propagation characteristics of the licensed spectrum (e.g., TV bands) than the ISM bands like larger coverage and the wall-penetrating ability [10]. Although the Wi-Fi-like service over whitespaces has been given different names such as Wi-Fi 2.0 [22], WhiteFi [3], and 802.11af [48], this chapter focuses on its general aspects of customer flow control

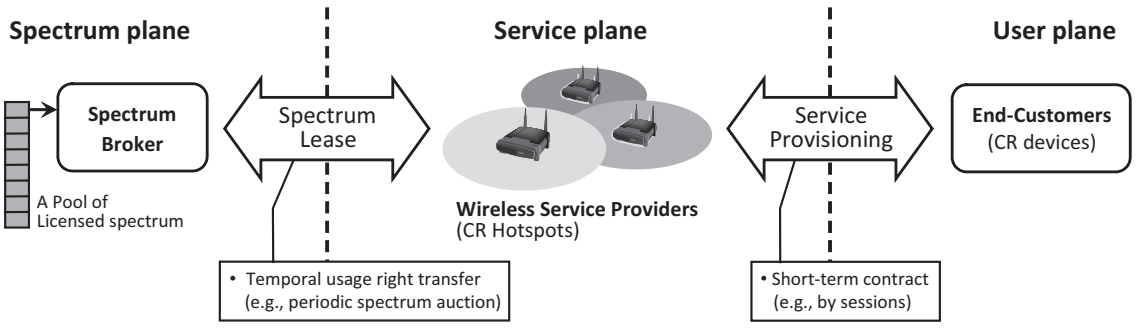

Figure 5.1: Inter-plane interactions in the dynamic spectrum market

under the time-varying spectrum availability.[1]

The concept of CR hotspots can be better understood in the framework of *dynamic spectrum market* (DSM) [44] (also called *secondary market*) in which the primary license holders can temporarily transfer their spectrum usage rights to CR users. The DSM consists of three interacting layers/planes—*spectrum*, *service*, and *user* planes—as shown in Fig. 5.1. In the spectrum plane, a spectrum broker (SB) leases licensed spectrum to the (CR) WSPs at the service plane, where the SB is either the regulatory authorities (e.g., FCC in USA and Ofcom in UK) or an authorized third-party. The WSPs compete with each other to lease as many spectrum bands as necessary which will be opportunistically utilized to provide the CR hotspot service to the CR users at the user plane.

The dynamic spectrum lease can be described by one of the three prevailing models in the CR literature: *dynamic exclusive-use*, *shared-use*, and *private commons* [5]. In the dynamic exclusive-use model, licensees can dynamically lease their spectrum to the lessees (i.e., secondary users (SUs)) who temporarily own an exclusive right to access the spectrum, but the spectrum leasing is not performed in real-time and the SUs' service should be the same type as the licensees. In the shared-use model,

[1]Note that Wi-Fi over whitespaces is not necessarily based on the same type of protocol as IEEE 802.11, as pointed out in [48].

SUs are allowed to freely access licensed bands opportunistically in the absence of primary users (PUs), without paying any leasing fees. Lastly, the private commons model enables more flexible integration of DSA in the licensed spectrum via *real-time* spectrum leasing by the *dynamic spectrum auction* where the licensees can also set their own rules on how their spectrum is used by the SUs. Among the three models, the private commons model is believed to be a viable market option that benefits both licensees and CR users [5] since the licensees can make extra profit via spectrum leasing (unlike shared-use) and the CR users are given full flexibility in utilizing the whitespaces (unlike dynamic exclusive-use).

5.1.1 Contributions

Our contribution in this chapter is two-fold. First, we propose a new spectrum reuse model called *preemptive spectrum lease* which is a realization of the private commons, as illustrated in Fig. 5.2. In our model, the license holders temporarily lease their channels to CR WSPs via *periodic* dynamic spectrum auction (e.g., hourly) and charge them for their opportunistic use of paid-but-idle channels. The WSPs are allowed to use the leased channels only when they are temporarily unoccupied by the PUs because the licensed users are given priority over the unlicensed CR users. Therefore, the CR users must vacate a channel to which PUs return (called *channel vacation*) where the channel state changes from 'available to SUs' to 'occupied by PUs', and should utilize the remaining idle channels afterwards. When PUs no longer transmit on the vacated channel, it can be used again by the SUs. Once a leasing term ends, the leased channels are all returned to the licensees and the WSPs must re-participate in the auction to lease new channels.

Next, we solve the profit maximization problem of a WSP by optimizing two types

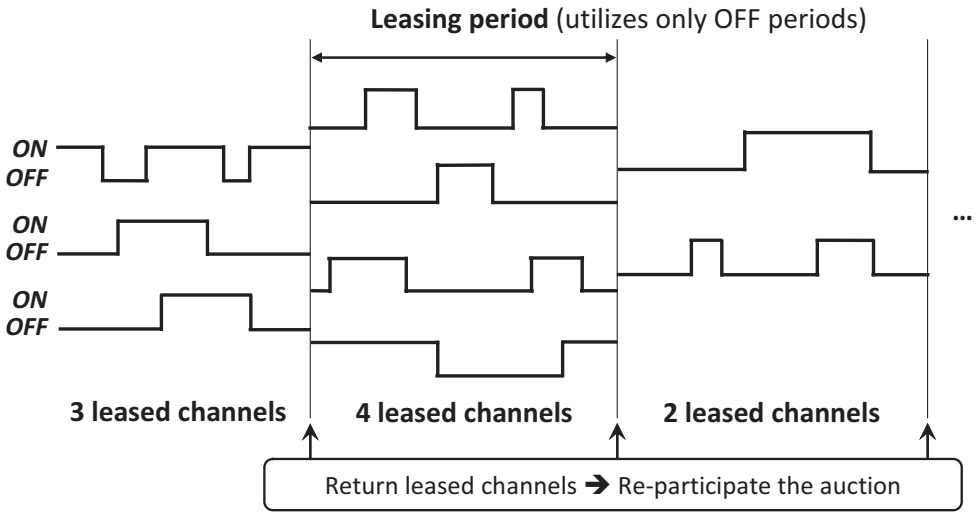

Figure 5.2: The preemptive spectrum lease model

of user control: admission and eviction. Admission control determines if a newly-arriving customer should be admitted to or rejected from the service, to achieve better profit. Although optimal user admission control in isolation was studied in [66] for the case of static spectrum availability, CR networks face a unique challenge—time-varying spectrum availability due to PUs' activities—that necessitates joint control of user admission and eviction. At channel vacation, the customers previously assigned to the channel (called *in-service users*) have to be relocated by the WSP to the other remaining idle channels. However, in case the remaining idle channels cannot fully support spectrum demands of all in-service users,[2] the WSP should determine which users to be evicted from its network. The evicted users will be compensated with some form of reimbursement, which may differ by the user-specific spectrum demands and thus affect the WSP's profit.

To derive the optimal user admission and eviction controls, we first model it as a semi-Markov decision process (SMDP) and a linear programming (LP) algorithm is

[2]QoS degradation (i.e., assigning less bandwidth than a user requested) is not considered in this chapter, which is our future work.

proposed to derive the solution. QoS provisioning for CR end-users is also considered by adding two constraints to the LP algorithm: the probability of blocking newly-arriving users and the probability of evicting/dropping in-service users, so that the WSP can strike a balance between profit maximization and customer satisfaction.

5.1.2 Organization

The rest of the chapter is organized as follows. Section 5.2 overviews related work, and then Section 5.3 introduces the system model and the basic assumptions used throughout this chapter. In Section 5.4, the problem of maximizing a WSP's profit is modeled as an SMDP and its relevant components are derived. Section 5.5 presents an LP-based SMDP algorithm to determine the optimal user admission and eviction policies with constraints on the blocking and dropping probabilities. Section 5.6 introduces a prioritized multi-class service at CR hotspots and derives its optimal user controls. The proposed scheme is evaluated in Section 5.7 via numerical analysis and in-depth simulation, and the chapter concludes with Section 5.8.

5.2 Related Work

Mutlu *et al.* [58] studied how to maximize a WSP's average profit, focusing on an optimal pricing policy without considering user admission control which could increase the WSP's profit further. Moreover, they assumed that PUs and SUs can simultaneously access the same channel, thus unneeding user eviction control, which is not possible if PUs are given priority over SUs. Ishibashi *et al.* [43] considered multi-homed PUs, where each PU is either conventional or CR-enabled. They investigated enhancement of resource utilization with cognitive PUs switching between channels, and derived the blocking and dropping probabilities in such a scenario. However, no priority in channel access is given to the conventional PUs, thus unac-

counting for user eviction. Wang *et al.* [95] proposed a primary-prioritized Markov approach where PUs have exclusive rights to access their own channels. Although they considered giving priority to PUs, user admission control was ignored and only one channel and two SUs were considered, thus limiting its applicability. Ross and Tsang [66] investigated the problem of optimal admission control on the users with different spectrum demands. However, their problem was limited to the case when channels are always available, thus unneeding user eviction control.

5.3 System Model

In this section, we introduce the system model and assumptions to be used throughout this chapter.

5.3.1 Channel Model

A channel is modeled as an ON/OFF alternating renewal process, as introduced in Chapter I. It is assumed that the transitions between ON and OFF states can be detected by either spectrum sensing or a PU signalling mechanism. First, spectrum sensing, as described in Chapter I, is a process of sampling the channel state (i.e., ON or OFF) to identify spectrum whitespaces, which has been discussed in Chapters II, III, and IV. Second, the PU signalling mechanism is a method with which the licensee indicates the presence/absence of the PUs in its channels so that the lessee can notice the status of the leased channels. Since the licensee can achieve extra profit via spectrum leasing, it is reasonable to assume that the licensee may be willing to build such an auxiliary mechanism to entice more CR WSPs to the secondary market and to protect its PUs more effectively.

Let C_i denote the capacity (or bandwidth) of channel i. In this chapter, we assume channel capacities are homogeneous, i.e., $C_i = C$, $\forall i$, for ease of presentation.

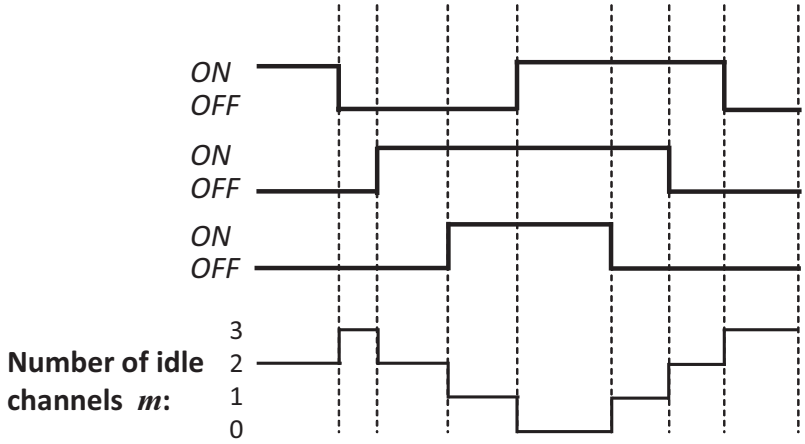

Figure 5.3: Time-varying channel capacity

However, our SMDP model can be easily extended to the case of heterogeneous channel capacities at the expense of increased state/action spaces. With M (possibly non-contiguous) leased channels, a WSP's instantaneous capacity is given as $m \cdot C$, $0 \leq m \leq M$, according to the ON/OFF channel-usage patterns, where m is the number of idle channels (i.e., channels in their OFF states) at that instant as shown in Fig. 5.3. We assume that the pool of idle channels is treated as one *logical channel*, whose capacity is equal to $m \cdot C$ bandwidth-units. This can be realized by the Orthogonal Frequency Division Multiplexing (OFDM) techniques with adaptive and selective allocation of OFDM sub-carriers, like NC-OFDM (Non-Contiguous OFDM) proposed in [64].

5.3.2 Spectrum Auction Model

We consider a multi-winner periodic spectrum auction [30, 97] where an SB (auctioneer) auctions off the licensed channels periodically (e.g., hourly, daily, or even weekly) every $T_{auction}$, and multiple WSPs bid for the number of channels they want to lease. Once a WSP wins M channels, it pays the (leasing) price of $p_{bid}(M)$ *per unit-time* to obtain temporary rights to reuse the channels for the period of $T_{auction}$.

After $T_{auction}$, the leased channels are returned to the licensees.

We make the following assumption on the bidding cost function $p_{bid}(M)$, $p_{bid}(0) = 0$, which is commonly accepted in the the CR auction market literature [44, 61].

Assumption 1. *$p_{bid}(M)$ is a positive, non-decreasing and convex function of M.*

This assumption is reasonable because the winning bid is likely to increase faster than proportionally to M due to the competition between WSPs contending for the limited amount of spectrum resources auctioned off in the market. The actual form of $p_{bid}(M)$ should depend on the auction market, and hence, we assume $p_{bid}(M)$ is given *a priori* in order to focus on user-control issues. For an illustrative purpose, our simulation in Section 5.7 will use $p_{bid}(M) = D_1 \cdot M^{D_2}, D_2 \geq 1$, which was introduced in [44,61] and satisfies Assumption 1. Note that D_2 represents the degree of competition in the auction.

5.3.3 Multi-class User QoS Model

A customer at a CR hotspot is a CR-capable device that is assumed to have a spectrum demand in one of the following K QoS-classes:

$$\mathbf{B} = (B_1, B_2, \ldots, B_K)^{\mathrm{T}},$$

where B_k is the bandwidth requirement of class-k customers and $^{\mathrm{T}}$ represents 'transpose'. Without loss of generality, we can assume $B_{min} = B_1 < B_2 < \ldots < B_K = B_{max}$. Note that we reserve k as the index of user class.

Based on selective OFDM sub-carrier allocation, each CR user is assumed to be capable of tuning its antenna to any portion of the logical channel for its bandwidth assignment of B_k, as illustrated in Fig. 5.4. In this way, at a channel's OFF→ON transition, the users on the channel can be redistributed to other idle channels, by

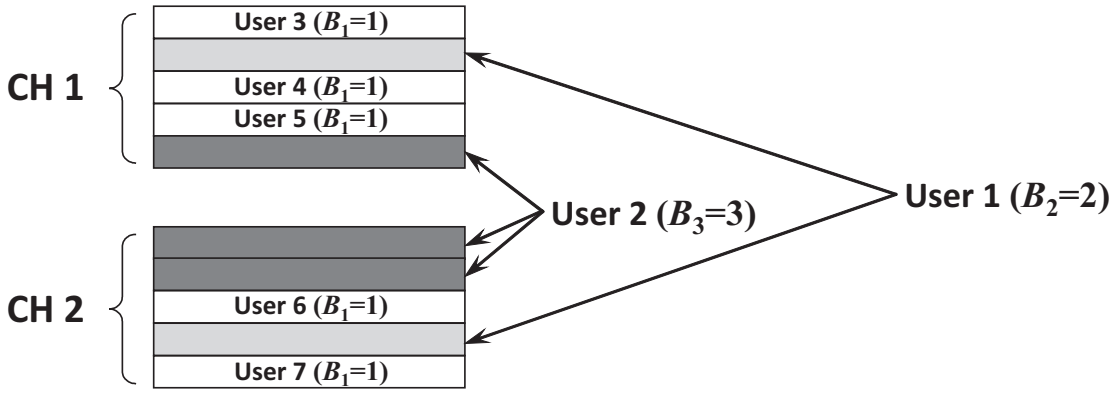

Figure 5.4: An example of channel allocation with $M = 2$, $K = 3$, and $C = 5$.

updating the mapping of OFDM subcarriers to the users. MAC-layer beaconing might be used to perform this re-mapping in real time.

We assume the arrival of class-k customers follows the Poisson distribution with rate λ_k, since the service requests from the CR users are made at the connection level and user-oriented connection requests are modeled well as a Poisson process [63]. For mathematical tractability, the service time of an in-service class-k customer is assumed exponentially distributed with mean $1/\mu_k$, capturing the reality of some applications such as phone-call traffic with exponentially-distributed talk spurt [87].

5.3.4 End-User Pricing Model

The revenue of a WSP is generated by the CR end-users who pay fees for their opportunistic spectrum usage. The vector of the usage fees for K QoS-classes, in terms of price *per* unit-time *per* unit-bandwidth, is denoted by

$$\mathbf{p} = (p_1, p_2, \ldots, p_K)^{\mathrm{T}}.$$

The arrival rate is price-dependent, and therefore, it is represented by $\lambda_k(p_k)$. $\lambda_k(p_k)$ is a non-increasing function of p_k, since a WSP advertising higher prices should expect less customer arrivals than the others offering lower prices. The actual

price-arrival relationship depends strongly on the WSP's tariff and the degree of competition, which must be treated as a separate marketing problem. Here we assume $\lambda_k(p_k)$ is given *a priori* and confine our discussion to the optimal user control. We leave $\lambda_k(p_k)$ as a general parameter in the analysis, and in Section 5.7 we will use an example of $\lambda_k(p_k) = \lambda_k^{max} e^{-\delta_k p_k}$ as introduced in [29], for an illustrative purpose. Here, λ_k^{max} indicates that the maximum user population at a CR hotspot is bounded, and δ_k represents the rate of decrease of the arrival rate as p_k increases, which is related to the degree of competition between WSPs.

5.4 SMDP Formulation

The profit maximization at a CR hotspot poses a unique challenge due to time-varying channel availability that necessitates joint user admission and eviction control by the CR WSP. In such a case, SMDP is a useful tool to determine the optimal actions achieving maximal profit, and thus in this section we formulate the system as an SMDP. We first show the validity of SMDP formulation for the problem considered, and then we derive the basic and essential components of the SMDP by accounting for time-varying channel availability and possible actions to be taken for user admission and eviction. In Section 5.5, we will use the derived components to construct our proposed LP algorithm that determines the optimal actions and achieves the maximal profit.

5.4.1 System State and State Space

We start with the definition of system state as

$$\mathbf{s} = (\mathbf{n}, \mathbf{w}), \text{ and } \begin{cases} \mathbf{n} = (n_1, n_2, \ldots, n_K)^{\mathrm{T}}, \\ \mathbf{w} = (w_1, w_2, \ldots, w_M)^{\mathrm{T}}, \end{cases} \tag{5.1}$$

where n_k is the number of class-k customers in service, and w_i is the channel state defined as

$$w_i = \begin{cases} 1, & \text{channel } i \text{ is occupied by PUs (i.e., ON),} \\ 0, & \text{channel } i \text{ is } \textit{not} \text{ occupied by PUs (i.e., OFF).} \end{cases}$$

Then, the sub-state-space of $\mathbf{w}$, denoted by $\Lambda_{\mathbf{w}}$, and the sub-state-space of $\mathbf{n}$ given $\mathbf{w}$, denoted by $\Lambda_{\mathbf{n}|\mathbf{w}}$, are defined as

$$\begin{aligned} \Lambda_{\mathbf{w}} &= \{\mathbf{w} : w_i \in \{0, 1\}\}, \\ \Lambda_{\mathbf{n}|\mathbf{w}} &= \{\mathbf{n} : n_k \geq 0,\ \mathbf{n}^{\mathrm{T}}\mathbf{B} \leq mC,\ m = (\mathbf{1} - \mathbf{w})^{\mathrm{T}}\mathbf{1}\}, \end{aligned}$$

where m is the number of idle channels and $\mathbf{1}$ is a vector of 1's. Therefore, the state space Λ is given as

$$\Lambda = \{\mathbf{s} : \mathbf{w} \in \Lambda_{\mathbf{w}}, \mathbf{n} \in \Lambda_{\mathbf{n}|\mathbf{w}}\}.$$

5.4.2 Possible Actions and Action Space

In our SMDP formulation, an *action* is taken and updated at each *decision epoch* under the chosen policy, where a natural choice of the decision epoch is the instant when a channel's state changes, i.e., (1) at a class-k customer's arrival/departure and (2) at channel i's state-transition (ON→OFF or OFF→ON).

We define the action at a certain decision epoch as

$$\boldsymbol{\alpha} = (\mathbf{a}, \mathbf{b}), \text{ and } \begin{cases} \mathbf{a} = (a_1, a_2, \ldots, a_K)^{\mathrm{T}}, \\ \mathbf{b} = (b_1, b_2, \ldots, b_K)^{\mathrm{T}}, \end{cases}$$

where $\mathbf{a}$ is the admission policy for future customer arrivals such that

$$a_k = \begin{cases} 0, & \textit{reject} \text{ all future class-}k \text{ arrivals,} \\ 1, & \textit{admit} \text{ all future class-}k \text{ arrivals,} \end{cases}$$

and $\mathbf{b}$ is the eviction policy for *in-service* customers where b_k indicates the number of class-k customers to be evicted *at the time of channel vacation*, i.e., at state-transition OFF→ON on a certain channel. That is, even if $\mathbf{b} \neq \mathbf{0}$, we do not evict any customer if the next event is an arrival, departure, or state-transition ON→OFF.

Then, for a given state $\mathbf{s}$, the action space A is defined as

$$A(\mathbf{s}) = \begin{cases} \{\boldsymbol{\alpha} : \mathbf{a} = \mathbf{0},\ \ \mathbf{b} = \mathbf{0}\}, & \text{if } m = 0, \\ \{\boldsymbol{\alpha} : \mathbf{a} \in A_1(\mathbf{s}),\ \ \mathbf{b} \in A_2(\mathbf{s})\}, & \text{otherwise,} \end{cases} \tag{5.2}$$

with $A_1(\mathbf{s})$ and $A_2(\mathbf{s})$ being defined as

$$A_1(\mathbf{s}) = \{\ \mathbf{a} :\ \ a_k \in \{0,1\};\quad a_k = 0 \text{ if } (\mathbf{n} + \mathbf{u}_k)^{\mathrm{T}}\mathbf{B} > mC\ \}, \tag{5.3}$$

$$\begin{aligned} A_2(\mathbf{s}) = \{\ \mathbf{b} :\ \ & 0 \le b_k \le n_k;\quad \mathbf{b} = \mathbf{0} \quad \text{if} \quad \mathbf{n}^{\mathrm{T}}\mathbf{B} \le (m-1)C; \\ & (\mathbf{n} - \mathbf{b} + \mathbf{u}_k)^{\mathrm{T}}\mathbf{B} > (m-1)C, \text{ for } \forall k \text{ s.t.} \\ & b_k \neq 0, \text{ and } (\mathbf{n} - \mathbf{b})^{\mathrm{T}}\mathbf{B} \le (m-1)C\ \}, \end{aligned} \tag{5.4}$$

where $\mathbf{u}_j$ is a unit vector with a single 1 at the j-th position and 0's elsewhere. In the definition of $A_2(\mathbf{s})$, the constraint

$$(\mathbf{n} - \mathbf{b} + \mathbf{u}_k)^{\mathrm{T}}\mathbf{B} > (m-1)C \text{ for } \forall k \text{ s.t. } b_k \neq 0$$

implies that $\mathbf{b}$ should be *minimal* so as not to evict more in-service customers than necessary. That is, $\mathbf{b}$ is *not* minimal if there exists k such that $\mathbf{b}' = \mathbf{b} - \mathbf{u}_k$ and $(\mathbf{n} - \mathbf{b}')^{\mathrm{T}}\mathbf{B} \le (m-1)C$, i.e., evicting one less customer than $\mathbf{b}$ still fits in $(m-1)$ channels. Obviously, the choice of minimal $\mathbf{b}$ for given $\mathbf{s}$ is not unique. For example, in case $m = 2$, $C = 5$ and $\mathbf{B} = (1, 2)$, there are three possible minimal $\mathbf{b}$'s for $\mathbf{n} = (5, 2)$: $\mathbf{b} = (4, 0)$, $\mathbf{b} = (2, 1)$ and $\mathbf{b} = (0, 2)$.

5.4.3 Validity of SMDP Formulation

Before deriving the other essential components of the SMDP, we need to check if the system under consideration can be modeled as an SMDP. In [93], an SMDP is defined as follows.

Definition 1. *A dynamic system is said to be a semi-Markov decision process if the following property is satisfied: if at a decision epoch the action $\boldsymbol{\alpha}$ is chosen in state $\boldsymbol{s}$, then the time until the state at, and revenue/cost incurred until, the next decision epoch depend only on $\boldsymbol{s}$ and $\boldsymbol{\alpha}$.*

To check if a system under consideration satisfies Definition 1, we first consider (1) a combined process of K-class user arrivals and departures, (2) M independent processes of channel-state transitions, and (3) a combined process of (1) and (2).

A combined process of user arrivals and departures

Inter-arrival and inter-departure times of class-k customers are all assumed to be exponentially distributed. Since the arrival and departure processes are independent of each other, the inter-event time, denoted by T_0, of the combined random process is also exponentially distributed with mean $1/\rho$, where $\rho := \mathbf{n}^{\mathrm{T}}\boldsymbol{\mu} + \mathbf{a}^{\mathrm{T}}\boldsymbol{\lambda}$, $\boldsymbol{\lambda} = (\lambda_1, \lambda_2, \ldots, \lambda_K)^{\mathrm{T}}$, and $\boldsymbol{\mu} = (\mu_1, \mu_2, \ldots, \mu_K)^{\mathrm{T}}$.

M independent processes of channel-state transitions

For generally-distributed ON/OFF periods, the time until the next state-transition on channel i depends not only on w_i but also on the elapsed time since the last state-transition, denoted by e_i. To satisfy the conditions in Definition 1, the previous definition of state $\mathbf{s}$ can be extended as

$$\mathbf{s} = (\mathbf{n}, \mathbf{w}, \mathbf{e}), \quad \mathbf{e} = (e_1, e_2, \ldots, e_M)^{\mathrm{T}}.$$

This approach, however, is impractical since e_i is continuous, introducing infinitely many possible states.

To derive a mathematically tractable but reasonably accurate model, we take an approximation-based approach using renewal theory [20] as follows.

Proposition 1 (Cox [20]). *Given that a renewal process of channel i has started a long time ago, the residual time in the current state, regardless of how much time has elapsed since the last state-transition, has the pdf of*

$$\begin{aligned} (1 - F_{T^i_{OFF}}(t))/E[T^i_{OFF}], t > 0, \quad \text{if } w_i = 0, \\ (1 - F_{T^i_{ON}}(t))/E[T^i_{ON}], t > 0, \quad \text{if } w_i = 1, \end{aligned} \tag{5.5}$$

where $F_{T^i_{OFF}}(t)$ and $F_{T^i_{ON}}(t)$ are the cumulative distribution functions (cdfs) of T^i_{OFF} and T^i_{ON}.

Proposition 1 indicates that as the current time progresses farther away from the time origin of a renewal channel, the pdf of the remaining time until the next state-transition will converge to Eq. (5.5). Note that exponential distribution is the only instance with which Eq. (5.5) coincides with $f_{T^i_{OFF}}(t)$ and $f_{T^i_{ON}}(t)$.

Using this property, we can keep the definition of $\mathbf{s}$ same as Eq. (5.1) while approximating the system as an SMDP because the pdfs in Eq. (5.5) do not depend on e_i's and are thus memoryless. In Section 5.7, we will show that this approximation, in fact, produces reasonably accurate results.

The overall combined process

Using the fact that the combined arrival/departure process and renewal processes of M channels are independent of each other, the cdf of the remaining time T until

the *next* decision epoch is given as

$$\begin{aligned} P(T \leq t) &= 1 - P(T = \min(T_0, T_1, \ldots, T_M) > t) \\ &= 1 - P(T_0 > t, T_1 > t, \ldots, T_M > t) \\ &= 1 - \prod_{l=0}^{M} P(T_l > t) = 1 - \prod_{l=0}^{M} (1 - P(T_l \leq t)), \end{aligned} \tag{5.6}$$

where T_l $(1 \leq l \leq M)$ is a random variable representing the residual time until the next state-transition on channel l whose pdf is given as Eq. (5.5).

As a result, the system model considered in this chapter becomes an SMDP since it possesses the properties in Definition 1:

- The time until the next decision epoch depends only on $(\mathbf{s}, \boldsymbol{\alpha})$ since Eq. (5.6) is a function of $\mathbf{n}$, $\mathbf{a}$, $\mathbf{w}$.
- The state $\mathbf{s}' = (\mathbf{n}', \mathbf{w}')$ at the next decision epoch depends only on $\mathbf{s}$ and $\boldsymbol{\alpha}$ such that (1) $\mathbf{n}' = \mathbf{n} + \mathbf{u}_k$, $\mathbf{w}' = \mathbf{w}$, at a class-k user's arrival, (2) $\mathbf{n}' = \mathbf{n} - \mathbf{u}_k$, $\mathbf{w}' = \mathbf{w}$, at a class-k user's departure, (3) $\mathbf{n}' = \mathbf{n} - \mathbf{b}$, $\mathbf{w}' = \mathbf{w} + \mathbf{u}_i$, at channel i's OFF→ON transition, and (4) $\mathbf{n}' = \mathbf{n}$, $\mathbf{w}' = \mathbf{w} - \mathbf{u}_i$, at channel i's ON→OFF transition.
- The revenue and cost accrued until the next decision epoch depend only on $\mathbf{s}$ and $\boldsymbol{\alpha}$ since they are a function of $\mathbf{n}$, $\mathbf{b}$, and the time until the next decision epoch. The definition of revenue and cost will be detailed in Section 5.4.6.

5.4.4 Decision Epochs

The expected time between two decision epochs, denoted by $\tau_{\mathbf{s}}(\boldsymbol{\alpha})$, is determined as

$$\tau_{\mathbf{s}}(\boldsymbol{\alpha}) = \int_0^\infty t f_T(t) dt, \quad f_T(t) = \frac{dP(T \leq t)}{dt},$$

where $P(T \leq t)$ is from Eq. (5.6).

For example, with exponentially-distributed ON and OFF durations with mean $1/\mu^i_{ON}$ and $1/\mu^i_{OFF}$, the expected time between two decision epochs is determined as

$$\tau_{\mathbf{s}}(\boldsymbol{\alpha}) = \left[\mathbf{n}^{\mathrm{T}}\boldsymbol{\mu} + \mathbf{a}^{\mathrm{T}}\boldsymbol{\lambda} + (\mathbf{1}-\mathbf{w})^{\mathrm{T}}\boldsymbol{\mu_{OFF}} + \mathbf{w}^{\mathrm{T}}\boldsymbol{\mu_{ON}}\right]^{-1},$$

where $\boldsymbol{\mu_{OFF}} = (\mu^1_{OFF}, \mu^2_{OFF}, \ldots, \mu^M_{OFF})^{\mathrm{T}}$ and $\boldsymbol{\mu_{ON}} = (\mu^1_{ON}, \mu^2_{ON}, \ldots, \mu^M_{ON})^{\mathrm{T}}$. This result can be understood intuitively as follows. Since channel i's residual time in ON (or OFF) state is exponentially distributed with mean $1/\mu^i_{ON}$ (or $1/\mu^i_{OFF}$), the time between state-transitions becomes exponentially distributed with mean $1/((1-w_i)\mu^i_{OFF} + w_i\mu^i_{ON})$. Therefore, with M independent channels, the combined random process is also exponentially distributed with mean $\left[(\mathbf{1}-\mathbf{w})^{\mathrm{T}}\boldsymbol{\mu_{OFF}} + \mathbf{w}^{\mathrm{T}}\boldsymbol{\mu_{ON}}\right]^{-1}$. As a result, the combined process of user arrivals/departures with M channel state-transitions becomes exponentially distributed with mean $\left[\mathbf{n}^{\mathrm{T}}\boldsymbol{\mu} + \mathbf{a}^{\mathrm{T}}\boldsymbol{\lambda} + (\mathbf{1}-\mathbf{w})^{\mathrm{T}}\boldsymbol{\mu_{OFF}} + \mathbf{w}^{\mathrm{T}}\boldsymbol{\mu_{ON}}\right]^{-1}$.

5.4.5 State-Transition Probability

The probability that the state of the SMDP switches from $\mathbf{s} = (\mathbf{n}, \mathbf{w})$ to $\mathbf{s}' = (\mathbf{n}', \mathbf{w}')$ at the next decision epoch is given as in Eq.(5.7), where T_a, T_{-a}, T_d, and T_{-d} are exponentially-distributed random variables with mean $1/a_k\lambda_k$, $1/(\rho - a_k\lambda_k)$, $1/n_k\mu_k$, and $1/(\rho - n_k\mu_k)$.

$$p_{\mathbf{s},\mathbf{s}'}(\boldsymbol{\alpha}) = \begin{cases} P(T_a \le T_{-a},\ T_a \le T_1,\ \ \ldots,\ T_a \le T_M), & \text{at a class-}k\text{ user's arrival,} \\ P(T_d \le T_{-d},\ T_d \le T_1,\ \ \ldots,\ T_d \le T_M), & \text{at a class-}k\text{ user's departure,} \\ P(T_i \le T_0,\ T_i \le T_1,\ \ \ldots,\ T_i \le T_M), & \text{at channel } i\text{'s OFF}\leftrightarrow\text{ON,} \end{cases}$$
$$= \begin{cases} \int_0^\infty \int_{t_a}^\infty \cdots \int_{t_a}^\infty \left\{ f_{T_a}(t_a) f_{T_{-a}}(t_{-a}) f_{T_1}(t_1) \cdots f_{T_M}(t_M) \right\} dt_{-a} dt_1 \cdots dt_M dt_a, \\ \int_0^\infty \int_{t_d}^\infty \cdots \int_{t_d}^\infty \left\{ f_{T_d}(t_d) f_{T_{-d}}(t_{-d}) f_{T_1}(t_1) \cdots f_{T_M}(t_M) \right\} dt_{-d} dt_1 \cdots dt_M dt_d, \\ \int_0^\infty \int_{t_i}^\infty \cdots \int_{t_i}^\infty \{ f_{T_0}(t_0) f_{T_1}(t_1) \cdots f_{T_M}(t_M) \} dt_0 \underbrace{dt_1 \cdots dt_M}_{\text{except } t_i} dt_i. \end{cases} \tag{5.7}$$

For example, for exponentially-distributed ON/OFF periods, we have

$$p_{\mathbf{s},\mathbf{s}'}(\boldsymbol{\alpha}) = \begin{cases} a_k \lambda_k \tau_{\mathbf{s}}(\boldsymbol{\alpha}), & \mathbf{n}' = \mathbf{n} + \mathbf{u}_k, & \mathbf{w}' = \mathbf{w}, & \text{class-}k\text{ arrival,} \\ n_k \mu_k \tau_{\mathbf{s}}(\boldsymbol{\alpha}), & \mathbf{n}' = \mathbf{n} - \mathbf{u}_k, & \mathbf{w}' = \mathbf{w}, & \text{class-}k\text{ departure,} \\ \mu^i_{OFF} \tau_{\mathbf{s}}(\boldsymbol{\alpha}), & \mathbf{n}' = \mathbf{n} - \mathbf{b}, & \mathbf{w}' = \mathbf{w} + \mathbf{u}_i, & \text{channel } i\text{: OFF}\rightarrow\text{ON,} \\ \mu^i_{ON} \tau_{\mathbf{s}}(\boldsymbol{\alpha}), & \mathbf{n}' = \mathbf{n}, & \mathbf{w}' = \mathbf{w} - \mathbf{u}_i, & \text{channel } i\text{: ON}\rightarrow\text{OFF.} \end{cases}$$

5.4.6 Revenue and Reimbursement Cost

Let $r_{\mathbf{s}}(\boldsymbol{\alpha})$ and $c_{\mathbf{s}}(\boldsymbol{\alpha})$ denote the expected revenue and the cost incurred by customers until the next decision epoch if action $\boldsymbol{\alpha}$ is chosen at state $\mathbf{s}$, respectively. Since the revenue comes from the usage fee paid by the admitted customers, $r_{\mathbf{s}}(\boldsymbol{\alpha})$ is given as

$$r_{\mathbf{s}}(\boldsymbol{\alpha}) = \sum_k p_k B_k n_k \tau_{\mathbf{s}}(\boldsymbol{\alpha}).$$

Assuming a fixed amount of reimbursement I_k for an evicted class-k customer, $c_{\mathbf{s}}(\boldsymbol{\alpha})$ is

$$c_{\mathbf{s}}(\boldsymbol{\alpha}) = \sum_k I_k b_k \cdot q^{\mathcal{V}}_{\mathbf{s}}(\boldsymbol{\alpha}),$$

where $\tau_{\mathbf{s}}(\boldsymbol{\alpha})$ does not contribute to the equation since the reimbursement is a one-time cost at channel vacation. $q_{\mathbf{s}}^{\mathcal{V}}(\boldsymbol{\alpha})$ is the probability that the event of channel vacation will happen at the next decision epoch. We also let $q_{\mathbf{s}}^{\mathcal{A},k}(\boldsymbol{\alpha})$ denote the probability that the event of a class-k user's arrival will occur and then be accepted at the next decision epoch. Then, we have

$$\begin{aligned} q_{\mathbf{s}}^{\mathcal{V}}(\boldsymbol{\alpha}) &= \sum_{\substack{\mathbf{s}'\in\Lambda \text{ s.t. } \mathbf{n}'=\mathbf{n}-\mathbf{b}, \\ \mathbf{w}'=\mathbf{w}+\mathbf{u}_i \text{ for some } i}} p_{\mathbf{s},\mathbf{s}'}(\boldsymbol{\alpha}), \\ q_{\mathbf{s}}^{\mathcal{A},k}(\boldsymbol{\alpha}) &= \sum_{\substack{\mathbf{s}'\in\Lambda \text{ s.t.} \\ \mathbf{n}'=\mathbf{n}+\mathbf{u}_k, \mathbf{w}'=\mathbf{w}}} p_{\mathbf{s},\mathbf{s}'}(\boldsymbol{\alpha}). \end{aligned}$$

5.5 Optimal User Control via a Linear Programming Algorithm

In this section, we propose an LP algorithm based on the essential SMDP components derived in the previous section, that can maximize the profit at CR hotspots by determining the optimal action $\boldsymbol{\alpha}$ at each possible system state $\mathbf{s}$ subject to the QoS constraints such as keeping the blocking and dropping probabilities below certain thresholds. There are three well-known methods for optimally solving the SMDP problem: *policy-iteration*, *value-iteration*, and *linear programming* (LP) [93], and of these, we adopt LP because it is the best-known to model the QoS-constrained optimization problem thanks to its flexibility to include additional equality and inequality constraints.

5.5.1 Linear Programming SMDP Algorithm: Constrained QoS

Here we formulate a 3-step LP algorithm with the constraints on the probability of blocking class-k arrivals (denoted by P_b^k), and the probability of dropping/evicting class-k in-service customers (denoted by P_d^k). This 3-step algorithm follows the gen-

eral format of the LP algorithm recommended in [93], but its mathematical content is our own development.

***Step 1*:** Find the optimal basic solution $z^*_{\mathbf{s},\boldsymbol{\alpha}}$ to the following linear programming problem ($z_{\mathbf{s},\boldsymbol{\alpha}} \geq 0$):

$$\textbf{Maximize} \sum_{\mathbf{s}\in\Lambda} \sum_{\boldsymbol{\alpha}\in A(\mathbf{s})} \left(r_{\mathbf{s}}(\boldsymbol{\alpha}) - c_{\mathbf{s}}(\boldsymbol{\alpha})\right) z_{\mathbf{s},\boldsymbol{\alpha}}$$

Subject to

$$\begin{aligned}
&\sum_{\boldsymbol{\alpha}\in A(\mathbf{s}')} z_{\mathbf{s}',\boldsymbol{\alpha}} - \sum_{\mathbf{s}\in\Lambda} \sum_{\boldsymbol{\alpha}\in A(\mathbf{s})} p_{\mathbf{s},\mathbf{s}'}(\boldsymbol{\alpha}) z_{\mathbf{s},\boldsymbol{\alpha}} = 0, \;\; \mathbf{s}' \in \Lambda, \\
&\sum_{\mathbf{s}\in\Lambda} \sum_{\boldsymbol{\alpha}\in A(\mathbf{s})} \tau_{\mathbf{s}}(\boldsymbol{\alpha}) z_{\mathbf{s},\boldsymbol{\alpha}} = 1, \\
&P_b^k \leq \gamma_{block}^k, \;\; \forall k, \\
&P_d^k \leq \gamma_{drop}^k, \;\; \forall k,
\end{aligned} \tag{5.8}$$

P_b^k and P_d^k in Eq. (5.8) are determined as

$$\begin{aligned}
P_b^k &= \sum_{\mathbf{s}\in\Lambda} \sum_{\substack{\boldsymbol{\alpha}\in A(\mathbf{s}) \\ \text{s.t. } a_k=0}} \tau_{\mathbf{s}}(\boldsymbol{\alpha}) z_{\mathbf{s},\boldsymbol{\alpha}}, \\
P_d^k &= \frac{\mathcal{V}^k}{\mathcal{A}^k},
\end{aligned} \tag{5.9}$$

where

$$\begin{aligned}
\mathcal{A}^k &= \sum_{\mathbf{s}\in\Lambda} \sum_{\boldsymbol{\alpha}\in A(\mathbf{s})} \tau_{\mathbf{s}}(\boldsymbol{\alpha}) z_{\mathbf{s},\boldsymbol{\alpha}} q_{\mathbf{s}}^{\mathcal{A},k}(\boldsymbol{\alpha}) \cdot \frac{1}{\tau_{\mathbf{s}}(\boldsymbol{\alpha})}, \\
\mathcal{V}^k &= \sum_{\mathbf{s}\in\Lambda} \sum_{\boldsymbol{\alpha}\in A(\mathbf{s})} \tau_{\mathbf{s}}(\boldsymbol{\alpha}) z_{\mathbf{s},\boldsymbol{\alpha}} q_{\mathbf{s}}^{\mathcal{V}}(\boldsymbol{\alpha}) \cdot \frac{b_k}{\tau_{\mathbf{s}}(\boldsymbol{\alpha})},
\end{aligned}$$

and $z_{\mathbf{s},\boldsymbol{\alpha}} = x_{\mathbf{s},\boldsymbol{\alpha}}/\tau_{\mathbf{s}}(\boldsymbol{\alpha})$ with $x_{\mathbf{s},\boldsymbol{\alpha}}$ denoting the fraction of time that the system is in state $\mathbf{s}$ when action $\boldsymbol{\alpha}$ is chosen. Therefore, $\mathcal{A}^k$ implies the expected number of class-k accepted arrivals per unit-time and $\mathcal{V}^k$ implies the expected number of class-k evictions per unit-time.

The form of P_d^k makes this a nonlinear programming (NLP) problem. Fortunately, however, by properly manipulating the constraint $P_d^k \leq \gamma_{drop}^k$, it can be converted to a linear programming (LP) problem as follows:

$$\begin{aligned} \frac{\mathcal{V}^k}{\mathcal{A}^k} &\leq \gamma_{drop}^k \;\Rightarrow\; \mathcal{V}^k - \gamma_{drop}^k \mathcal{A}^k \leq 0 \\ &\Rightarrow \sum_{\mathbf{s}\in\Lambda} \sum_{\boldsymbol{\alpha}\in A(\mathbf{s})} \left(q_{\mathbf{s}}^{\mathcal{V}}(\boldsymbol{\alpha}) \cdot b_k - \gamma_{drop}^k q_{\mathbf{s}}^{\mathcal{A},k}(\boldsymbol{\alpha}) \cdot 1\right) z_{\mathbf{s},\boldsymbol{\alpha}} \leq 0, \end{aligned}$$

which is a linear constraint on $z_{\mathbf{s},\boldsymbol{\alpha}}$'s.

***Step 2*:** Start with a non-empty set

$$S := \left\{ \mathbf{s} | \sum_{\boldsymbol{\alpha}\in A(\mathbf{s})} z_{\mathbf{s},\boldsymbol{\alpha}}^* > 0 \right\},$$

and for any state $\mathbf{s} \in S$, set the decision as

$$R^*(\mathbf{s}) := \boldsymbol{\alpha} \text{ for some } \boldsymbol{\alpha} \text{ such that } z_{\mathbf{s},\boldsymbol{\alpha}}^* > 0.$$

***Step 3*:** If $S = \Lambda$, then the algorithm terminates with the optimal policy R^*. Otherwise, determine some state $\mathbf{s} \notin S$ and action $\boldsymbol{\alpha} \in A(\mathbf{s})$ such that $p_{\mathbf{s},\mathbf{s}'}(\boldsymbol{\alpha}) > 0$ for some $\mathbf{s}' \in S$. For the chosen $\mathbf{s}$, set $R^*(\mathbf{s}) := \boldsymbol{\alpha}$ and update $S := S \cup \{\mathbf{s}\}$, and then repeat Step 3.

By repeatedly performing Step 3, the algorithm runs until S becomes Λ. The computational complexity of executing this final step is trivial since $p_{\mathbf{s},\mathbf{s}'}(\boldsymbol{\alpha}) > 0$ has already been computed in Step 1 for all possible combinations of $(\mathbf{s}, \mathbf{s}', \boldsymbol{\alpha})$. In addition, the optimality of the derived policy is guaranteed in [93], although the algorithm may not produce a unique solution due to the conditions 'some $\boldsymbol{\alpha}$' and 'some $\mathbf{s}'$' in Steps 2 and 3.

Then, the *optimal profit* g^* per unit-time is determined as

$$g^* = \sum_{\substack{\mathbf{s}\in\Lambda \\ \boldsymbol{\alpha}=R^*(\mathbf{s})}} (r_{\mathbf{s}}(\boldsymbol{\alpha}) - c_{\mathbf{s}}(\boldsymbol{\alpha}))z_{\mathbf{s},\boldsymbol{\alpha}} \;\; - \;\; p_{bid}(M). \tag{5.10}$$

5.5.2 Complexity of SMDP Algorithm

The complexity of the proposed algorithm is measured by the size of the search space $\Lambda \times A(\mathbf{s})$. In Fig. 5.5, one can see that $|\Lambda \times A(\mathbf{s})|$ increases almost exponentially as M or K increases, because $|\Lambda_{\mathbf{w}}| = 2^M$ and $|A_1(\mathbf{s})| = 2^K$ in the worst case. However, the complexity issue can be managed properly in the real scenarios due to the following two reasons.

First, in commercial applications, a reasonable range of (M, K) could be $1 \leq K, M \leq 3$ in which case we have a moderate and reasonable level of complexity since $|\Lambda \times A(\mathbf{s})| \leq 2,167$ in Fig. 5.5. For example, $K = 3$ for a service with Gold, Silver, and Bronze classes, and $K = 2$ for a service with Premium and Basic classes. In fact, the premium/basic classification is commonly found in today's commercial Wi-Fi hotspot services. In addition, if we compare the *effective* capacity of our Wi-Fi-like service over whitespaces with that of the traditional Wi-Fi, a CR hotspot utilizing M ON/OFF channels has $M \cdot (1-u)C$ provided the channels have a similar utilization factor of u such that

$$u = E[T^i_{ON}]/\{E[T^i_{ON}] + E[T^i_{OFF}]\},$$

while the traditional Wi-Fi utilizing a single and always-idle channel has C. In practice, licensed bands with lower utilization (e.g., $u < 0.5$) have more whitespaces, and thus they are more preferred for DSA deployment. In such channels, it is sufficient to have $M \geq 2$ to achieve a capacity equal to or larger than C. As a result, most practical scenarios will incur manageable complexity.

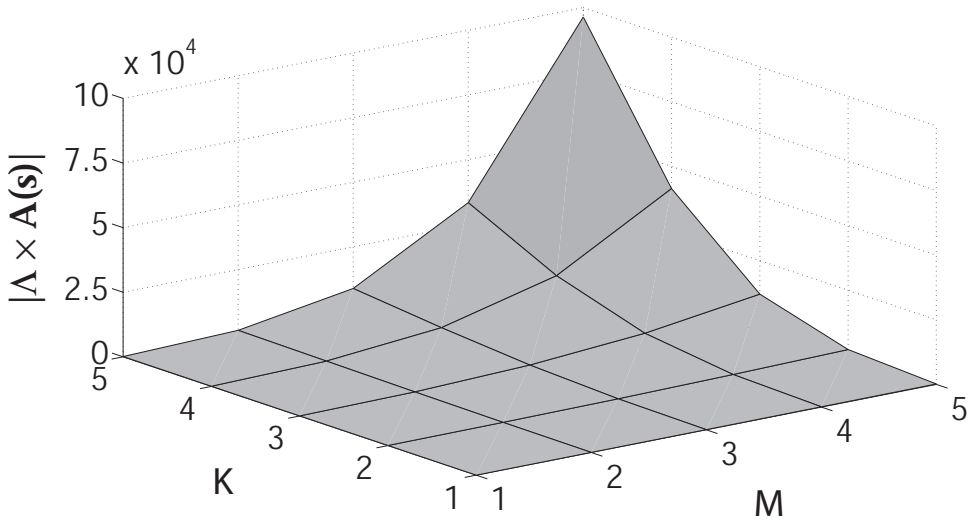

Figure 5.5: The size of the search space according to (M,K)

Next, the LP can be solved *off-line* before a WSP starts a new spectrum-leasing period (i.e., $T_{auction}$), so the derived optimal control can be stored in a database. Using the database, the WSP can perform user admission control in real time by simply looking up the database upon every user arrival/departure or channel ON/OFF transition.

5.6 Prioritized Multi-Class User Control

So far, we have investigated the optimal user control at CR hotspots for multi-class customers, each requiring a different level of QoS, without assuming any priority in service provisioning between them. In this section, we introduce the case when different priority is given to each user class, and discuss how optimal actions are derived in such a case.

Without loss of generality, we assume that a larger-index class is given higher priority, i.e., class K gets the highest priority and class 1 gets the lowest priority in either admission or eviction control. This type of service may be viewed as a hybrid service of two types of today's commercial Wi-Fi services—*free* (e.g., at some coffee

$$A_1(\mathbf{s}) = \Bigg\{ \mathbf{a} : a_K = \begin{cases} 1, & \text{if } (n_K+1)B_K \le mC, \\ 0, & \text{otherwise,} \end{cases} \quad \text{and}$$
$$a_{k<K} = \begin{cases} 1, & \text{if } \sum_{l=k+1}^{K} n_l B_l + (n_k+1)B_k \le mC, \\ 0, & \text{otherwise.} \end{cases} \Bigg\}. \tag{5.11}$$

$$A_2(\mathbf{s}) = \Bigg\{ \mathbf{b} : b_K = \beta_K, \quad \text{and} \quad b_{k<K} = \begin{cases} n_k, & \text{if } \sum_{l=k+1}^{K} n_l B_l \ge (m-1)C, \\ \beta_k, & \text{otherwise.} \end{cases} \Bigg\},$$
$$\beta_K = \min\Big\{ n_K \ge \beta \ge 0 : (n_K - \beta)B_K \le (m-1)C \Big\}, \tag{5.12}$$
$$\beta_k = \min\left\{ n_k \ge \beta \ge 0 : \sum_{l=k+1}^{K} n_l B_l + (n_k - \beta)B_k \le (m-1)C \right\}.$$

$$c_k^{\kappa} = \begin{cases} 0, & \text{if } \kappa \le k, \\ n_k, & \text{if } \kappa > k, \sum_{l=k+1}^{K} n_l B_l + B_\kappa > mC, \quad \textit{where} \\ \omega_{min}, & \text{otherwise,} \end{cases} \tag{5.13}$$
$$\omega_{min} = \min\Big\{ \omega : 0 \le \omega \le n_k, \text{ and } \sum_{l=k+1}^{K} n_l B_l + B_\kappa + (n_k - \omega)B_k \le mC \Big\}.$$

---

shops) and *charged* Wi-Fi access (e.g., AT&T Wi-Fi access). For example, for $K = 2$, by making $p_2 > 0$ and $p_1 = 0$, customers with less important jobs may choose a best-effort free service (class 1) while customers with important or resource demanding jobs, such as multimedia applications, may choose a reliable-but-fee-paying service (class 2).

In prioritized admission control (p-AC), user eviction is allowed not only at the time of channel vacation but also at the customer arrivals. Under this new policy, an arriving user is *always* accepted for the service *unless* there is no room even after evicting all lower-class users. When accepting the newly-arrived user, the system should evict a certain number of lower-priority in-service users, but no more than

necessary. To model such an action, we need to modify the action space $A_1(\mathbf{s})$ in Eq. (5.3) to express the prioritized admission control, as shown in Eq.(5.11).

In prioritized eviction control (p-EC), an in-service user is *never* evicted from the system *unless* there is no room even after evicting all lower-class users. This rule is modeled by modifying the action space $A_2(\mathbf{s})$ in Eq. (5.4) as shown in Eq.(5.12).

Note that if both p-AC and p-EC are employed, the action at given state $\mathbf{s}$ is uniquely determined as can be seen from Eqs. (5.11) and (5.12). In case either p-AC or p-EC is not applied, however, the LP algorithm in Section 5.5 should still be used in deriving optimal actions.

For the prioritized service, we may need to modify/re-define some SMDP components introduced earlier. First, to differentiate user eviction at customer arrivals from user eviction at channel vacation, we re-define the action $\boldsymbol{\alpha}$ as

$$\boldsymbol{\alpha} = (\mathbf{a}, \mathbf{b}, \mathbf{c}^1, \ldots, \mathbf{c}^K). \tag{5.14}$$

In Eq.(5.14), $\mathbf{c}^\kappa$, $1 \le \kappa \le K$, is defined as

$$\mathbf{c}^\kappa = (c_1^\kappa, c_2^\kappa, \ldots, c_K^\kappa)^{\mathrm{T}},$$

where c_k^κ is the number of class-k in-service users to be evicted if the next event is a class-κ customer arrival, which is determined as in Eq.(5.13).

Then, upon a class-κ customer's arrival, we have $\mathbf{n}' = \mathbf{n} + \mathbf{u}_\kappa a_\kappa - \mathbf{c}^\kappa a_\kappa$ instead of $\mathbf{n}' = \mathbf{n} + \mathbf{u}_\kappa$. Note that when p-AC is not applied, we set $c_k^\kappa = 0, \forall (k, \kappa)$.

Next, P_d^k is re-defined as

$$\begin{aligned} P_d^k &= \frac{\mathcal{V}^k + \mathcal{V}_{arr}^k}{\mathcal{A}^k}, \\ \mathcal{V}_{arr}^k &= \sum_{\mathbf{s}\in\Lambda} \sum_{\boldsymbol{\alpha}\in A(\mathbf{s})} \sum_{\kappa} \tau_{\mathbf{s}}(\boldsymbol{\alpha}) z_{\mathbf{s},\boldsymbol{\alpha}} q_{\mathbf{s}}^{\mathcal{A},\kappa}(\boldsymbol{\alpha}) \cdot \frac{c_k^\kappa a_\kappa}{\tau_{\mathbf{s}}(\boldsymbol{\alpha})}, \end{aligned}$$

where $\mathcal{A}^k$ and $\mathcal{V}^k$ are the same as in Section 5.5, and $\mathcal{V}^k_{arr}$ implies the expected number of class-k evictions per unit-time due to the arrivals with higher priority.

Finally, the reimbursement cost $c_{\mathbf{s}}(\boldsymbol{\alpha})$ is updated as

$$c_{\mathbf{s}}(\boldsymbol{\alpha}) = \sum_k I_k b_k \cdot q^{\mathcal{V}}_{\mathbf{s}}(\boldsymbol{\alpha}) + \sum_\kappa \sum_k I_k c^\kappa_k a_\kappa \cdot q^{\mathcal{A},\kappa}_{\mathbf{s}}(\boldsymbol{\alpha}).$$

5.7 Performance Evaluation

In this section, we first present the system state of a WSP according to the optimal user admission/eviction control, and show the robustness of the approximation of Eq. (5.5) in Section 5.4.3. Then, we evaluate the impact of various system parameters on the achieved profit g^* such as the optimal control, the number of leased channels M, and the service tariff $\mathbf{p}$. Finally, we introduce the tradeoff between two QoS metrics, the probability of blocking and the probability of dropping.

In all simulation experiments, we randomly generated customer arrivals and departures according to the Poisson distributions as we assumed, and randomly produced ON/OFF periods according to either exponential or Erlang distribution.[3] At each decision epoch, an action is taken in accordance with the set of optimal actions determined by the analysis (via solving the LP). In addition, we consider the un-prioritized multi-class service.

Each simulation ran for 3,000 time-units and the same simulation repeats 10 times to observe its average performance. The simulation parameters used in this section are summarized in Tables 5.1 and 5.2. In Table 5.1, I_k is set to be $\epsilon_I \cdot$ 100% of the average usage charge until the normal departure (not eviction) of an admitted class-k user. In Table 5.2, $\gamma_{block} = \gamma^k_{block}$ and $\gamma_{drop} = \gamma^k_{drop}$ for all k.

[3] In Section 5.7.2 we test both exponential and Erlang distributions; otherwise, ON/OFF periods are assumed to be exponentially distributed. For the Erlang case, we consider pdfs of $(\eta^i_{ON})^2 t \cdot e^{-\eta^i_{ON} \cdot t}$ and $(\eta^i_{OFF})^2 t \cdot e^{-\eta^i_{OFF} \cdot t}$, $t > 0$, where $\eta^i_{ON} = 2/E[T^i_{ON}]$ and $\eta^i_{OFF} = 2/E[T^i_{OFF}]$.

Channel	$C = 5, \quad E[T^i_{OFF}] = 10,\ E[T^i_{ON}] = 5,\ \forall i$
Auction	$p_{bid}(M) = 0.7 \cdot M^2$
Customers	$B_k = k, \qquad \mu_k = 1/7,\ \forall k,$ $\lambda_k(p_k) = \lambda_k^{max} e^{-p_k}$, where $(\lambda_1^{max}, \lambda_2^{max}, \lambda_3^{max}) = (5.5, 4.5, 5.5)$
Eviction	$I_k = \epsilon_I \times p_k B_k / \mu_k,\ \epsilon_I = 0.5$

Table 5.1: The list of common test parameters

Section	M	K	γ_{block}	γ_{drop}	$\mathbf{p}$
5.7.1	3	2	1.0	1.0	$(1, 1.5)^{\mathrm{T}}$
5.7.2	1-5	3	1.0	1.0	$(1, 1.5, 2)^{\mathrm{T}}$
5.7.3	1-5	3	1.0	1.0	$(1, 1.5, 2)^{\mathrm{T}}$
5.7.3	1-5	3	1.0	1.0	$(1, 1.5, 2)^{\mathrm{T}}$
5.7.3	3	2	1.0	1.0	$0.5 \leq p_1, p_2 \leq 3.5$
5.7.4	4	3	0.65-0.85	0.25-0.65	$(1, 1.5, 2)^{\mathrm{T}}$

Table 5.2: The list of test-specific parameters

5.7.1 System State Transition by Optimal Control

Fig. 5.6 illustrates the optimal actions derived by the proposed SMDP algorithm in the form of state-transition diagram, when $M = 3$ and $K = 2$. For simplicity, the state-transition diagram is drawn for $m = 2$ (i.e., when there are two idle channels) and only the transitions by the user arrivals are presented. As shown, the optimal admission policy deliberately rejects certain arrivals to maximize the profit, disabling some possible state-transitions (shaded regions). It is also observed that the derived optimal control is not threshold-type [67] as found in traditional networks with static spectrum availability.

5.7.2 Approximation Accuracy of Eq. (5.5)

Fig. 5.7 shows the difference between the analytically-predicted results given by Eq. (5.10) and the simulation results, for two different ON/OFF distributions: expo-

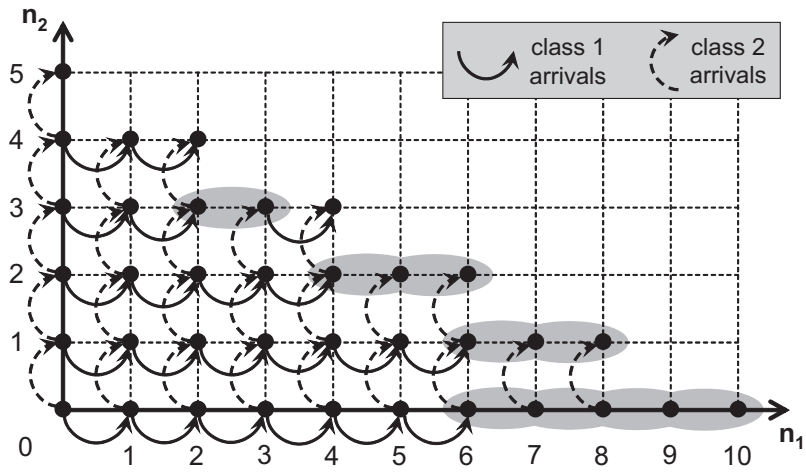

Figure 5.6: The state-transition diagrams of the proposed SMDP algorithm, according to user arrivals (shown for $m = 2$)

nential and Erlang. To focus on the accuracy of our analysis, we plot $g^* + p_{bid}(M)$. In Fig. 5.7(a), it is seen that the two results match well each other since there exists no approximation error in case ON/OFF periods are exponentially-distributed. On the other hand, when ON/OFF periods are Erlang-distributed as in Fig. 5.7(b), there exists only up to 4.4% difference between the simulated and analytic results showing that the approximation in Eq. (5.5) produces reasonably accurate results. The difference gets slightly larger as M grows due to the increase in the number of channels where approximation is used.

5.7.3 Achieved Optimal Profit by SMDP Algorithm

We now show the optimal profit achieved by the proposed SMDP under various test scenarios. We first compare the optimal profit of SMDP with the profit of the simple complete-sharing (CS) algorithm [66], and show the impact of the system parameters on the achieved profit such as the number of leased channels and the service tariff.

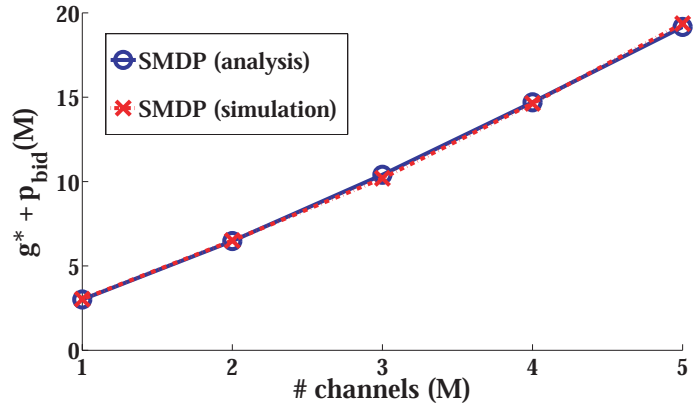

(a) Exponential distribution

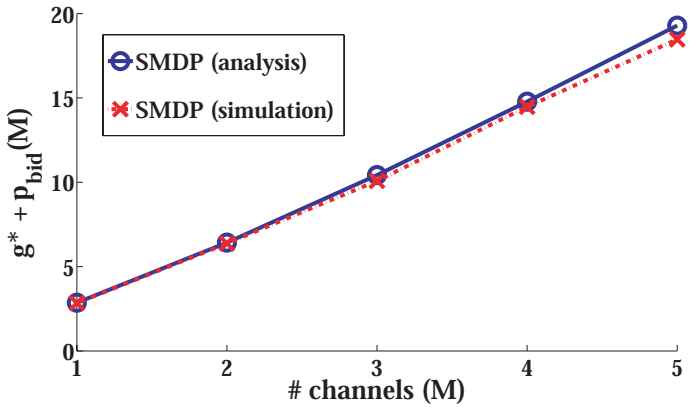

(b) Erlang distribution

Figure 5.7: Approximation accuracy of Eq. (5.5) for two types of ON/OFF distributions

Optimal vs. Non-optimal Control

We compare the performance of the proposed SMDP algorithm with the CS algorithm in terms of g^* and $g^* + p_{bid}(M)$. The CS algorithm provides a simple admission control that accepts any arrivals as long as there is room in the WSP's spectrum resources. Since CS is not designed to deal with eviction control, we consider two possible variations of CS: CS with random eviction (denoted by 'CS + Random'), and CS with optimal eviction control (denoted by 'CS + EC'). At channel vacation, 'CS + Random' chooses the users to evict one-by-one through random selection, until the remaining users can fit in the available idle channels. On

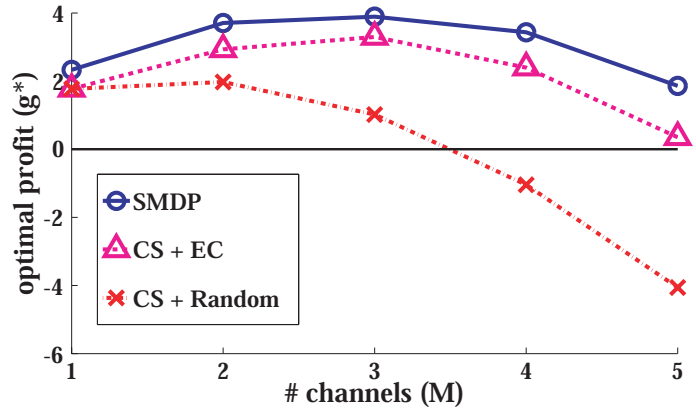

(a) optimal profit g^*

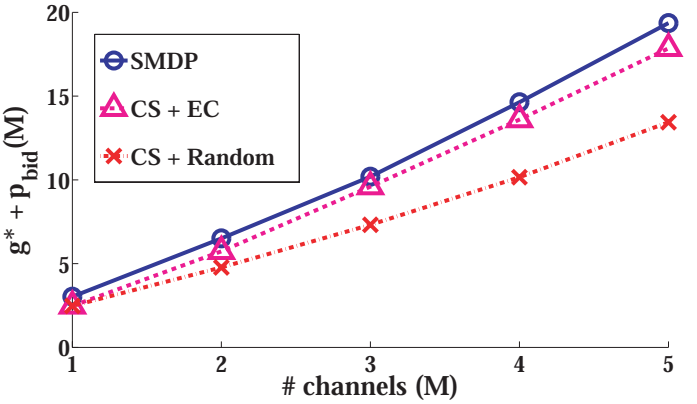

(b) $g^* + p_{bid}(M)$

Figure 5.8: Comparison of SMDP and two variations of CS in terms of their achieved profits

the other hand, 'CS + EC' is derived by applying our SMDP procedure in Sections 5.4 and 5.5 by updating $A_1(\mathbf{s})$ in Eq. (5.3) as

$$A_1(\mathbf{s}) = \left\{ \mathbf{a} : \quad a_k = \left\{ \begin{array}{ll} 0 & \text{if } (\mathbf{n} + \mathbf{u}_k)^{\mathrm{T}} \mathbf{B} > mC, \\ 1 & \text{otherwise.} \end{array} \right\} \right. .$$

Fig. 5.8 shows that SMDP always achieves more profit than CS. In the tested scenario, SMDP achieves up to 44% more profit than 'CS + Random' and up to 22.5% more profit than 'CS + EC', in terms of $g^* + p_{bid}(M)$.[4] Comparison of 'CS + EC'

[4]The reason why we consider $g^* + p_{bid}(M)$ is to eliminate the effect of the bidding price for fair comparison, focusing on the profit achievement solely by the optimal control, since $p_{bid}(M)$ is given and thus cannot be optimized.

and 'CS + Random' shows that the performance of CS is enhanced significantly by employing the optimal eviction control. In addition, the performance gap between the optimal SMDP and 'CS + EC' is much smaller than the gap between 'CS + EC' and 'CS + Random', suggesting that eviction control makes more impact on the achieved profit than the admission control does. It also shows that 'CS + EC' coincides with 'CS + Random' at $M = 1$ since there exists only one possible eviction control at channel vacation (i.e., evict all users), and the performance gap between two becomes more significant as M grows. This implies that the effect of eviction control becomes dominant as the number of leased channels increases, due to the time-varying spectrum availability.

Impact of Number of Leased Channels M

In Fig. 5.8(a), one can see that g^* varies with M, having a peak value at $M = 3$. This phenomenon stems from the tradeoff between the revenue generated by customers (i.e., $g^* + p_{bid}(M)$) and the bidding cost (i.e., $p_{bid}(M)$), because (1) a larger M generates more revenue and less reimbursement cost due to more room available to accommodate user arrivals, but (2) the gain will eventually be saturated due to the bounded user population, and therefore, leasing more channels than necessary becomes counter-productive, considering that $p_{bid}(M)$ grows faster than proportionally to M as assumed in Section 5.3.2. Therefore, finding a proper M is essential to profit maximization which can be achieved by determining and comparing $g^*(M)$ for various M using the proposed SMDP algorithm.

Impact of Service Tariff p

Due to the price-dependent arrival rate (i.e., $\lambda_k(p_k) = \lambda_k^{max} e^{-p_k}$), varying p_k may produce a different amount of profit. To show its impact on g^*, we evaluated the case

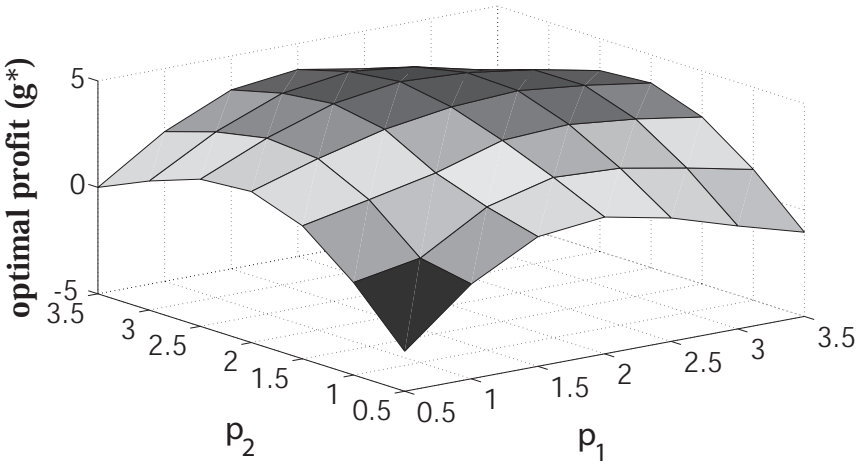

Figure 5.9: Optimal profit with various end-user pricing

of $M = 3$ and $K = 2$ while varying $\mathbf{p}$ such that $0.5 \leq p_1, p_2 \leq 3.50$. Fig. 5.9 plots the resulting g^*. It can be seen that as either p_1 or p_2 (or both) gets closer to 0.5 or 3.5, the resultant profit decreases dramatically due to the bounded user arrivals by λ_k^{max} (the case of 0.5) and decrease of the user arrival rate by e^{-p_k} (the case of 3.5), respectively. As a result, the profit function becomes concave, where the largest profit can be attained at $\mathbf{p} = (2.0, 2.5)$. Therefore, a WSP must consider the impact of its pricing policy on the overall profit, for which research on market demands and customer statistics should be helpful to find the price–arrival rate relationship.

5.7.4 Tradeoffs between Two QoS Constraints

Fig. 5.10 plots the tradeoff between P_b and P_d. To show the relationship between the two, we first fix $\gamma_{block} = 1.0$ and vary γ_{drop} in (a). Similarly, in (b), we fix $\gamma_{drop} = 1.0$ and vary γ_{block}. As γ_{drop} decreases, the QoS requirement on P_d becomes stricter so that more in-service users may be protected from eviction at channel vacation. For this, user arrivals must be blocked more often since the longer stay of in-service users implies less idle resources for newly-arriving users. Thus, P_b increases to compensate for the decrease of P_d which can be observed from Fig. 5.10(a) and (b),

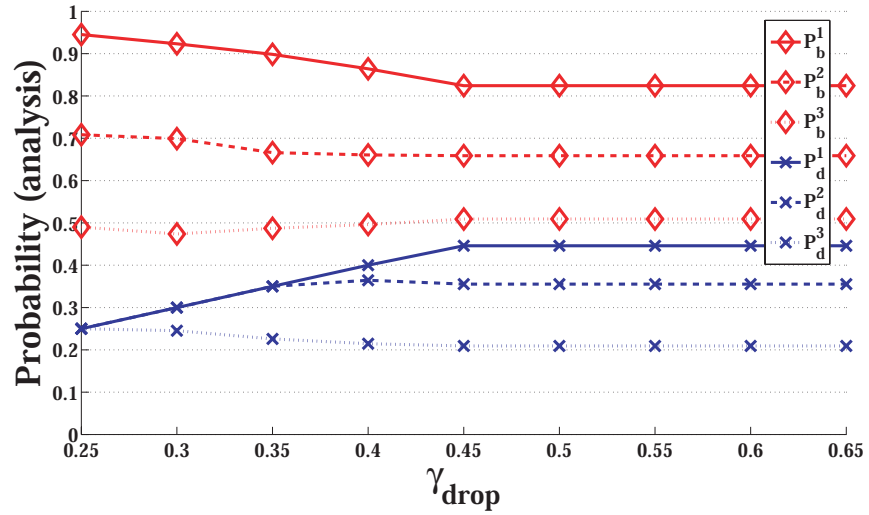

(a) Varying γ_{drop}

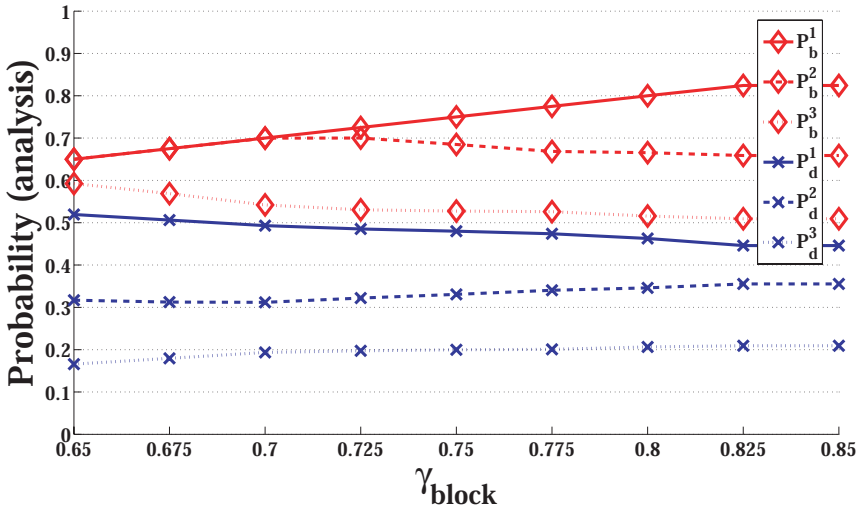

(b) Varying γ_{block}

Figure 5.10: The tradeoffs between P_b and P_d

more apparently at class 1. By contrast, as γ_{block} decreases, the QoS requirement on P_b becomes stricter so that less users may be rejected upon their arrival. To accommodate more users, the WSP has to reserve more room by evicting more users at channel vacation, thus increasing P_d. This phenomenon is clearly seen in Fig. 5.10(b) at class 1.

5.8 Conclusion

In this chapter, we proposed the optimal admission and eviction control of CR users to maximize a WSP's profit at a CR hotspot. The problem was modeled as an SMDP, and an LP algorithm was proposed to derive the optimal actions. The two QoS constraints—user blocking and dropping probabilities—have also been considered to strike a balance between profit maximization and user satisfaction. We also introduced two types of prioritized user control to enable differentiated service provisioning. The proposed LP algorithm is shown to outperform the CS algorithm, and its sensitivity to the number of channels and the chosen pricing policy has been studied.

CHAPTER VI

WHITESPACE UTILIZATION PART II: PRICE AND QUALITY COMPETITION BETWEEN CR SERVICE PROVIDERS

6.1 Introduction

The commercial use of dynamic spectrum access (DSA) has been encouraged by the FCC's ruling released in 2008 [28] that allows unlicensed radio operation in the DTV bands by fixed and portable devices. The fixed devices represent high-power stationary transceivers designed for the last-mile services in rural areas such as IEEE 802.22 [1], and the portable devices represent short-range communication devices in urban areas such as customer terminals for WiFi-like Internet access in spectrum whitespaces (WS), often referred to as *Wi-Fi 2.0* [3, 22, 52, 85]. Of these, Wi-Fi 2.0 is considered as a promising commercial application of DSA with much higher speed and less collision than today's Wi-Fi using the ISM band, thanks to the improved propagation characteristics of the WS such as larger coverage and the wall-penetrating ability of the UHF/VHF bands [10].

The Wi-Fi 2.0 can be modeled as a three-tier dynamic spectrum market (DSM) [5] consisting of three types of network entity: spectrum license holders, WSPs, and cognitive radio (CR) customers, as illustrated in Fig. 6.1. The license holders can

Figure 6.1: The three-tier Wi-Fi 2.0 market

temporarily lease their spectrum to the WSPs via the multi-winner periodic spectrum auction managed by the spectrum broker (SB). Once a WSP wins a channel at the auction, it provides Internet access to the CR customers (or end-users) by utilizing the leased spectrum, at popular public sites like coffee shops, libraries, or airports. Once a leasing term ends, all channels are returned to the licensees and the WSPs go through the auction again.

We employ the preemptive spectrum lease model in Chapter V. In this model, when a WSP leases an ON/OFF channel, the primary users (PUs) of the channel can preempt the leased channel for their own use during ON periods, thus restricting the secondary users (SUs) to accessing only OFF periods as illustrated in Fig. 6.2. Hence, the licensee collects the channel leasing fee only for the OFF periods. In fact, this model is a realization of the *private commons* model in [5] which is considered as a viable market option to benefit both PUs and SUs by enabling shared channel access between PUs and SUs while making extra profit by leasing unused portions of their spectrum.

In this chapter, we consider a duopoly Wi-Fi 2.0 network[1] where two co-located WSPs face price and quality competitions. Each WSP leases a licensed channel with time-varying availability due to the ON-OFF channel usage patterns, and hence upon

[1]This chapter studies duopoly for the ease of analysis, but the duopoly scenario can still provide us enough insight into the network dynamics of Wi-Fi 2.0. In fact, the procedures introduced in Sections 6.5 and 6.6 can be extended to the multi-WSP case, which is left as our future work.

appearance of PUs the WSP should evict all in-service customers from its network (called *channel vacation*) to protect the PUs.[2] We assume the WSP provides the evicted customers with a monetary compensation by (partially) reimbursing their service charges for the sake of customer satisfaction. Therefore, a WSP should lease a channel with a proper *quality* in terms of channel utilization by PUs, that incurs less eviction and smaller leasing cost. Each WSP should also determine the optimal *price* strategy in terms of the service tariff, because a higher price than its competitor will result in less customer arrivals and less profit according to the customers' preference on services. However, the price must be set high enough to be profitable, exceeding the sum of the channel leasing and eviction costs.

6.1.1 Contributions

Our contribution in this chapter is three-fold. First, we model the interaction between WSPs as a joint game with price and quality competitions while accounting for time-varying spectrum availability. The existing game-theoretic approaches to the dynamic spectrum market [23, 44, 46] have been limited to static idle channels, and to the best of our knowledge, this is the first attempt to incorporate the effect of time-varying channel availability in the game-theoretic framework. Next, we analyze the market dynamics using a Markov chain and derive the Nash Equilibria (NE) of the price and quality games. As to quality competition, we also discover the market entry barrier for a WSP. Finally, we perform an extensive numerical analysis to provide insightful results about the market dynamics of the Wi-Fi 2.0 network.

[2] Although the WSP can also keep customers in the system while suspending its service during ON periods, it cannot achieve seamless service provisioning.

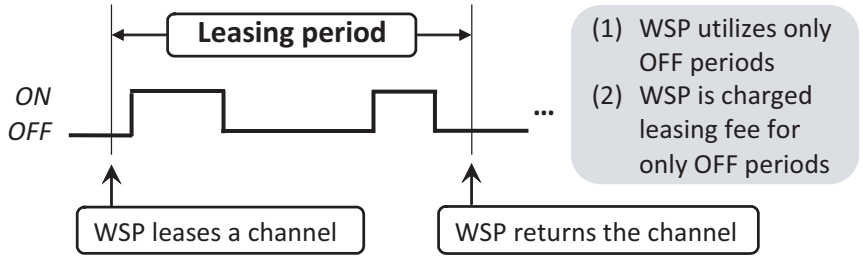

Figure 6.2: The preemptive lease model with ON-OFF channels

6.1.2 Organization

The rest of the chapter is organized as follows. Section 6.2 briefly reviews related work, and Section 6.3 introduces the system model and assumptions used in this chapter. Section 6.4 models the problem as a Markov Chain and derives the profit and cost functions. Then, Section 6.5 and Section 6.6 formulate and analyze the price and quality competitions, respectively. The market dynamics under various network conditions are shown via an extensive numerical analysis in Section 6.7, and the chapter concludes with Section 6.8.

6.2 Related Work

Jia and Zhang [44] studied price and capacity competition in a duopoly DSA market, assuming that the customer arrival rate is determined by a quadratic utility function. However, it may not apply to our case where customers choose a service based on price. Duan *et al.* [23] studied a similar problem with consideration to physical-layer characteristics of heterogeneous end-users, and derived threshold-type pricing rules. However, they assumed that the spectrum leasing cost is constant and does not depend on the total demand in the spectrum auction. Kasbekar *et al.* [46] considered a hierarchical game of quantity–price competition, with a two-level prioritized service available to the end-users. None of the above-mentioned

work, however, considered time-varying spectrum availability, while assuming that a leased channel is always idle during a leasing term.

6.3 System Model

In this section, we describe the system model and assumptions used throughput the chapter.

6.3.1 Channel Model

We follow the channel model introduced in Chapter I. We also assume that WSP i ($i = 1, 2$) leases a single channel with the capacity of C_i from the spectrum auction[3] where each channel has exponentially distributed ON and OFF periods with rate λ_i^{ON} and λ_i^{OFF}. Then, the channel utilization by PUs, denoted by u_i,[4] is given as

$$u_i = \frac{1/\lambda_i^{ON}}{(1/\lambda_i^{ON} + 1/\lambda_i^{OFF})} = \frac{\lambda_i^{OFF}}{(\lambda_i^{ON} + \lambda_i^{OFF})}.$$

Estimation of the channel parameters (i.e., λ_i^{ON}, λ_i^{OFF}, and u_i) is possible via spectrum sensing, as discussed in Chapter II. Detection of the ON/OFF patterns can also be achieved via spectrum sensing, which has also been discussed in Chapters II, III, and IV.

We assume homogeneous channel capacities such that $C_i = C, \forall i$, which would be the case when the same type of licensed bands are considered (e.g., multiple DTV channels).

[3]In this chapter, we use i as an index of a WSP and $-i$ as an index of the competitor of WSP i, by slightly abusing the notation i which was previously reserved as channel index in Chapter I. However, this does not incur any ambiguity within the chapter since we only discuss single-channel WSPs.

[4]Note that this chapter uses u_i instead of u^i for the ease of notation.

6.3.2 Auction Model

We consider a multi-winner periodic spectrum auction [30, 97], where WSP i leases a channel with the utilization of u_i and pays the leasing fee of L_i *per* unit-time. To describe the form of L_i, we introduce the concept of *effective* channel capacity, denoted by C_i^{eff}, given as

$$C_i^{eff} = (1 - u_i)C,$$

which implies the total effective amount of leased spectrum available for WSP i.

Then, the DSA auction model in [44, 61] has shown that the unit price function l, i.e., the leasing price *per* unit-bandwidth, is given as

$$l = \gamma_1 \left(C_i^{eff} + C_{-i}^{eff} \right)^{\gamma_2}, \gamma_1 > 0, \gamma_2 \geq 1,$$

which is a positive, non-decreasing and convex function of $(C_i^{eff} + C_{-i}^{eff})$. That is, the leasing cost depends on the total spectrum demand in the auction market, where γ_1 is the baseline cost when the total demand is unity. In addition, the leasing cost increases faster than proportionally to the total demand (i.e., $C_i^{eff} + C_{-i}^{eff}$) due to the competition between WSPs for the limited spectrum resources auctioned off, where the degree of competition is described by γ_2.

Finally, the leasing cost function L_i of WSP i is given as

$$L_i = C_i^{eff} \cdot l = \overline{\gamma}_1 (1 - u_i)(2 - u_i - u_{-i})^{\gamma_2}, \tag{6.1}$$

where $\overline{\gamma}_1 = \gamma_1 C^{1+\gamma_2} > 0$ is the normalized γ_1.

6.3.3 Service Model

Customer arrivals and departures

We assume that customer arrivals follow a Poisson distribution with rate λ and their service time is exponentially distributed with mean $1/\mu$. We define $\rho := \lambda/\mu$

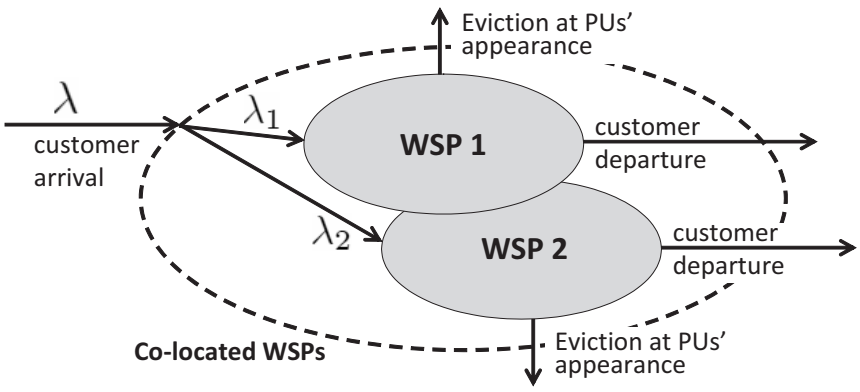

Figure 6.3: A duopoly Wi-Fi 2.0 network

and assume $0 < \rho < 1$. In addition, the bulk customer arrivals are split into two flows such that WSP i has arrival rate λ_i and $\lambda = \lambda_i + \lambda_{-i}$ as shown in Fig. 6.3.

We assume that each customer demands the bandwidth of B ($B \leq C$) where C is a multiple of B. Then, by defining $\alpha := C/B$ (≥ 1), which is a positive integer, we can have up to α concurrent in-service customers at a WSP.

Service price

An in-service customer at WSP i is charged by p_i *per* unit-time, where it is assumed $\underline{\Pi}_i \leq p_i \leq \overline{\Pi}$. $\overline{\Pi}$ is referred to as the *monopoly price* above which WSP i would have no customer arrivals because customers may not choose the 'best-effort' CR service if the 'guaranteed' legacy service offers more competitive price. Therefore, $\overline{\Pi}$ is determined by the tariff of the legacy services (e.g., 3G networks) and is assumed given a priori. On the other hand, $\underline{\Pi}_i$ is called the *marginal price* under which the WSP cannot make profit due to the channel leasing and user eviction cost. $\underline{\Pi}_i$ will be derived in Section 6.5.

Service discovery and preference

We assume a WSP broadcasts beacons at its leased channel while it is idle (i.e., OFF), to indicate its network is in service. Then, an arriving customer scans a

predetermined range of channels (e.g., a list of DTV channels reserved for Wi-Fi 2.0) to find in-service WSPs at its location, and selects the one advertising smallest service price.[5] In case the WSP chosen by the customer is fully occupied by SUs, the customer is assumed to leave the Wi-Fi 2.0 site.[6]

When a WSP's channel is occupied by PUs (i.e., ON), it cannot broadcast beacons and no customer visits its network. Therefore, even if $p_i > p_{-i}$, WSP i can have arrivals while WSP $-i$'s channel is busy. In summary, when $p_i > p_{-i}$, (1) $\lambda_i = 0$ and $\lambda_{-i} = \lambda$ while WSP $-i$'s channel is idle, and (2) $\lambda_i = \lambda$ and $\lambda_{-i} = 0$ while WSP $-i$'s channel is busy and WSP i's channel is idle. In addition, when $p_i = p_{-i}$, we have $\lambda_i = \lambda_{-i} = \lambda/2$ while both WSPs have idle channels.

User eviction

At appearance of PUs, a WSP should evict all in-service customers from the network to protect the PUs.[7] Each evicted user is compensated by a reimbursement of I, where $I = \beta \cdot p_i/\mu$, $\beta > 0$, i.e., β times the average service charge of a normally terminated session without eviction. We also assume $\beta \leq 1$ to make the compensation upper-bounded by what customers pay on average. In addition, we assume $\lambda_i^{OFF}/\mu = (1/\mu)/\left(1/\lambda_i^{OFF}\right) < 1$, because it is not beneficial to lease a channel that cannot serve even a single session in an OFF period.

[5] One can consider other factors in service preference including QoS, data rate, and channel quality. In this chapter, we focus on the price as a sole factor.

[6] This is a reasonable assumption since the WSP-customer relationship is volatile due to the flexible design of CR devices [52]. That is, CR customers may choose different services (e.g., Wi-Fi, 3G networks) by reconfiguring themselves if the desired WSP's service is not instantly available.

[7] We assume the evicted customers will use alternative services such as Wi-Fi or 3G networks, due to the flexibility of the CR devices.

6.4 Two-Stage Market Competition

The market competition between WSPs can be modeled as a two-stage game, consisting of price and quality games. The quality game is performed periodically at every auction, where each WSP competes for the desired quality of spectrum resources to lease, in terms of u_i. The quality game is a one-shot game, and thus a WSP cannot return or change the leased channel during a leasing term. During a leasing term, two WSPs perform a price competition to determine the optimal price p_i for their maximal profit. The quality game is also called a *full*-game in the sense that the optimal quality of spectrum is determined by assuming the NE prices of the two WSPs achieved at a price *sub*-game.

As the main objective of a WSP is to maximize its profit, the profit function must be analytically derived before investigating the price and quality competition. To derive the profit, we define the system state of WSP i as $s_i = (m_i, n_i)$ where m_i is the channel state such that

$$m_i = \begin{cases} 0 & \text{if channel is busy,} \\ 1 & \text{if channel is idle,} \end{cases}$$

and n_i is the number of in-service customers with $n_i \in [0, m_i\alpha]$. Then, the system state transition can be modeled as a Markov Chain under the assumption of Poisson arrivals, exponential service times, and exponential ON and OFF periods.

Fig. 6.4 illustrates the state-transition diagram of the Markov Chain. The horizontal transitions represent the state transitions by the customer arrivals and departures, and the vertical transitions represent the state transitions due to ON-OFF channel state changes. A customer arrival is accepted by the system if $n_i < m_i\alpha$. When an idle channel becomes busy, all n_i customers are evicted from the system.

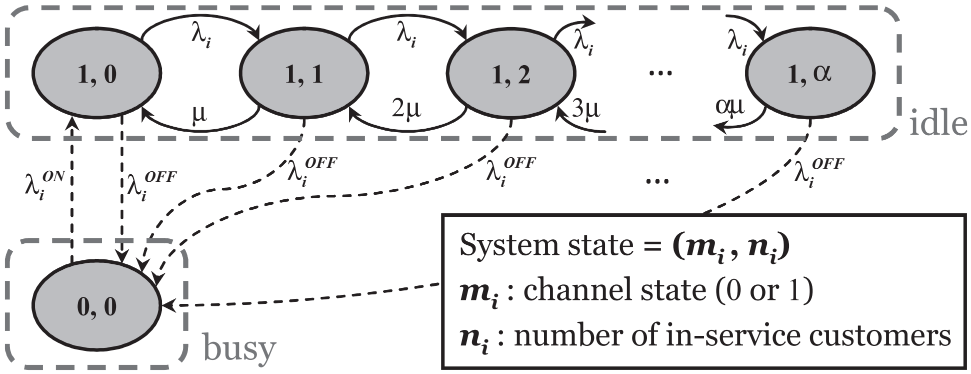

Figure 6.4: State transition of WSP i's system

From Fig. 6.4, we first notice that

$$\begin{aligned} \pi_{0,0} &= u_i, \\ \sum_{n_i=0}^{\alpha} \pi_{1,n_i} &= 1 - u_i, \end{aligned}$$

where $\pi_{s_i} = \pi_{m_i,n_i}$ denotes the stationary distribution of the system. Then, the global balance equations can be derived in a matrix form as follows.

$$\mathbf{A} \begin{pmatrix} \pi_{1,0} & \pi_{1,1} & \dots & \pi_{1,\alpha} \end{pmatrix}^{\mathrm{T}} = \begin{pmatrix} u \cdot \frac{\lambda_i^{ON}}{\mu} & 0 & \dots & 0 \end{pmatrix}^{\mathrm{T}}, \tag{6.2}$$

where

$$\mathbf{A} = \begin{pmatrix} f(0) & -1 & 0 & 0 & \dots & 0 & 0 & 0 \\ -\rho_i & f(1) & -2 & 0 & \dots & 0 & 0 & 0 \\ 0 & -\rho_i & f(2) & -3 & \dots & 0 & 0 & 0 \\ \cdots & \cdots & \cdots & \cdots & \cdots & \cdots & \cdots & \cdots \\ 0 & 0 & 0 & 0 & \dots & -\rho_i & f(\alpha-1) & -\alpha \\ 0 & 0 & 0 & 0 & \dots & 0 & -\rho_i & f(\alpha)-\rho_i \end{pmatrix},$$

by defining $f(k) := \rho_i + \lambda_i^{OFF}/\mu + k$ and $\rho_i := \lambda_i/\mu$. Therefore, using Eq.(6.2) the stationary probability is found as

$$\begin{pmatrix} \pi_{1,0} & \pi_{1,1} & \dots & \pi_{1,\alpha} \end{pmatrix}^{\mathrm{T}} = \mathbf{A}^{-1} \begin{pmatrix} u \cdot \frac{\lambda_i^{ON}}{\mu} & 0 & \dots & 0 \end{pmatrix}^{\mathrm{T}}.$$

Although a numerical analysis can be used to find $\mathbf{A}^{-1}$, the stationary probability in a closed-form is preferred in analyzing the price and quality games to obtain an insight in the form of the price and quality NEs. Therefore, we approximate the original Markov Chain by applying a state decomposition technique introduced in [33].

According to [33], we can group the states in Fig. 6.4 with the same m_i (i.e., the states in the same row) together as long as the vertical state-transition rates are much smaller than the horizontal state-transition rates. In DSA, this condition is expected to be met in many applications because spectrum reuse is intended for under-utilized channels with relatively longer ON/OFF periods (e.g., TV bands) compared to the customer arrival/departure by the SUs. In Section 6.7, we will quantify the impact of this approximation on the accuracy of the analysis through extensive numerical experiments.

After the decomposition, the system becomes $M/M/\alpha/\alpha$ while the channel is idle. Hence, we can express π_{s_i} as

$$\pi_{s_i} \approx \pi_{n_i|m_i} \cdot P(m_i) = \begin{cases} u_i & \text{if } s_i = (0,0), \\ \pi_{n_i} \cdot (1-u_i) & \text{if } m_i = 1. \end{cases}$$

where π_{n_i} is the stationary probability of a $M/M/\alpha/\alpha$ system such that

$$\pi_{n_i}(\rho_i) = \frac{(\rho_i)^{n_i}/n_i!}{\sum_{n=0}^{\alpha}(\rho_i)^n/n!}, \ \forall n_i. \tag{6.3}$$

Then, revenue and eviction cost occurs only when channel is idle because $n_i = 0$ for a busy channel. Hence, for $m_i = 1$, we derive the revenue rate $R(p_i, \rho_i)$ (the

average revenue per unit time) and the eviction cost $E(p_i, \rho_i)$ as follows:

$$\begin{aligned} R(p_i, \rho_i) &= \sum_{n_i=0}^{\alpha} p_i n_i \cdot \pi_{n_i}(\rho_i) = p_i \rho_i \frac{\sum_{n=0}^{\alpha-1} (\rho_i)^n / n!}{\sum_{n=0}^{\alpha} (\rho_i)^n / n!} \\ E(p_i, \rho_i) &= \sum_{n_i=0}^{\alpha} I n_i \cdot \pi_{n_i}(\rho_i) \cdot \lambda_i^{OFF} = \beta \frac{\lambda_i^{OFF}}{\mu} R(p_i, \rho_i) \end{aligned}$$

where λ_i^{OFF} is the transition probability due to the OFF→ON transition of an idle channel.

The derived $R(p_i, \rho_i)$ and $E(p_i, \rho_i)$ will become our bases in the later sections to calculate the profit rate of WSP i under the various market conditions. For the ease of notation, we define

$$\Delta(p_i, \rho_i) := R(p_i, \rho_i) - E(p_i, \rho_i).$$

6.5 Price Competition Analysis

In this section, we investigate a price competition sub-game to find the best tariff strategy of WSP i in terms of p_i, when (u_i, u_{-i}) are given. We also study the necessary condition for the existence of the price NE and derive the NE at such conditions. The derived price NE will be applied to the quality full-game in Section 6.6, in determining the profit at the equilibrium price for a given set of quality.

6.5.1 Three Pricing Strategies

At WSP i, the price of the competitor WSP $-i$ (i.e., p_{-i}) is known since the WSP $-i$ advertises its tariff via the beacons. Then, the WSP i can take one of the following three pricing strategies according to the relationship between p_i and p_{-i}: (1) $p_i < p_{-i}$, (2) $p_i > p_{-i}$, and (3) $p_i = p_{-i}$. We overview each strategy to derive the conditional profit of WSP i.

• Under strategy 1 ($p_i < p_{-i}$): WSP i can monopolize the market and hence its profit is maximized at $p_i = p_{-i} - \epsilon$, $\epsilon > 0$, where ϵ can be arbitrarily small. In this case, the profit rate of WSP i becomes

$$F_i^{\{p_i<p_{-i}\}} = (1 - u_i) \cdot \Delta(p_{-i} - \epsilon, \rho) - L_i. \tag{6.4}$$

• Under strategy 2 ($p_i > p_{-i}$): WSP i loses the entire market to its competitor (i.e., $\lambda_i = 0$ and $\lambda_{-i} = \lambda$) if WSP $-i$ has an idle channel (i.e., $m_{-i} = 1$). On the contrary, while $m_{-i} = 0$, it becomes $\lambda_i = \lambda$ and $\lambda_{-i} = 0$ if WSP i's channel is idle. Therefore, with probability $u_{-i} \cdot (1-u_i)$, the stationary probability of WSP i's system follows Eq. (6.3). In this case, WSP i's profit is maximized at $p_i = \overline{\Pi}$ since WSP $-i$ is out-of-service, and thus WSP i's profit rate is given as

$$F_i^{\{p_i>p_{-i}\}} = (1 - u_i)u_{-i} \cdot \Delta(\overline{\Pi}, \rho) - L_i. \tag{6.5}$$

• Under strategy 3 ($p_i = p_{-i}$): Here, we need to consider two cases. First, when $m_i = m_{-i} = 1$, two WSPs take an equal share of the market such that $\lambda_i = \lambda_{-i} = \lambda/2$. Second, when $m_i = 1$ and $m_{-i} = 0$, we have $\lambda_i = \lambda$ and $\lambda_{-i} = 0$ since the arriving customers cannot find the service beacons of WSP $-i$. Therefore, by setting $p_i = p_{-i}$, the profit rate of WSP i becomes

$$F_i^{\{p_i=p_{-i}\}} = (1 - u_i)\Big\{u_{-i} \cdot \Delta(p_{-i}, \rho) + (1 - u_{-i}) \cdot \Delta(p_{-i}, \frac{\rho}{2})\Big\} - L_i. \tag{6.6}$$

6.5.2 Optimal Price Strategy

The goal of WSP i is to maximize its profit by optimally determining its price p_i for a given p_{-i}. Hence, we will compare the profit rates of the three pricing strategies in Section 6.5.1 to derive the optimal p_i.

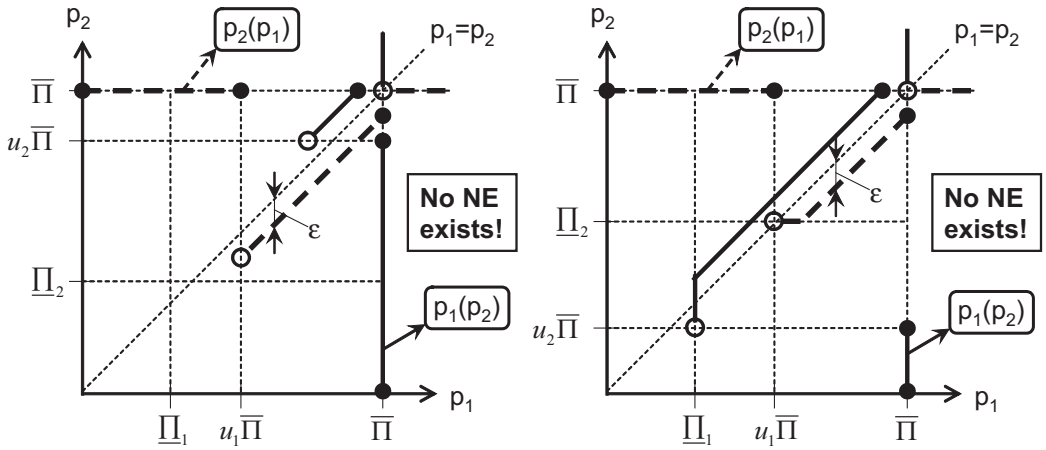

(a) $\underline{\Pi}_1 \le u_1\overline{\Pi}$, $\underline{\Pi}_2 \le u_2\overline{\Pi}$ (b) $\underline{\Pi}_1 \le u_1\overline{\Pi}$, $\underline{\Pi}_2 > u_2\overline{\Pi}$

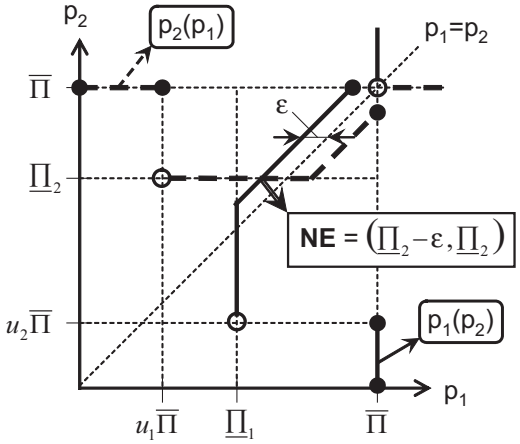

(c) $\underline{\Pi}_1 > u_1\overline{\Pi}$, $\underline{\Pi}_2 > u_2\overline{\Pi}$

Figure 6.5: Nash Equilibrium of the price competition

Comparison of price strategies 1 and 3

We first compare strategies 1 and 3 in terms of their profit rates given by Eqs. (6.4) and (6.6) as follows (when $\epsilon \to 0^+$):

$$F_i^{\{p_i<p_{-i}\}} - F_i^{\{p_i=p_{-i}\}} = (1-u_i)(1-u_{-i})p_{-i}\left(1-\beta\frac{\lambda_i^{OFF}}{\mu}\right)A_r \tag{6.7}$$

where

$$A_r \;:=\; \rho\left\{\frac{\sum_{n=0}^{\alpha-1}\rho^n/n!}{\sum_{n=0}^{\alpha}\rho^n/n!} - \frac{1}{2}\cdot\frac{\sum_{n=0}^{\alpha-1}(\rho/2)^n/n!}{\sum_{n=0}^{\alpha}(\rho/2)^n/n!}\right\}.$$

Lemma 6.5.1. *For $0 < \rho < 1$ and $\alpha \geq 1$, $A_r > 0$.*

Proof. See Appendix A. □

Theorem 6.5.1. *Price strategy 3 ($p_i = p_{-i}$) is strictly dominated by price strategy 1 ($p_i < p_{-i}$).*

Proof. In Eq.(6.7), $\left(1 - \beta\lambda_i^{OFF}/\mu\right) > 0$ since $\beta \leq 1$ and $\lambda_i^{OFF}/\mu < 1$ by our assumption, and $A_r > 0$ by Lemma 6.5.1. Therefore, we have $F_i^{\{p_i<p_{-i}\}} > F_i^{\{p_i=p_{-i}\}}$, $\forall p_{-i}$, which completes the proof. □

Comparison of price strategies 1 and 2

Next, we compare strategies 1 and 2 in terms of their profit rates given by Eqs. (6.4) and (6.5) as follows (when $\epsilon \to 0^+$):

$$F_i^{\{p_i<p_{-i}\}} - F_i^{\{p_i>p_{-i}\}} = (1 - u_i) \quad (p_{-i} - u_{-i}\overline{\Pi}) \left(1 - \beta\frac{\lambda_i^{OFF}}{\mu}\right) \frac{\rho \sum_{n=0}^{\alpha-1} \rho^n/n!}{\sum_{n=0}^{\alpha} \rho^n/n!}. \quad (6.8)$$

Theorem 6.5.2. *The optimal price strategy is*

- *Strategy 1 ($p_i = p_{-i} - \epsilon$), if $p_{-i} > u_{-i} \cdot \overline{\Pi}$,*
- *Strategy 2 ($p_i = \overline{\Pi}$), if $p_{-i} \leq u_{-i} \cdot \overline{\Pi}$.*

Proof. By Theorem 6.5.1, price strategy 3 cannot be optimal. Hence, we only need to compare strategies 1 and 2. In the proof of Theorem 6.5.1, it has been shown that $\left(1 - \beta\lambda_i^{OFF}/\mu\right) > 0$. Therefore, by considering the form of Eq. (6.8), it is seen that strategy 1 is optimal (i.e., $F_i^{\{p_i<p_{-i}\}} > F_i^{\{p_i>p_{-i}\}}$) if $p_{-i} > u_{-i} \cdot \overline{\Pi}$; otherwise strategy 2 is optimal. □

6.5.3 Nash Equilibrium of the Price Competition

Using the derived optimal price strategy, we can find the Nash Equilibrium of the price competition. We first describe how to determined the marginal price for each WSP, and then derive the NE and its existence condition.

Finding the Marginal Price

We define the marginal price $\underline{\Pi}_i$ as the minimal price to guarantee a non-negative profit for WSP i even at the worst case. That is, when $p_i = \underline{\Pi}_i$, the WSP i should be able to achieve at least a break-even (zero profit) regardless of p_{-i}.

When we fix $p_i = \underline{\Pi}_i$, the profit rate F_i previously given as Eqs. (6.4),(6.5),(6.6) becomes

- $F_i^{\{p_i<p_{-i}\}} = (1-u_i)\cdot\Delta(\underline{\Pi}_i,\rho) - L_i$,
- $F_i^{\{p_i>p_{-i}\}} = (1-u_i)\cdot u_{-i}\Delta(\underline{\Pi}_i,\rho) - L_i$,
- $F_i^{\{p_i=p_{-i}\}} = (1-u_i)\left\{u_{-i}\Delta(\underline{\Pi}_i,\rho) + (1-u_{-i})\Delta(\underline{\Pi}_i,\frac{\rho}{2})\right\} - L_i$.

It can be observed that $F_i^{\{p_i>p_{-i}\}}$ is the worst. Therefore, to guarantee $F_i \geq 0$, we need to set

$$\underline{\Pi}_i = \frac{L_i/u_{-i}}{(1-u_i)\cdot\Delta(\underline{\Pi}_i,\rho)/\underline{\Pi}_i} = \frac{L_i/u_{-i}}{(1-u_i)\chi_i(\rho)} = \frac{\overline{\gamma}_1(2-u_i-u_{-i})^{\gamma_2}}{u_{-i}\chi_i(\rho)}, \tag{6.9}$$

where Eq.(6.1) is applied. Here, $\chi_i(\rho_i)$ is defined as

$$\chi_i(\rho_i) \;:=\; \left(1-\beta\frac{\lambda_{OFF}^i}{\mu}\right)\rho_i\frac{\sum_{n=0}^{\alpha-1}(\rho_i)^n/n!}{\sum_{n=0}^{\alpha}(\rho_i)^n/n!}. \tag{6.10}$$

Note that if the determined $\underline{\Pi}_i$ satisfies $\underline{\Pi}_i > \overline{\Pi}$, WSP i cannot make positive profit for any p_i since $\lambda_i = 0$ for $p_i > \overline{\Pi}$ making the profit strictly negative such as $F_i = -L_i$. Therefore, WSP i should opt out of the market when $\underline{\Pi}_i > \overline{\Pi}$ in order not to incur any channel leasing cost. In the next section, this will be modeled as forcing

$u_i = 1$ at the quality competition where the channel leasing cost becomes zero since $C_i^{eff} = 0$.

Finding the Nash Equilibrium

To find the NE, we consider the case where $\underline{\Pi}_i \leq \overline{\Pi}$ and $\underline{\Pi}_{-i} \leq \overline{\Pi}$ so that both WSPs may participate in the market competition. Fig. 6.5 shows the NE of the price competition, where the solid plot represents $p_1(p_2)$, i.e., the best response function of WSP 1 given p_2, and the dashed plot represents $p_2(p_1)$. The best response functions are drawn by following the optimal strategy in Theorem 6.5.2. Note that WSP i never decreases its price p_i smaller than $\underline{\Pi}_i$, and hence $p_i(p_{-i})$ is lower-bounded by $\underline{\Pi}_i$.

It can be seen from Figs. 6.5(a),(b) that there exists no NE when (1) $\underline{\Pi}_i \leq u_i\overline{\Pi}$ and $\underline{\Pi}_{-i} \leq u_{-i}\overline{\Pi}$, or (2) $\underline{\Pi}_i \leq u_i\overline{\Pi}$ and $\underline{\Pi}_{-i} > u_{-i}\overline{\Pi}$, since $p_1(p_2)$ and $p_2(p_1)$ never intersect with each other.

As shown in Fig. 6.5(c), the NE exists when $\underline{\Pi}_i > u_i\overline{\Pi}$ and $\underline{\Pi}_{-i} > u_{-i}\overline{\Pi}$, where the NE is given as $(\underline{\Pi}_2 - \epsilon, \underline{\Pi}_2)$ for $\underline{\Pi}_2 > \underline{\Pi}_1$. Due to symmetry, the NE becomes $(\underline{\Pi}_1, \underline{\Pi}_1 - \epsilon)$ for $\underline{\Pi}_1 > \underline{\Pi}_2$. Therefore, as $\epsilon \to 0$, there exist a unique NE described as follows in Theorem 6.5.3.

Theorem 6.5.3. *The NE of the price competition exists only when* $\underline{\Pi}_i > u_i\overline{\Pi}$ *and* $\underline{\Pi}_{-i} > u_{-i}\overline{\Pi}$*, and the unique NE is determined as* $(p_1, p_2) = (p^*, p^*)$*, where* $p^* = \max\{\underline{\Pi}_1, \underline{\Pi}_2\}$ *and* $\underline{\Pi}_i$ *is given as in Eq.(6.9).*

6.6 Quality Competition Analysis

The goal of the quality competition is to find the best channel to lease with optimal quality in terms of u_i that achieves maximal profit of WSP i at the equi-

librium price found in Section 6.5. Having the NE of the price competition as $p_i = p_{-i} = \max\{\underline{\Pi}_1, \underline{\Pi}_2\}$, the resulting profit of WSPs is given as Eq. (6.6), and we want to find the best response function $u_i(u_{-i})$ to maximize such profit.

As introduced in the channel model, $u_i = \lambda_i^{OFF}/(\lambda_i^{OFF} + \lambda_i^{ON})$, and thus there exist infinitely many possible pairs of $(\lambda_i^{OFF}, \lambda_i^{ON})$ for a given u_i. Therefore, we would like to consider a scenario where $\lambda_i^{OFF} = \lambda^{OFF}, \forall i$, representing the case when channels have identically distributed intervals between PU activities. It is also possible to consider another scenario where $\lambda_i^{ON} = \lambda^{ON}, \forall i$ (i.e., the duration of PU activities follows the same distribution over channels), which is left as our future work.

Note that even though the optimal u_i can be found for any $\gamma_2 \geq 1$, we are particularly interested in the case of $\gamma_2 = 1$ as an illustrative example.

6.6.1 Market entry barrier

WSP i's profit becomes strictly negative in case its marginal price becomes greater than the monopoly price (i.e., $\underline{\Pi}_i > \overline{\Pi}$), because there will be no customer arrival while the channel leasing fee must be still paid. If this happens, the WSP would rather shut down its service by leasing no channel (equivalently, leasing a channel with $u_i = 1$). Therefore, there exists a market entry condition for a WSP, which is described by $\underline{\Pi}_i \leq \overline{\Pi}$. For a given u_{-i}, this condition results in the following interval of u_i:

$$2 - \left(1 + \frac{\overline{\Pi}\chi_i(\rho)}{\overline{\gamma}_1}\right) u_{-i} \leq u_i. \tag{6.11}$$

In addition, the same claim applies to WSP $-i$ by switching the role of i and $-i$.

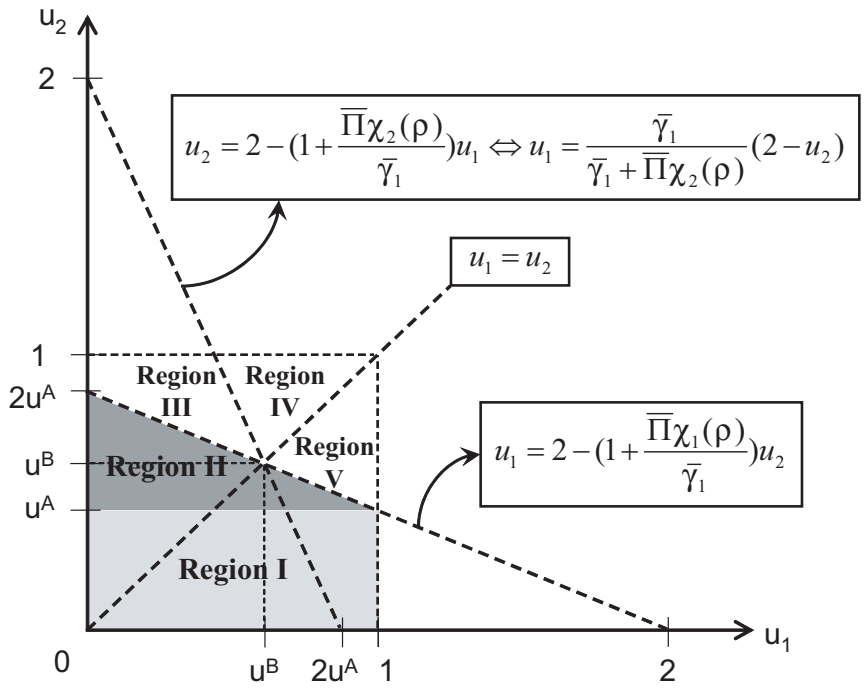

Figure 6.6: Five decision regions of (u_1, u_2)

6.6.2 Region-specific optimal quality strategies

According to the market entry points of the two WSPs, we can divide the area of (u_1, u_2) into five regions as shown in Fig. 6.6.

Region I and II (below the market entry barrier)

The region I is a rectangular area where $0 \leq u_i \leq 1$ and $0 \leq u_{-i} < u^A$. The region represents the case when WSP i cannot overcome the market entry barrier and it leaves the market. Therefore, the best response function in $u_{-i} \in [0, u^A)$ is $u_i(u_{-i}) = 1$.

The region II, that does not include the line $u_i = 2 - \left(1 + \overline{\Pi}\chi_i(\rho)/\overline{\gamma}_1\right) u_{-i}$, also belongs to the case when WSP i cannot overcome the market entry barrier. However, the region does not include $u_i = 1$, and hence no possible solution exists. As a result, we can ignore this region in deriving $u_i(u_{-i})$.

Region III (a monopoly market)

The region III includes the line $2 - \left(1 + \overline{\Pi}\chi_i(\rho)/\overline{\gamma}_1\right) u_{-i} = u_i$, but excludes the line $u_{-i} = 2 - \left(1 + \overline{\Pi}\chi_{-i}(\rho)/\overline{\gamma}_1\right) u_i$. Therefore, $p_{-i} > \overline{\Pi}$ in the region due to the market entry condition, and thus WSP $-i$ will not have any customer arrival. As a result, WSP i monopolizes the market with $p_i = \overline{\Pi}$. With the monopoly price, WSP i's profit rate becomes

$$F_i^{III} = (1 - u_i) \times \left\{\overline{\Pi}\chi_i(\rho) - \overline{\gamma}_1(2 - u_{-i} - u_i)\right\} \tag{6.12}$$

Region IV (a duopoly market)

In the region IV, both WSPs can enter the market, and satisfy the condition $u_i \leq u_{-i}$ where we have $\underline{\Pi}_i \leq \underline{\Pi}_{-i}$. Therefore, the NE price becomes $p^* = \underline{\Pi}_{-i}$ and WSP i's profit rate becomes

$$\begin{aligned} F_i^{IV} =& (1 - u_i) \times \left\{(u_{-i}\chi_i(\rho) + (1 - u_{-i})\chi_i(\rho/2))\, p^* - \overline{\gamma}_1(2 - u_{-i} - u_i)\right\} \\ =& \overline{\gamma}_1(1 - u_i)(2 - u_{-i} - u_i)\,(\psi - u_i) \cdot \frac{1}{u_i}, \end{aligned} \tag{6.13}$$

where $\psi = u_{-i} + (1 - u_{-i})\chi_i(\rho/2)/\chi_{-i}(\rho)$. For $u_i \in \left[\frac{\overline{\gamma}_1}{\overline{\gamma}_1 + \overline{\Pi}\chi_{-i}(\rho)}(2 - u_{-i}), u_{-i}\right]$, Eq. (6.13) is maximized at $u_i = \frac{\overline{\gamma}_1}{\overline{\gamma}_1 + \overline{\Pi}\chi_{-i}(\rho)}(2 - u_{-i})$, because $F_i \to \infty$ as $u_i \to 0$ and $u_{-i} \leq \psi < 1 \leq (2 - u_{-i})$ where $\psi < 1$ is given by Lemma 6.5.1.

Region V (a duopoly market)

Similar to the region IV, the region V also belongs to the duopoly market. As seen, the region satisfies the condition $u_i \geq u_{-i}$ where we have $\underline{\Pi}_i \geq \underline{\Pi}_{-i}$. Therefore, the NE price becomes $p^* = \underline{\Pi}_i$, and WSP i's profit rate becomes

$$F_i^V = (u_i - 1)(u_i + u_{-i} - 2) \cdot \frac{\overline{\gamma}_1(1 - u_{-i})\chi_i(\rho/2)}{u_{-i}\chi_i(\rho)}. \tag{6.14}$$

Then, due to the form of the region V, two distinct cases are considered. First, for $u_{-i} \in [u^A, u^B)$, we have $0 < 2 - \left(1 + \overline{\Pi}\chi_i(\rho)/\overline{\gamma}_1\right) u_{-i} \leq u_i \leq 1$. Since $1 \leq (2 - u_{-i})$, Eq. (6.14) is maximized at $u_i = 2 - \left(1 + \overline{\Pi}\chi_i(\rho)/\overline{\gamma}_1\right) u_{-i}$.

Next, for $u_{-i} \in [u^B, 1]$, we have $u_i \in [u_{-i}, 1]$, and thus Eq. (6.14) is maximized at $u_i = u_{-i}$.

6.6.3 Optimal quality strategy

Finally, we derive the optimal quality strategy, i.e., the best response function $u_i(u_{-i})$ for all possible intervals of u_{-i}. As already shown, the best response function in $u_{-i} \in [0, u^A)$ is $u_i(u_{-i}) = 1$. For $u_{-i} \in [u^A, u^B)$, we compare the regions II and V, but as pointed out earlier, we can ignore the region II. Therefore, the best response function in $u_{-i} \in [u^A, u^B)$ is $u_i(u_{-i}) = 2 - \left(1 + \overline{\Pi}\chi_i(\rho)/\overline{\gamma}_1\right) u_{-i}$.

For $u_{-i} \in [u^B, 1]$, we need to compare all three regions (III, IV, and V) in order to determine the best response function. First, it can be easily shown that the best profit in the region V cannot exceed the best profit of the region IV for the following reason. The maximal profit of the region V for $u_{-i} \in [u^B, 1]$ is achieved at $u_i = u_{-i}$, which is a shared line with region IV. However, $u_i = u_{-i}$ does not provide the maximal profit in the region IV, and thus the maximal profit of the region IV is larger than that of the region V.

Next, for given u_{-i}, let u_i^{IV} denote the optimal u_i in the region IV such as $u_i^{IV} = \frac{\overline{\gamma}_1}{\overline{\gamma}_1 + \overline{\Pi}\chi_{-i}(\rho)}(2 - u_{-i})$. Let us also consider $u_i = u_i^{IV} - \epsilon$, $\epsilon > 0$, which is in the region III. If we compare Eq. (6.13) at $u_i = u_i^{IV}$ and Eq. (6.12) at $u_i = u_i^{IV} - \epsilon$ for an arbitrarily small ϵ, then we can easily observe that the leasing cost is arbitrarily close to each other in both regions while $\overline{\Pi}\chi_i(\rho) > (u_{-i}\chi_i(\rho) + (1 - u_{-i})\chi_i(\rho/2))\,\underline{\Pi}_{-i}$. Therefore, we can conclude that the best profit in the region IV cannot exceed the

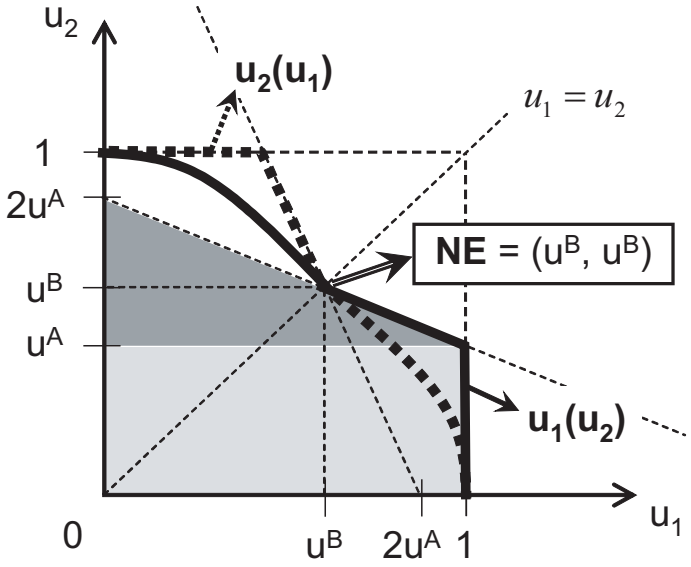

Figure 6.7: The Nash Equilibrium of the quality competition

profit in the region III at $u_i = u_i^{IV} - \epsilon$, and thus the best response function exists in the region III.

Fig. 6.7 plots the resulting best response $u_i(u_{-i})$ for $u_{-i} \in [0, 1]$, where $u_{-i}(u_i)$ is also drawn using the symmetry. It is observed that, regardless of the optimal u_i in the region III, there exists a NE of the quality game at (u^B, u^B) where u^B is an intersection of $u_i = u_{-i}$ and $u_i = 2 - \left(1 + \overline{\Pi}\chi_i(\rho)/\overline{\gamma}_1\right) u_{-i}$, resulting in Theorem 6.6.1 as follows.

Theorem 6.6.1. *The NE of the quality competition exists at* $(u_1, u_2) = (u^*, u^*)$, *where* $u^* = 2\overline{\gamma}_1/\{2\overline{\gamma}_1 + \overline{\Pi}\chi_1(\rho)\}$.

Note that there exist two additional NEs other than $(u_1, u_2) = (u^*, u^*)$: $(\tilde{u}, 1)$ and $(1, \tilde{u})$, where $0 \leq \tilde{u} < u^A$. However, according to the concept of the *focal point* introduced in [23, 59], these NEs are not likely to be chosen by the WSPs since such NEs exclude either WSP from the market thus impairing the fairness.

From Theorem 6.6.1, we obtain the following two corollaries.

Corollary 6.6.1. *At the NE of the quality competition, the NE price becomes* $p^* = \overline{\Pi}$.

Proof. By applying $u_i = u_{-i} = u^*$ to Eq. (6.9), we obtain $\underline{\Pi}_i = \overline{\Pi}$ since $\chi_1(\rho) = \chi_2(\rho)$. Therefore, $p^* = \overline{\Pi}$ by Theorem 6.5.3. □

Corollary 6.6.2. *The NE of the quality competition satisfies the equilibrium price existence condition.*

Proof. Since $\underline{\Pi}_i = \overline{\Pi}$, we have $\underline{\Pi}_i > u_i\overline{\Pi}$ and $\underline{\Pi}_{-i} > u_{-i}\overline{\Pi}$ for $u_i = u_{-i} = u^* \neq 1$. □

6.6.4 Discussion

WSPs may, in reality, not be able to find the channel that exactly matches their needs, whose utilization factor equals u^*. In such a case, they should make a reasonable assumption that both WSPs would act rationally to bid for the best matching channel whose utilization factor is closest to u^*. This strategy is reasonable in that the quality competition is a one-shot game performed once at each periodic auction, and thus a WSP cannot make any adjustment on its leased channel until the next auction.

In case u takes its value from a countable set in a discrete manner, the quality competition becomes a combinatorial matching problem that should consider all possible pairs of (u_1, u_2) from the given channel set. The problem formulation in such a case becomes quite different from the procedure presented in this chapter, as the best response function is no more continuous. We leave the case as our future work.

The quality competition problem can be further extended to a joint quantity/quality competition when we consider WSPs, each operating with multiple channels. That

is, WSP i leases more than one channel, say M_i channels, and combine them into a one logical channel with a larger capacity (e.g., $M_i \cdot C$). In such a case, we need to find the best quantity/quality pair of (M_i, u_i),[8] for a given pair of (M_{-i}, u_{-i}). Hence, the decision space becomes $\mathbb{N} \times [0, 1]$ where $\mathbb{N}$ is a set of natural numbers, with additional complexity coming from the choice of M_i. We also leave such extension as our future work.

6.7 Evaluation of Wi-Fi 2.0 Network Dynamics

We now conduct an extensive numerical analysis to provide insight into the market dynamics of the Wi-Fi 2.0 network. First, we compare the profit observed from a simulated scenario with the analytically-derived profit to investigate the condition under which our state decomposition approach can be applied with a tolerable approximation error. Next, we study the fundamental tradeoffs between the network parameters at equilibrium, including the arrival rate λ, the leasing cost $\overline{\gamma}_1$, and the eviction cost β.

In each scenario, we set a list of common parameters as follows: $C = 5$, $B = 1$, and $\gamma_2 = 1$.

6.7.1 Approximation accuracy in state decomposition

We compare the profit observed from the simulation with the profit given by the analysis to derive the condition under which state decomposition performs reasonably well. In the simulation, we randomly generate 200 pairs of exponential ON and OFF periods and also emulate user arrivals and departures. A simulation is run by applying the optimal price and quality found by the analysis, and repeats 10 times to derive the average performance. Other simulation parameters are set as $\overline{\Pi} = 2$,

[8] Assuming all M_i channels are of the same quality u_i.

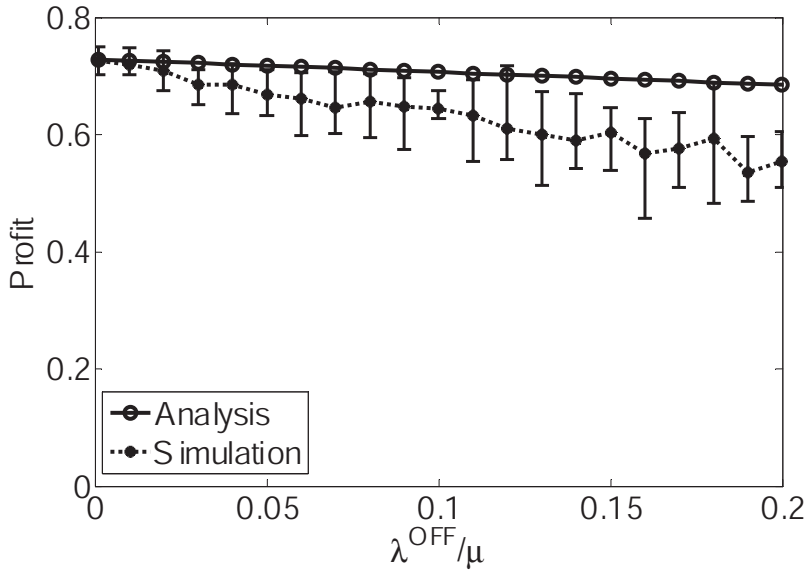

Figure 6.8: Decomposition approximation accuracy

$\rho = 0.9$, $\overline{\gamma}_1 = 0.1$, and $\beta = 0.25$.

From Fig. 6.8, one can see that the profit predicted by analysis gets fairly close to the actual achieved profit at a small λ^{OFF}/μ, and the gap between them gradually increases as λ^{OFF}/μ grows. At $\lambda^{OFF}/\mu = 0.1$, the approximation error is found to be less than 9.5%, which becomes around 15% at $\lambda^{OFF}/\mu = 0.15$. In case the tolerable error is less than 10%, the state decomposition approach is effective for $\lambda^{OFF}/\mu \leq 0.1$, implying that an OFF period, on average, can accommodate at least 10 consecutive user sessions. Note that this is a plausible scenario since DSA targets to reuse under-utilized channels with relatively larger ON/OFF periods than customer arrivals/departures.

6.7.2 Impact of arrival rate and leasing cost

In Fig. 6.9(a), we plot the achieved profit of a WSP at its equilibrium while varying the arrival rate λ (equivalently ρ). The leasing cost is also varied by testing three selected values of $\overline{\gamma}_1$. In this test, the simulation parameters are set as $\overline{\Pi} = 1$,

$\mu = 1/5$, $\lambda^{OFF} = 1/500$, $\lambda^{ON} = 1/50$, and $\beta = 0.25$. It can be seen that as the arrival rate increases (i.e., $\rho \to 1$), the WSP achieves more profit due to the increased revenue. The profit also enhances as $\overline{\gamma}_1$ decreases, due to the less leasing cost by L_i.

In Fig. 6.9(b), we also plot the quality equilibrium u^* under the same test conditions. As the arrival rate increases, u^* is monotonically decreasing because the WSP can overcome the leasing cost by accommodating more customers using a less busy channel (i.e., smaller u^*). Therefore, when $\rho \to 0$, the best strategy is to leave the market by setting $u^* = 1$. On the other hand, at the same ρ, u^* increases as $\overline{\gamma}_1$ increases, because it can compensate the increased leasing cost by leasing a less idle channel.

6.7.3 Impact of eviction cost

In Fig. 6.9(c), we plot the achieved profit at equilibrium versus the average OFF period (i.e., $1/\lambda^{OFF}$) under the various eviction costs given by β. Other simulation parameters are set as $\overline{\Pi} = 1$, $\rho = 0.9$, $\overline{\gamma}_1 = 0.3$, and $\lambda^{ON} = 1/50$.

At the same $1/\lambda^{OFF}$, a larger profit is achieved at a smaller β due to the amount of reimbursement to the evicted users, and the difference becomes more pronounced as $1/\lambda^{OFF}$ decreases. This implies that eviction becomes more dominant in a dynamic channel environment (i.e., channels with small ON and OFF periods) than in a static environment, due to more frequent evictions.

6.8 Conclusion

In this chapter, we studied the competition between WSPs in the duopoly Wi-Fi 2.0 network while considering time-varying spectrum availability. We modeled the problem as a joint price and quality game where two co-located WSPs compete for

leasing limited spectrum resources and enticing customers to their service. A WSP's profit function is derived by considering the dependency of revenue on the pricing policy, the eviction cost due to the reimbursement of the evicted customers, and the channel leasing cost. It is shown that the price game has a unique NE at a larger marginal price of the two WSPs, and the quality game has a NE that balances the marginal price with the monopoly price. Using an extensive numerical analysis, we have demonstrated the fundamental tradeoffs in the Wi-Fi 2.0 network due to the factors, such as customer arrival rate, channel dynamics, and eviction cost.

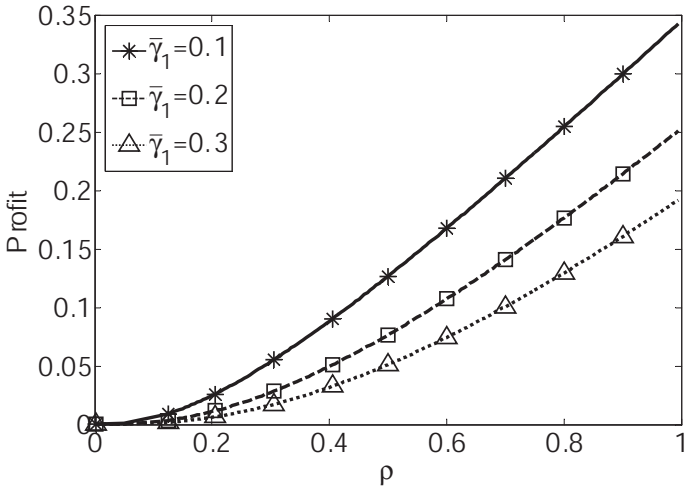

(a) Profit F_i vs. arrival rate λ

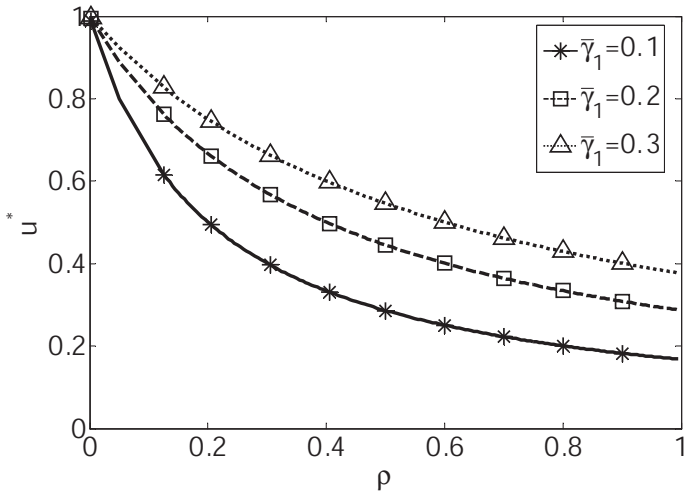

(b) Quality NE u^* vs. arrival rate λ

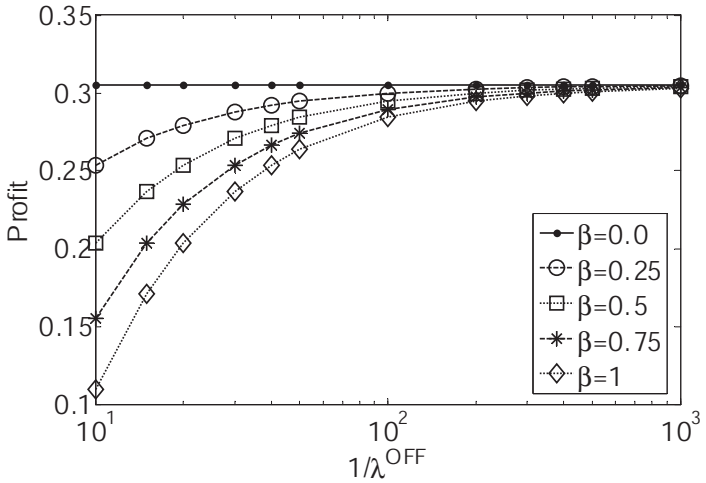

(c) Profit F_i vs. eviction cost β

Figure 6.9: Fundamental tradeoffs in the duopoly market

CHAPTER VII

Conclusion and Future Direction

This dissertation addresses the issues of efficient discovery and utilization of spectrum opportunities to better integrate the dynamic spectrum access (DSA) mechanism into the current wireless networking paradigm. This chapter summarizes our contributions and presents possible future research directions.

7.1 Research Contributions

The major contributions of this research are grouped into two categories: efficient opportunity discovery and efficient opportunity utilization. In particular, we addresses opportunity discovery in the context of spectrum sensing of in-band and out-of-band channels, and addresses opportunity utilization in the application of Wi-Fi-like whitespace utilization.

7.1.1 Contributions in Opportunity Discovery

The success of DSA hinges on how to strike a balance between the following two conflicting objectives: (1) to efficiently discover opportunities with minimal sensing overhead, and (2) to protect PUs against harmful interference from SUs. We addressed this issue by proposing two types of out-of-band sensing techniques and an in-band sensing scheme.

In Chapter II, we consider a bandwidth-craving CR network (CRN) which aims to discover as much opportunities as possible from out-of-band channels to achieve a higher throughput. We propose a periodic out-of-band sensing scheme that optimizes sensing-periods of multiple out-of-band channels to maximize the utilizable portion of opportunities. The utilizable opportunity implies the portion of opportunities discovered by out-of-band sensing which are uninterrupted by out-of-band sensing of other channels in case a sensor and a transceiver are co-located at each SU.

In Chapter III, we consider a bandwidth-limited CRN which seeks a specific amount of bandwidth determined as the sum of spectrum demands from all SUs in the CRN. In such a setup, we focus on the case where channel vacation incurs a shortage of spectrum opportunities and triggers reactive out-of-band sensing to find additional spectrum opportunities to compensate for the loss of bandwidth due to the channel vacation. We propose an optimal sequence of out-of-band channels that minimizes the delay in finding the necessary amount of opportunities to promote seamless service provisioning. The optimal sensing sequence is derived by dynamic programming (DP) with consideration of the heterogeneous channel characteristics, and a near-optimal sequencing algorithm is also proposed which reduces the computational complexity of DP by finding the suboptimal sequence in polynomial-time.

In Chapter IV, we study PU protection via periodic in-band sensing with an objective of detecting returning PUs at in-band channels within a hard deadline determined by the FCC requirement. Especially, we optimally schedule periodic in-band sensing by deriving optimal sensing-time and sensing-period incurring minimal sensing overhead while achieving all the PU detection requirements such as sensing latency, sensitivity, and accuracy. We also identify a tradeoff between energy and feature detection and compare the two schemes to determine a better detection

method in terms of sensing overhead according to the varying sensing environments.

7.1.2 Contributions in Opportunity Utilization

The discovered spectrum opportunities should be utilized in a way that SUs can benefit from DSA and the legacy spectrum can be used more efficiently. We focus on Wi-Fi-like whitespace applications where SUs can access the Internet via DSA-enabled access points (called CR hotspot) operated by the secondary wireless service providers (WSPs). Such applications may appear in early stages of DSA deployment due to its popularity in the current consumer market. In this context, we address two issues in the problem of WSP's profit maximization: (1) CR customer flow control at each CR hotspot, and (2) competition between co-located WSPs.

In Chapter V, we propose an optimal admission and eviction control of CR users at CR hotspots where a multi-class service is provided and spectrum availability is time-varying due to the ON/OFF channel usage patterns by PUs. We address the issues in the dynamic spectrum market (DSM) where the license holders lease their own spectrum to WSPs via dynamic spectrum auction. According to the system state in terms of the number of in-service customers, the arriving customers are either admitted or rejected, and at channel vacation in-service customers are selectively evicted from the service to fit into the remaining spectrum opportunities. The optimization problem is modeled as a semi-Markov decision process (SMDP) and a linear programming (LP) algorithm is formulated to derive the optimal control.

In Chapter VI, we consider price and quality competition between co-located WSPs where they compete for leasing the spectrum with the best quality at spectrum auction and for enticing more customers by providing more competitive pricing. The problem is modeled as a duopoly game and the Nash Equilibria of the service tariff

and the quality of the leased channel are derived.

7.2 Future Direction

This section describes possible future research directions related to the efficient integration of DSA into the future wireless networks.

7.2.1 Energy-efficient Spectrum-agile Networking

Although DSA may help support better quality-of-service (QoS) in wireless communications, the cost in deploying and managing CR sensors must be taken into account. Among the various issues in CR sensor management, energy efficiency is an interesting issue which can be addressed as follows. First, an efficient sensing algorithm needs to be developed to choose the best sensors to collaborate according to the sensors' heterogeneous lifetime distribution and their surrounding environments (e.g., fading). Next, to enhance the lifetime of each sensor, the sensing algorithm should be able to mitigate sensing overhead, radio reconfiguration time, and sensing report dissemination time. Finally, when there are multimedia users competing for a limited spectrum resource, a dynamic resource sharing algorithm can be developed to derive an optimal sharing strategy with minimal collision and contention, for which game theory can be adopted.

7.2.2 Coexistence of Heterogeneous Wireless Networks

Due to the exponential growth of wireless services, coexistence of heterogeneous networks has become a serious issue. CR techniques may help mitigate such problems, since CR networks are inherently required to coexist with legacy systems. In the context of coexistence, "spectrum etiquette" implies a scheme that describes how collocated networks can share spectrum resources through resource negotiation,

renting, and contention. Therefore, we can extend the spectrum etiquette concept for coexistence of the various types of emerging wireless networks. Potential research topics include development of a spectrum etiquette protocol to enable spatial reuse of spectrum, and construction of cooperative and non-cooperative discovery mechanisms of neighboring networks.

7.2.3 Seamless Multimedia Communications

DSA can be adopted to achieve more reliable and seamless multimedia service provisioning. One possible direction is to use CR techniques in searching for extra bandwidth by collecting unused portion of the licensed spectrum, thus supporting multi-dimensional network objectives such as bandwidth, delay, data rates, and deadlines. DSA can be also used in cellular networks in terms of dynamic resource leasing between service providers to maintain seamless services and to exploit extra revenue from the temporary transfer of spectrum usage rights.

APPENDIX

APPENDIX A

Proof of Lemma 6.5.1

Let's consider the following:

$$\begin{aligned}
&\frac{\sum_{n=0}^{\alpha} \rho^n/n!}{\sum_{n=0}^{\alpha-1} \rho^n/n!} - 2 \cdot \frac{\sum_{n=0}^{\alpha} (\rho/2)^n/n!}{\sum_{n=0}^{\alpha-1} (\rho/2)^n/n!} \\
&= 1 + \frac{\rho^\alpha/\alpha!}{\sum_{n=0}^{\alpha-1} \rho^n/n!} - 2 \cdot \left(1 + \frac{(\rho/2)^\alpha/\alpha!}{\sum_{n=0}^{\alpha-1} (\rho/2)^n/n!} \right) \\
&= \frac{\rho^\alpha/\alpha!}{\sum_{n=0}^{\alpha-1} \rho^n/n!} - 1 - 2 \cdot \frac{(\rho/2)^\alpha/\alpha!}{\sum_{n=0}^{\alpha-1} (\rho/2)^n/n!} < 0,
\end{aligned}$$

since $\frac{\rho^\alpha/\alpha!}{\sum_{n=0}^{\alpha-1} \rho^n/n!} < 1$ because (1) $\rho^\alpha/\alpha! < 1$, for $0 < \rho < 1$ and $\alpha \geq 1$, and (2) $\sum_{n=0}^{\alpha-1} \rho^n/n! = 1 + \sum_{n=1}^{\alpha-1} \rho^n/n! > 1$. This completes the proof.

BIBLIOGRAPHY

BIBLIOGRAPHY

[1] IEEE 802.22 Working Group on Wireless Regional Area Networks. http://www.ieee802.org/22/.

[2] S.H.A. Ahmad, M. Liu, T. Javidi, Q. Zhao, and B. Krishnamachari. Optimality of Myopic Sensing in Multichannel Opportunistic Access. *IEEE Trans. Inf. Theory*, 55(9):4040–4050, September 2009.

[3] P. Bahl, R. Chandra, T. Moscibroda, R. Murty, and M. Welsh. White Space Networking with Wi-Fi like Connectivity. In *Proc. ACM SIGCOMM*, August 2009.

[4] J.O. Berger. *Statistical Decision Theory and Bayesian Analysis, second edition.* Springer Science, New York, NY, 2006.

[5] M.M. Buddhikot. Understanding Dynamic Spectrum Access: Models, Taxonomy and Challenges. In *Proc. IEEE DySPAN*, April 2007.

[6] M.M. Buddhikot and K. Ryan. Spectrum Management in Coordinated Dynamic Spectrum Access Based Cellular Networks. In *Proc. IEEE DySPAN*, November 2005.

[7] D. Cabric, S.M. Mishra, and R.W. Brodersen. Implementation Issues in Spectrum Sensing for Cognitive Radios. In *Proc. Asilomar Conference on Signals, Systems and Computers*, November 2004.

[8] W. Caldwell. Draft Recommended Practice. *IEEE 802.22-06/0242r06*, March 2007.

[9] N.B. Chang and M. Liu. Optimal Channel Probing and Transmission Scheduling for Opportunistic Spectrum Access. In *Proc. ACM MobiCom*, September 2007.

[10] J.M. Chapin and W.H. Lehr. The Path to Market Success for Dynamic Spectrum Access Technology. *IEEE Commun. Mag.*, 45(5):96–103, May 2007.

[11] H.-S. Chen, W. Gao, and D.G. Daut. Spectrum Sensing Using Cyclostationary Properties and Application to IEEE 802.22 WRAN. In *Proc. IEEE GLOBECOM*, November 2007.

[12] H.-S. Chen, W. Gao, and D.G. Daut. Spectrum Sensing for Wireless Microphone Signals. In *Proc. IEEE SECON*, June 2008.

[13] T. Chen, H. Zhang, G.M. Maggio, and I. Chlamtac. CogMesh: A Cluster-based Cognitive Radio Network. In *Proc. IEEE DySPAN*, Apr. 2007.

[14] C.-T. Chou. *Adaptive Quality-of-Service Provisioning in Wireless/Mobile Networks*. PhD thesis, The University of Michigan, 2004.

[15] C.-T. Chou, S. Shankar N, H. Kim, and K.G. Shin. What and How Much to Gain by Spectral Agility. *IEEE J. Sel. Areas Commun.*, 25(3):576–588, April 2007.

[16] G. Chouinard. WRAN Reference Model. *IEEE 802.22-04/0002r12*, September 2005.

[17] C. Cordeiro, K. Challapali, D. Birru, and S. Shankar N. IEEE 802.22: An Introduction to the First Wireless Standard based on Cognitive Radios. *Journal of Communications*, 1(1):38–47, April 2006.

[18] C. Cordeiro, K. Challapali, and M. Ghosh. Cognitive PHY and MAC Layers for Dynamic Spectrum Access and Sharing of TV Bands. In *Proc. ACM TAPAS*, August 2006.

[19] C. Cordeiro, M. Ghosh, D. Cavalcanti, and K. Challapali. Spectrum Sensing for Dynamic Spectrum Access of TV Bands. In *Proc. CrownCom*, July 2007.

[20] D.R. Cox. *Renewal Theory*. Butler & Tanner Ltd, London, UK, 1967.

[21] D. Datla, R. Rajbanshi, A.M. Wyglinski, and G.J. Minden. Parametric Adaptive Spectrum Sensing Framework for Dynamic Spectrum Access Networks. In *Proc. IEEE DySPAN*, Apr. 2007.

[22] S. Deb, V. Srinivasan, and R. Maheshwari. Dynamic Spectrum Access in DTV Whitespaces: Design Rules, Architecture and Algorithms. In *Proc. ACM MobiCom*, September 2009.

[23] L. Duan, J. Huang, and B. Shou. Competition with Dynamic Spectrum Leasing. In *Proc. IEEE DySPAN*, April 2010.

[24] FCC. Spectrum Policy Task Force Report. *ET Docket No. 02-135*, November 2002.

[25] FCC. Facilitating Opportunities for Flexible, Efficient, and Reliable Spectrum Use Employing Cognitive Radio Technologies. *ET Docket No. 03-108*, December 2003.

[26] FCC. Notice of Proposed Rule Making and Order. *ET Docket No. 03-322*, December 2003.

[27] FCC. Notice of Proposed Rulemaking and Order. *ET Docket No. 04-113*, May 2004.

[28] FCC. Second Report and Order and Memorandum Opinion and Order. *FCC 08-260*, November 2008.

[29] G. Gallego and G.v. Ryzin. Optimal Dynamic Pricing of Inventories with Stochastic Demand over Finite Horizons. *Management Science*, 40(8):999–1020, August 1994.

[30] S. Gandhi, C. Buragohain, L. Cao, H. Zheng, and S. Suri. A General Framework for Wireless Spectrum Auctions. In *Proc. IEEE DySPAN*, April 2007.

[31] G. Ganesan and Y. Li. Cooperative Spectrum Sensing in Cognitive Radio Networks. In *Proc. IEEE DySPAN*, November 2005.

[32] S. Geirhofer, L. Tong, and B.M. Sadler. Dynamic Spectrum Access in the Time Domain: Modeling and Exploiting White Space. *IEEE Commun. Mag.*, 45(5):66–72, May 2007.

[33] S. Ghani and M. Schwartz. A Decomposition Approximation for the Analysis of Voice/Data Integration. *IEEE Trans. Commun.*, 42(7):2441–2452, July 1994.

[34] A. Ghasemi and E.S. Sousa. Collaborative Spectrum Sensing for Opportunistic Access in Fading Environments. In *Proc. IEEE DySPAN*, November 2005.

[35] A. Ghasemi and E.S. Sousa. Opportunistic Spectrum Access in Fading Channels Through Collaborative Sensing. *Journal of Communications*, 2(2):71–82, March 2007.

[36] L.P. Goh, Z. Lei, and F. Chin. DVB Detector for Cognitive Radio. In *Proc. IEEE ICC*, June 2007.

[37] A. Goldsmith. *Wireless Communications*. Cambridge University Press, Cambridge, NY, 2005.

[38] M. Gudmundson. Correlation Model for Shadow Fading in Mobile Radio Systems. *Electronic Letters*, 27(23):2145–2146, November 1991.

[39] B. Hamdaoui and K. G. Shin. OS-MAC: An Efficient MAC Protocol for Spectrum-Agile Wireless Networks. *IEEE Trans. Mobile Comput.*, 7(8):915–930, August 2008.

[40] N. Han, S. Shon, J.H. Chung, and J.M. Kim. Spectral correlation based signal detection method for spectrum sensing in IEEE 802.22 WRAN systems. In *Proc. ICACT*, February 2006.

[41] S. Haykin. Cognitive Radio: Brain-empowered Wireless Communications. *IEEE J. Sel. Areas Commun.*, 23(2):201–220, February 2005.

[42] A.T. Hoang and Y.-C. Liang. Adaptive Scheduling of Spectrum Sensing Periods in Cognitive Radio Networks. In *Proc. IEEE GLOBECOM*, November 2007.

[43] B. Ishibashi, N. Bouabdallah, and R. Boutaba. QoS Performance Analysis of Cognitive Radio-based Virtual Wireless Networks. In *Proc. IEEE INFOCOM*, April 2008.

[44] J. Jia and Q. Zhang. Competitions and Dynamics of Duopoly Wireless Service Providers in Dynamic Spectrum Market. In *Proc. ACM MobiHoc*, May 2008.

[45] H. Jiang, L. Lai, R. Fan, and H.V. Poor. Optimal Selection of Channel Sensing Order in Cognitive Radio. *IEEE Trans. Wireless Commun.*, 8(1):297–307, January 2009.

[46] G. S. Kasbekar, E. Altman, and S. Sarkar. A Hierarchical Spatial Game over Licenced Resources. In *Proc. GameNets*, June 2009.

[47] T. Keller and L. Hanzo. Adaptive Multicarrier Modulation: A Convenient Framework for Time-frequency Processing in Wireless Communications. *Proc. IEEE*, 88(5):611–640, May 2000.

[48] R. Kennedy and P. Ecclesine. IEEE P802.11af Tutorial. *IEEE 802.11-10/0742r0*, July 2010. https://mentor.ieee.org/802.11/dcn/10/11-10-0742-00-0000-p802-11af-tutorial.ppt.

[49] H. Kim, C. Cordeiro, K. Challapali, and K.G. Shin. An Experimental Approach to Spectrum Sensing in Cognitive Radio Networks with Off-the-Shelf IEEE 802.11 Devices. In *Proc. IEEE CCNC*, January 2007.

[50] H. Kim and K.G. Shin. Efficient Discovery of Spectrum Opportunities with MAC-Layer Sensing in Cognitive Radio Networks. *IEEE Trans. Mobile Comput.*, 7(5):533–545, May 2008.

[51] H. Kim and K.G. Shin. In-band Spectrum Sensing in Cognitive Radio Networks: Energy Detection or Feature Detection? In *Proc. ACM MobiCom*, September 2008.

[52] H. Kim and K.G. Shin. Understanding Wi-Fi 2.0: From the Economical Perspective of Wireless Service Providers. *IEEE Wireless Commun. Mag.*, 17(4):41–46, August 2010.

[53] L. Lai, H.E. Gamal, H. Jiang, and H.V. Poor. Cognitive Medium Access: Exploration, Exploitation and Competition. *IEEE Trans. Mobile Comput.*, 2010.

[54] X. Liu and S. Shankar N. Sensing-based Opportunistic Channel Access. *J. Mobile Netw. Appl.*, 11(4):577–591, August 2006.

[55] M. A. McHenry. NSF Spectrum Occupancy Measurements Project Summary. *Shared Spectrum Company Report*, August 2005.

[56] S.M. Mishra, A. Sahai, and R.W. Brodersen. Cooperative Sensing among Cognitive Radios. In *Proc. IEEE ICC*, June 2006.

[57] A. Motamedi and A. Bahai. MAC Protocol Design for Spectrum-agile Wireless Networks: Stochastic Control Approach. In *Proc. IEEE DySPAN*, April 2007.

[58] H. Mutlu, M. Alanyali, and D. Starobinski. Spot Pricing of Secondary Spectrum Usage in Wireless Cellular Networks. In *Proc. IEEE INFOCOM*, April 2008.

[59] R.B. Myerson. *Game Theory: Analysis of Conflict*. Harvard University Press, Cambridge, MA, 2002.

[60] N. Nie and C. Comaniciu. Adaptive channel allocation spectrum etiquette for cognitive radio networks. *Mobile Netw. Appl.*, 11(6):779–797, December 2006.

[61] D. Niyato and E. Hossain. A Game-Theoretic Approach to Competitive Spectrum Sharing in Cognitive Radio Networks. In *Proc. IEEE WCNC*, March 2007.

[62] P. Pawelczak, C. Guo, R.V. Prasad, and R. Hekmat. Cluster-based Spectrum Sensing Architecture for Opportunistic Spectrum Access Networks. *IRCTR-S-004-07 Report*, February 2007.

[63] V. Paxson and S. Floyd. Wide-Area Traffic: The Failure of Poisson Modeling. *IEEE/ACM Trans. Netw.*, 3(3):226–244, June 1995.

[64] R. Rajbanshi, Q. Chen, A.M. Wyglinski, G.J. Minden, and J.B. Evans. Quantitative Comparison of Agile Modulation Techniques for Cognitive Radio Transceivers. In *Proc. IEEE CCNC*, January 2007.

[65] T.S. Rappaport. *Wireless Communications: Principles and Practices*. Prentice Hall PTR, 2nd edition, 2002.

[66] K.W. Ross and D.H.K. Tsang. Optimal Circuit Access Policies in an ISDN Environment: A Markov Decision Approach. *IEEE Trans. Commun.*, 37(9):934–939, September 1989.

[67] K.W. Ross and D.H.K. Tsang. The Stochastic Knapsack Problem. *IEEE Trans. Commun.*, 37(7):740–747, July 1989.

[68] S.M. Ross. *Stochastic Processes*. John Wiley & Sons, Inc., New York, NY, 1983.

[69] A. Sahai and D. Cabric. Cyclostationary Feature Detection. *Tutorial presented at IEEE DySPAN 2005 (Part II)*, November 2005. http://www.eecs.berkeley.edu/ sahai/Presentations/Dy-SPAN05_part2.ppt.

[70] A. Sahai, R. Tandra, S.M. Mishra, and N. Hoven. Fundamental Design Tradeoffs in Cognitive Radio Systems. In *Proc. ACM TAPAS*, August 2006.

[71] S. Sankaranarayanan, P. Papadimitratos, and A. Mishra. A Bandwidth Sharing Approach to Improve Licensed Spectrum Utilization. In *Proc. IEEE DySPAN*, November 2005.

[72] S. Sengupta, M. Chatterjee, and S. Ganguly. An Economic Framework for Spectrum Allocation and Service Pricing with Competitive Wireless Service Providers. In *Proc. IEEE DySPAN*, April 2007.

[73] S. Shankar, C. Cordeiro, and K. Challapali. Spectrum Agile Radios: Utilization and Sensing Architectures. In *Proc. IEEE DySPAN*, November 2005.

[74] S. Shellhammer. An ATSC Detector using Peak Combining. *IEEE 802.22-06/0243r0*, November 2006.

[75] S. Shellhammer. Numerical Spectrum Sensing Requirements. *IEEE 802.22-06/0088r0*, June 2006.

[76] S. Shellhammer and G. Chouinard. Spectrum Sensing Requirements Summary. *IEEE 802.22-06/0089r1*, June 2006.

[77] S. Shellhammer, S. Shankar N., R. Tandra, and J. Tomcik. Performance of Power Detector Sensors of DTV Signals in IEEE 802.22 WRANs. In *Proc. ACM TAPAS*, August 2006.

[78] S. Shellhammer and R. Tandra. An Evaluation of DTV Pilot Power Detection. *IEEE 802.22-06/0188r0*, July 2006.

[79] S. Shellhammer and R. Tandra. Performance of the Power Detector with Noise Uncertainty. *IEEE 802.22-06/0134r0*, July 2006.

[80] S. Shellhammer, V. Tawil, G. Chouinard, M. Muterspaugh, and M. Ghosh. Spectrum Sensing Simulation Model. *IEEE 802.22-06/0028r10*, September 2006.

[81] T. Shu and M. Krunz. Throughput-efficient Sequential Channel Sensing and Probing in Cognitive Radio Networks Under Sensing Errors. In *Proc. ACM MobiCom*, September 2009.

[82] D. Simon. *Optimal State Estimation: Kalman, H_∞, and Nonlinear Approaches*. John Wiley & Sons, Inc., Hoboken, NJ, 2006.

[83] E. Sofer and G. Chouinard. WRAN Channel Modeling. *IEEE 802.22-05/0055r07*, September 2005.

[84] C.R. Stevenson, C. Cordeiro, E. Sofer, and G. Chouinard. Functional Requirements for the 802.22 WRAN Standard. *IEEE 802.22-05/0007r47*, January 2006.

[85] A. Stirling. White Spaces - the New Wi-Fi? *International Journal of Digital Television*, 1(1):69–83, 2010.

[86] A.P. Subramanian, H. Gupta, S.R. Das, and M.M. Buddhikot. Fast Spectrum Allocation in Coordinated Dynamic Spectrum Access Based Cellular Networks. In *Proc. IEEE DySPAN*, April 2007.

[87] S.N. Subramanian and T. Le-Ngoc. Traffic Modeling in a Multimedia Environment. In *Proc. IEEE CCECE/CCGEI*, 1995.

[88] C. Sun, W. Zhang, and K.B. Letaief. Cluster-based Cooperative Spectrum Sensing in Cognitive Radio Systems. In *Proc. IEEE ICC*, June 2007.

[89] R. Tandra and A. Sahai. Fundamental Limits on Detection in Low SNR under Noise Uncertainty. In *Proc. WirelessCom*, June 2005.

[90] R. Tandra and A. Sahai. SNR Walls for Feature Detectors. In *Proc. IEEE DySPAN*, April 2007.

[91] H. Tang. Some Physical Layer Issues of Wide-band Cognitive Radio Systems. In *Proc. IEEE DySPAN*, November 2005.

[92] V. Tawil. DTV Signal Captures. *IEEE 802.22-06/0038r0*, March 2006.

[93] H.C. Tijms. *Stochastic Modelling and Analysis: A Computational Approach*. John Wiley & Sons, New York, NY, 1986.

[94] E. Visotsky, S. Kuffner, and R. Peterson. On Collaborative Detection of TV Transmissions in Support of Dynamic Spectrum Sharing. In *Proc. IEEE DySPAN*, November 2005.

[95] B. Wang, Z. Ji, and K.J.R. Liu. Primary-Prioritized Markov Approach for Dynamic Spectrum Access. In *Proc. IEEE DySPAN*, April 2007.

[96] J. Wang, M. S. Song, S. Santhiveeran, K. Lim, G. Ko, K. Kim, S. H. Hwang, M. Ghosh, V. Gaddam, and K. Challapali. First Cognitive Radio Networking Standard for Personal/Portable Devices in TV White Spaces. In *Proc. IEEE DySPAN*, April 2010.

[97] Y. Wu, B. Wang, K.J.R. Liu, and T.C. Clancy. A Multi-Winner Cognitive Spectrum Auction Framework with Collusion-Resistant Mechanisms. In *Proc. IEEE DySPAN*, October 2008.

[98] S. Xu, Y. Shang, and H. Wang. SVD based Sensing of a Wireless Microphone Signal in Cognitive Radio Networks. In *Proc. ICCS*, June 2008.

[99] Q. Zhao, L. Tong, and A. Swami. Decentralized Cognitive MAC for Dynamic Spectrum Access. In *Proc. IEEE DySPAN*, November 2005.